

# **COMPUTATIONAL ANALYSIS OF WARPAGE OF COMPOSITE LAMINATES**

TOWARDS DIGITAL TWINS OF LAMINATES FABRICATED FROM AN  
AUTOMATION LINE



# **COMPUTATIONAL ANALYSIS OF WARPAGE OF COMPOSITE LAMINATES**

TOWARDS DIGITAL TWINS OF LAMINATES FABRICATED FROM AN  
AUTOMATION LINE

## **Proefschrift**

om het masterdiploma te behalen  
aan de Technische Universiteit Delft,  
op gezag van de dr. ir. Marcel Sluiter,  
in het openbaar te verdedigen op woensdag 9 oktober 2019 om 14:00 uur

door

**Haralambos ALKIVIADES**

Physicist,  
Aristotelio University of Thessaloniki,  
geboren te Limassol, Cyprus.

Dit proefschrift is goedgekeurd door de

promotor: Dr. M. Sluiter

Samenstelling promotiecommissie:

*Voorzitter,*

Dr. M. Sluiter, Technische Universiteit Delft

*leidinggevende,*

Dr. M.A. Bessa, Technische Universiteit Delft

*Onafhankelijke leden:*

Dr. P. Dey, Technische Universiteit Delft

*bedrijfsafgevaardigde:*

Mr. M. Muilwijk, Airborne Composite Automation

Dr. M.A. Bessa heeft in belangrijke mate aan de totstandkoming van het proefschrift bijgedragen.



Copyright © 2019 by Haralambos Alkiviades

An electronic version of this dissertation is available at  
<http://repository.tudelft.nl/>.

# SUMMARY

## **Haralambos Alkiviades**

Airborne Composites Automation recently installed an automation product line that creates flat thermoplastic laminates intended for consumer electronics industry. However, due to the composite nature of the material and the process parameters, the final product is deformed, as a result of internal residual stresses. The purpose of this thesis is to use Finite Element Analysis methods in order to build up digital twins of the composite laminates undergoing the manufacturing process composed by several pressing cycles in order to predict their final warpage. Hence, this work aims at characterizing and predicting the real cause for warpage, offering an opportunity to minimizing it. Since the parameterization of the simulations is automated, this work is a first step towards the use of data-driven methods that enable analysis and design of future laminates under different process parameters.



# CONTENTS

<b>Summary</b>	<b>v</b>
<b>1 Introduction</b>	<b>1</b>
<b>2 Literature Review</b>	<b>5</b>
2.1 Basics of thermoplastics . . . . .	5
2.1.1 Thermoforming Process . . . . .	7
2.2 Origin of residual stresses . . . . .	8
2.3 Predicting residual stresses in thermoforming . . . . .	12
2.3.1 Heat Transfer analysis . . . . .	12
2.3.2 Constitutive modeling . . . . .	14
2.3.3 Viscoelasticity . . . . .	18
2.3.4 Friction Model . . . . .	26
<b>3 Influence of the Thermal gradient</b>	<b>27</b>
3.1 Material Properties . . . . .	27
3.1.1 Composite properties . . . . .	28
3.1.2 Tool properties . . . . .	30
3.2 Heat transfer analysis module . . . . .	32
3.2.1 Heat Transfer Simulations . . . . .	32
3.2.2 Heat Transfer Experiments . . . . .	36
3.2.3 Conclusions from heat transfer analysis . . . . .	39
3.3 Coupled Temperature-Displacement Simulations . . . . .	41
<b>4 Tool-Part Interaction</b>	<b>45</b>
4.1 Tool-Part finite element analyses . . . . .	46
4.1.1 Simulation Results . . . . .	48
4.1.2 Simulation Conclusions . . . . .	56
4.2 Tool-Part Experiments . . . . .	56
4.2.1 Experimental Conclusions . . . . .	60
<b>5 Viscoelasticity</b>	<b>63</b>
5.1 Implementation in finite element analysis . . . . .	63
5.2 Computational predictions with viscoelasticity . . . . .	65
5.3 Viscoelasticity Conclusion . . . . .	71
<b>6 Discussion</b>	<b>73</b>
<b>7 Conclusion</b>	<b>75</b>
<b>References</b>	<b>77</b>
<b>A Appendix A</b>	<b>81</b>
A.1 Heat Transfer Simulation . . . . .	81

<b>B</b>	<b>Appendix B</b>	<b>111</b>
B.1	Cycle's Simulation . . . . .	111
B.2	Warpage Simulation . . . . .	127
B.3	Discrete rigid Plates . . . . .	127
B.4	Viscoelastic Scripts . . . . .	131
<b>C</b>	<b>Appendix C</b>	<b>133</b>



# 1

## INTRODUCTION

**I**N recent years, the use of fibre reinforced polymer composites in high performance structural applications has increased significantly due to improvements in processing technology that enables the production of parts of very high quality. With increasing production rates of structures, there is a demand for time- and cost-efficient manufacturing processes for large scale production. Traditional manufacturing techniques for composite materials are generally slow as a typical production cycle involves labour-intensive ply collation by either hand lay-up or the use of preforms followed by long curing cycles [1]. On the other hand, Airborne Composites Automation (ACA) was able to construct an automated manufacturing technique where robotic engineering and science replace time consuming and expensive manual layup processes by laying the thermoplastic composite into the process line. To complete consolidation, several pressing cycles are used which combine mechanical and thermal loads simultaneously with the help of pressing plates and robotic hands.

The purpose of this work is to create the whole process using Finite Element (FE) modeling techniques in order to find what processing parameters cause the deformation and how to optimize it. The complexity of the modeling and process simulation is attributed to the multi-physics and multi-scale nature of the composites. Moreover, worth mentioning is that, the specific process does not exist from previous authors, so a general digital computational twin for this new product line is important for the next generation of composite automation.

The automated product line is used to manufacture laminates that will be applied to lap-top cases, among other possible applications. Therefore, the flatness of the laminates is particularly important for their functionality as well as visual appeal. However, this project has an important practical constraint: the material properties are not experimentally determined because the purpose of this thesis is to focus on simulating the process and to automate the input of the parameters involved. Moreover, it will provide working material for future work, concerning press consolidation, thermoforming, stamping and in general forming techniques. Therefore, this research has limited experimental input beyond simple characterizations of the final shape of the laminate (the output of this re-

search). Therefore, the research goal is to create a general computational strategy that can be adopted for predicting the residual stress build-up and subsequent warping of any composite laminates manufactured by the automation line.

The manufacturing process is called the "Falcon Line" with the purpose of producing thermoplastic laminates at a fast pace without any human involvement. The whole process is very fast (a matter of minutes) where in each full run, 4 flat laminates are produced. Moreover, the process is labour free, which allows for 24/7 production, reducing vastly the manufacturing cost of the composite parts.

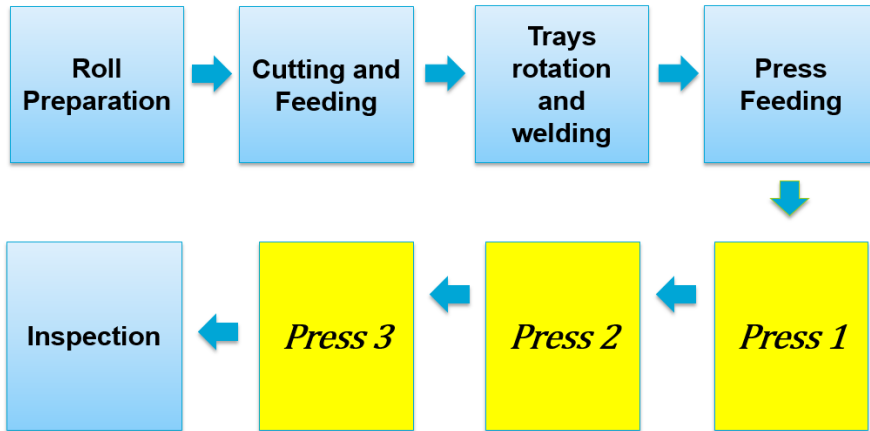


Figure 1.1: Schematic Representation of the Falcon Line

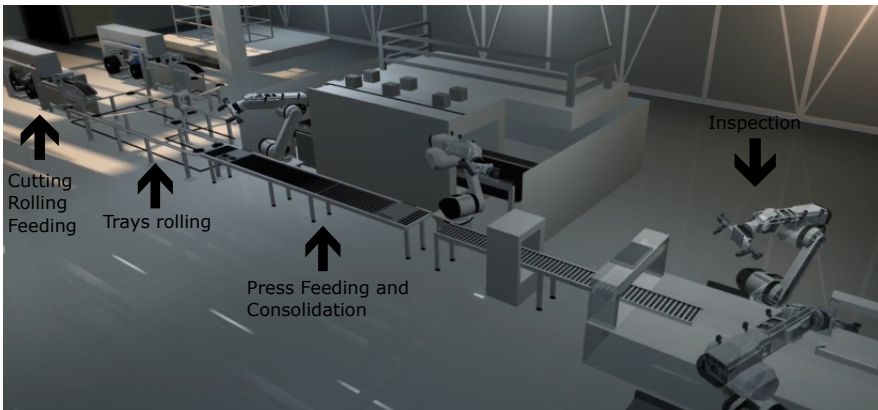


Figure 1.2: Falcon Line

The line is a combination of several steps (Figure 1.1). Also, Figure 1.2 shows the line from a digital movie that represents the real product line. Two rollers feed the system using trays that are moving into trailing lines. With correct cutting and placement, the two rollers provide laminates with different orientations and the laminate sequence is controlled automatically by choosing it before the start of feed process. At the moment, only

two directions can be chosen (0 and 90 Degrees) creating cross-ply laminates. After feeding, the laminates are welded with ultrasonic welding at two spots for the robot to easily grab them and place them into the consolidation pressing machine. The system handles four composite laminates at a time (Figure 4.17), where steel plates and a compatibility layer sheet are also used separately. With the help of robotic hands, the structure is moving through the press (plates, compatibility layer and laminates). The pressing machine consists of 3 presses, each one applying different temperature and pressure values, which is the main focus of this thesis. Moreover, the time that the loads are applied is important and also the time of the transportation from each press to the next, as it controls the heating and cooling profile of the laminates. After consolidation, the last step is the inspection of the laminate's quality, which measures the deviation of the laminates from flatness. From the stages, many variables affect the outcome of the material's quality.

The first laminates fabricated by this process showed non-negligible warpage. Warpage is characterized by a distortion of the composite laminate that leads to a different final shape after the manufacturing process is finished, as compared to the intended design [2]. In our case, warpage stands for the deviation from the flatness of initially flat laminates (the laminates must be as flat as possible in order to meet the design requirements) [3] – see Figure 1.3 exemplifying a laminate at the end of the Falcon line. Moreover, the laminates were extracted having concave shape (edges touching the compatibility layer). Then, the user turned over the laminates (convex shape) and measured the distance from all the laminate's corners to the flat reference plate. The final warpage is defined as the average of the 4 measured distances for each laminate individually. Typically, residual stresses generated during the production steps are the culprit for this defect. In general, there are multiple factors associated to composite warpage that can have two origins:

1. **Intrinsic sources:** arising from the material and the part itself. For example, material anisotropy, heterogeneity, thermo-mechanical properties, stacking sequence and part shape can strongly affect warpage of composite laminates. Non-symmetric laminate sequences, fibre misalignments, non-homogeneous distribution of fibers or defects (e.g. matrix voids), and moisture absorption are typical factors that lead to warpage [4].
2. **Extrinsic sources:** process related issues, such as kinetics of the forming process, and thermal gradient profiles that depend on mechanical tool-part interaction [5].

Chapter 2 provides a literature review about this subject and elaborates on the sources of composite warpage. Chapter 3 shows the influence of a temperature gradient on the development of stresses and also of the deformation of the material. Both computational and also experimental efforts will be compared and analyzed. Chapter 4 illustrates the mechanical interaction from a tool to the laminate that will deform the material, which again, both computational and experimental work will be illustrated. Chapter 5 will only provide a computational technique to simulate viscoelastic material, which may open doors for future work either computationally or experimentally. In the Appendix, all the coding will be explained in detail that was used for the simulations and also, coding for future work will be provided.



Figure 1.3: Warped laminate from Falcon Line

# 2

## LITERATURE REVIEW

**I**N this chapter the origin of residual stresses and their role on the material's behavior is provided, as well as analytical models describing this behavior. A brief introduction about thermoplastic polymers composites and the relevant manufacturing process in this thesis is also included.

### 2.1. BASICS OF THERMOPLASTICS

Thermoplastics are high density polymers where the interaction between polymer chains usually occurs via van der Waals forces [6] that weakly attract neutral molecules to each other. Unlike thermosets that are rigidly crosslinked by permanent bonds between chains, thermoplastics can be reheated and molded into a wide range of shapes multiple times [7], which makes them recyclable. Thermoplastics do not undergo a curing process (no permanent cross-links), so the manufacturing process is significantly faster than for thermosets.

Airborne's Falcon Line currently uses a composite supplied by Sabic [8] that has a polycarbonate thermoplastic matrix. This polymer has an amorphous structure [9], and undergoes different temperature and pressure cycles. In amorphous polymers, the material transitions from a liquid/fluid state into a glassy/solid one once it reaches the glass transition temperature. This temperature is important because it affects the mechanical properties of the material significantly. The glass transition temperature  $T_g$  should not be confused with the melting temperature  $T_m$ , since the latter is the "solid-liquid" transition in one step and can only occur for crystalline materials. Figure 2.1 shows the difference between the two temperatures,  $T_g$  and  $T_m$ , comparing an amorphous material, a semi-crystalline and a crystalline configuration. The glass transition presents features of a  $2^{nd}$  order transition since thermal studies often indicate that the molar Gibbs energies, molar enthalpies, and the molar volumes of the two phases, i.e., the melt and the glass, are equal, while the heat capacity and the expansivity are discontinuous (but for other properties such as Elastic Modulus vs Temperature, the glass transition is of  $1^{st}$  order [11, 55]). However, the glass transition is generally not regarded as a thermodynamic transition in view of the inherent difficulty in reaching equilibrium in a polymer glass or in a polymer

melt at temperatures close to the glass-transition temperature. The figure highlights the variation of volume as a function of temperature [10].

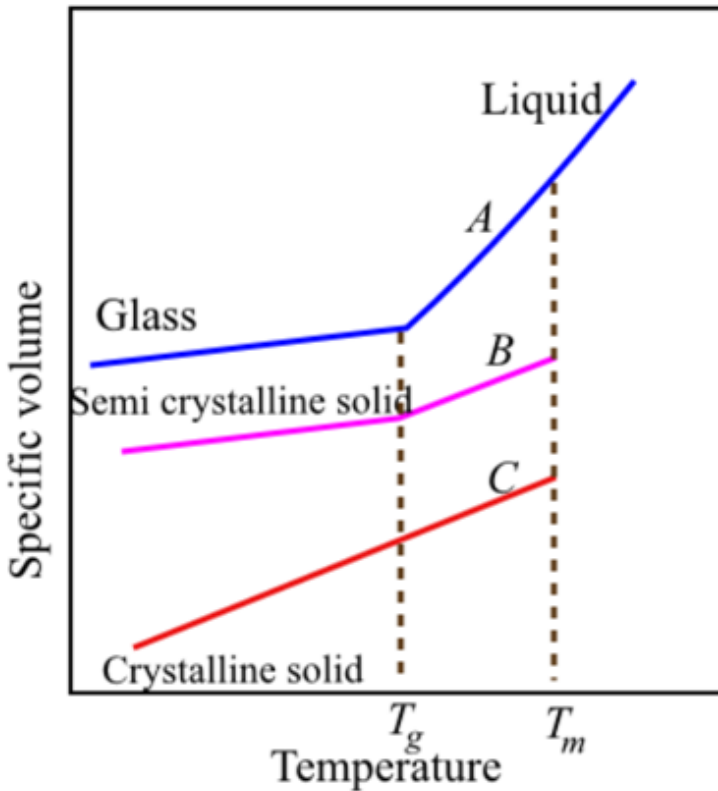


Figure 2.1: Volume Vs Temperature for solids [10].

Figure 2.2 shows how the Young's Modulus of a polyetheretherketone (PEEK) thermoplastic polymer changes as temperature increases, where it is clear the significant decrease of the Modulus value after  $T_g$  is surpassed. As temperature rises above  $T_g$ , material volume increases and facilitates the movement of molecular chains which affects thermal and elastic properties [11].

Several factors affect the transition into a glassy state:

1. Mobility of the polymer chains as the temperature increases.
2. Presence of plasticizers, which tend to separate chains from each other and increase the free volume. In this case, chains can slide past each other more easily, lowering  $T_g$  and making the polymer more pliable [11].
3. External pressure which tends to increase the glass transition temperature (smaller free volume).

The effect of pressure has been investigated by different authors, in a technique called

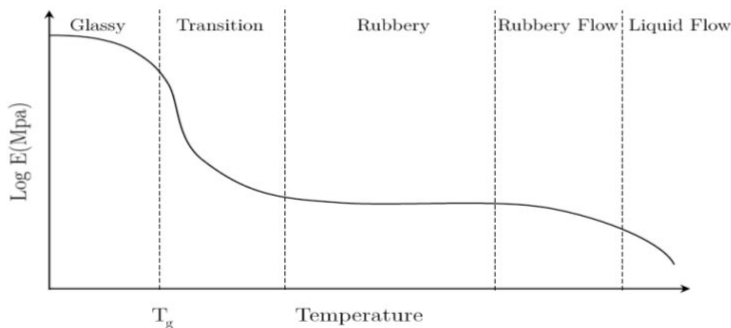


Figure 2.2: Young's Modulus vs Temperature for PEEK [12].

"Compression Induced Solidification" (CIS) [13, 14]. Using this technique, the user can manipulate the glass transition temperature concerning their manufacturing applications.

### 2.1.1. THERMOFORMING PROCESS

Thermoplastic parts can be manufactured by a myriad of techniques [15, 16]. However, this thesis focuses on the thermoforming or stamping process which is similar but not the same as Airborne's Falcon line. Falcon's Line best description is **press consolidation**, but it has some similarities with different forming techniques (so, the description of theoretical techniques is for the reader to get an understanding of the several existing forming techniques of thermoplastic products). Thermoforming is a manufacturing process where the thermoplastic polymer is heated until it is easily pliable so that it can be introduced into a mold by applying pressure such that the product is formed into the desirable shape after consolidation. The process is mainly used for smaller scale products but it is suitable for high production rates [17]. Moreover, a difference between regular thermoforming techniques and Falcon Line is that some thermoforming techniques use an already consolidated part due to the nature of thermoplastics to be remolded [18]. As shown in Figure 2.3, there are many different types of forming techniques (e.g. vacuum forming, pressure forming and mechanical forming) with their own advantages and limitations (cost, intended shape for the product, application, etc.). After consolidation, the excess material is then trimmed away and the formed part is released. Excess material can be reground, mixed with unused plastic, and reformed again into new thermoplastic sheets.

Thermoplastics and especially thermoplastic composites can have significant residual stresses after being manufactured. Residual stresses are the stresses that remain in the material after the originally induced stresses have been removed [19]. This kind of stresses can be desirable or undesirable, depending on the application. This thesis aims at creating an automated finite element analysis process to simulate the effects of residual stresses on thermoplastic composite parts manufactured by thermoforming. Therefore, understanding the origin of residual stresses is of key importance.

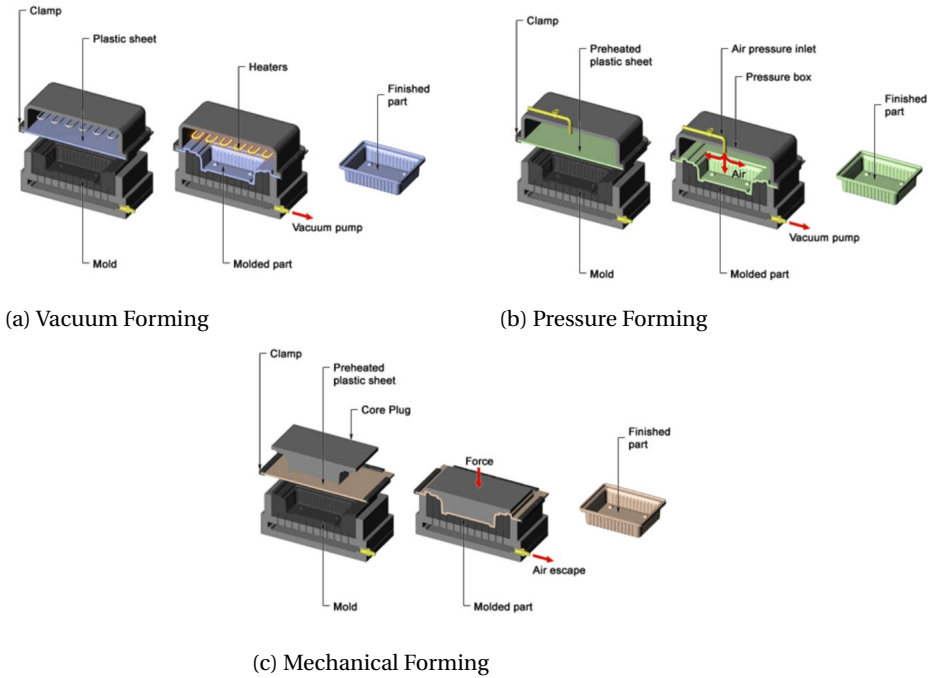


Figure 2.3: Thermoforming techniques

## 2.2. ORIGIN OF RESIDUAL STRESSES

The residual stresses are generated during cooling of the material from its final hold temperature. Since these stresses are generated inside the material, they are typically separated into three main categories:

1. *Micro-mechanical or constituent level* where the mismatch between coefficients of thermal expansion (CTE) [20] is the most important factor. After heating the material to a temperature higher than  $T_g$  or  $T_m$ , during cool down, the thermoplastic matrix tends to shrink volumetrically at a different rate than the fibres [21]. For example, Figure 2.4 illustrates the effect of the small negative CTE of carbon fibers that induces longitudinal compressive stresses in the matrix when heating the composite, as opposed to the tensile stresses that originate from the thermoplastic matrix on the transverse direction. A typical value for the CTE of the carbon fibers is  $a_C \approx -0.1 \cdot 10^{-6} K^{-1}$  while a polycarbonate matrix would have  $a_m \approx 65 \cdot 10^{-6} K^{-1}$ . Evidently, higher CTE mismatches cause larger residual stresses. Note that the matrix's CTE is temperature dependent [22].
2. *Meso-mechanical or lamination level* concerns ply to ply interactions due to the stacking sequence. Figure 2.5 summarizes this phenomenon, where interlaminar shear stresses arise between layers. If the laminate is unbalanced, for example considering a stacking sequence of [0,90,90] (which is 3 layers of the specific orientation of unidirectional laminates), then it will bend even when subjected to an axial force – see Figure 2.8 for a finite element simulation conducted by the author of



this thesis. Ply thickness or the presence of multiple plies with the same fiber direction ("block effect") also affect the residual stresses that arise, as the "block" has high elastic modulus that causes high shear stresses to the adjacent layer, eventually causing bending [21].

3. *Macro-mechanical or Global level* pertains to boundary effects that cause, for example, thermal gradients in the material. Different thermal distributions through the thickness of the material can introduce compressive residual stresses at surface plies and tensile stresses in the centre plies, as illustrated in Figure 2.6. Unbalanced cooling and thick laminates can also affect material phase formation in different locations, for example surface plies could have different phases than centre plies (important for semi-crystalline polymers [23]). This, will create constraints in the material where the surfaces solidify quicker than the centre [21].

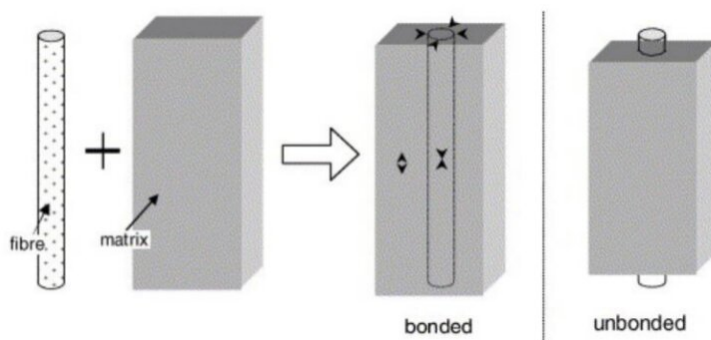


Figure 2.4: *Micro-level*: Compressive stresses from the fibres and tensile stresses from the matrix [21].

Cooling strongly affects the solidification/liquefaction of the composite through the thickness, and can cause different phase transformations [24] (in this thesis, only change in properties and not phase transformations are applied and used). The temperature in which the material does not have internal stresses is called stress-free temperature (SFT), and corresponds to a state where polymer chains have enough kinetic energy to avoid entanglements. Close to  $T_g$ , both elastic and viscous properties of the material become important, so stresses start to build up as the temperature decreases. Figure 2.9 shows a PVT diagram with the variation of specific volume when cooling in an isobaric environment for amorphous thermoplastic materials [13]. Comparing the 3 pressure configurations  $p_0$ ,  $p_1$  and  $p_2$ , where  $p_0 > p_1 > p_2$ , increasing the pressure, the glass transition temperature will decrease respectively  $T_{g0} < T_{g1} < T_{g2}$ . In this diagram, the previously mentioned effect of pressure on the  $T_g$  is evident, as well as the variation of free volume with both pressure and temperature.

The **cooling rate** is another parameter with significant importance. As the cooling rate increases, there is less time for residual stresses to relax and unwanted deformations occur in the final material. Figure 2.10 shows how the glass transition temperature  $T_g$  is affected by the cooling rate. The cooling rate also affects adhesion between the two constituents, as increasing the cooling rate leads to interfacial shear stress [21] which can lead to fibre

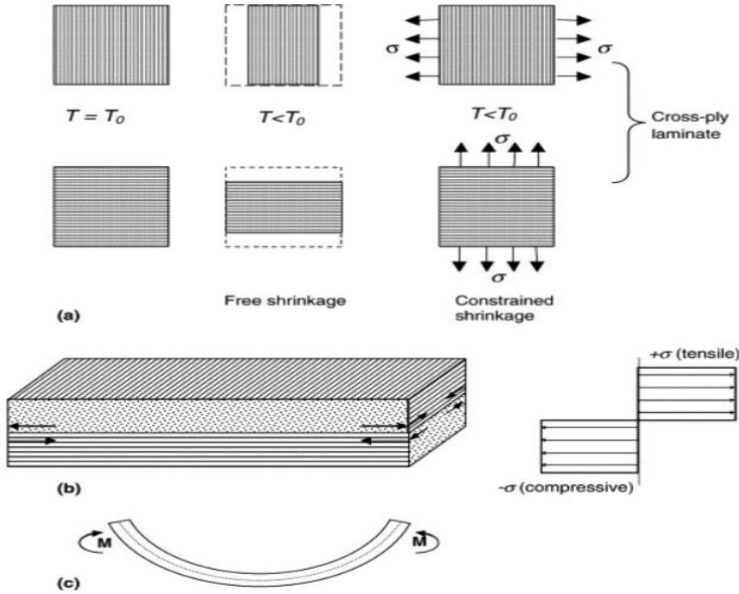


Figure 2.5: *Meso-level*: Interlaminar interaction concerning the layup sequence and block effect [21].

debonding and interfacial crack growth between the laminates.

The effect of cooling rate on composite residual stresses has been investigated by different authors. Guo et al. [25] created a micro-scale finite element model that predicts the response of a glass fibre/epoxy composite subjected to thermal stresses. Teixeira-Dias et al. [26] investigated similar effects for metal matrix composites. The accuracy of these and other investigations hinges on the quality of the material laws needed in the finite element analyses. They can include linear elasticity, viscoelasticity and friction models that affect the generation of residual stresses. Since residual stresses are sensitive to the drop of temperature between processing and working temperature, the higher the  $\Delta T$ , the higher the final value of the residual stresses and also the higher the strain in the respective material. To calculate that, the simple equation:

$$\varepsilon_{thermal} = \alpha \cdot \Delta T \quad (2.1)$$

can be used, where  $\varepsilon_{thermal}$  are the strains in each direction that were developed only from the temperature drop, and  $\alpha$  is the material's CTE. For linear elasticity, the strains are independent of the cooling rates, depending uniquely on  $\Delta T$ . If the effect of moisture is also important, the equation  $\varepsilon_{moisture} = \beta \cdot \Delta C$  can be used where  $\beta$  is the respective hygroscopic expansion coefficient and  $\Delta C$  is the difference between a dry composite and a composite with moisture

$$C = \frac{Moisture_{mass}}{Dry_{mass}} \cdot 100$$

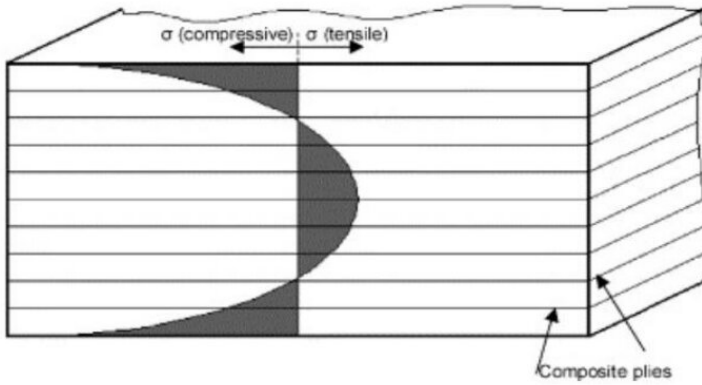


Figure 2.6: *Macro-level*: Stresses gradient through the thickness of the material [21].

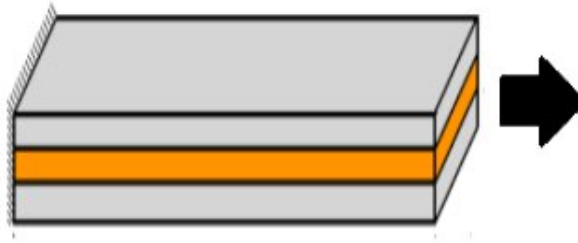


Figure 2.7: Schematic illustration of the boundary conditions for Figure 2.8.

[4].

Also, phase changes can affect the strains in the material, so the most appropriate equation [20] is

$$\epsilon_{total} = \epsilon_{thermal} + \epsilon_{moisture} + \epsilon_{PhaseChanges} \quad (2.2)$$

The above assumptions do not include any applied stress but only a temperature difference.

**Tool-part interaction** can also lead to the development of residual stresses [5, 21], as introduced in section 2.3.4, because the presence of tool affects the transfer of heat and can introduce friction. Concerning heat transfer, if there is a tool on only one side of the part, then this will cause a temperature gradient due to different heat transfer properties. This temperature gradient can affect the material microstructure in different locations, eventually leading to residual stresses and warping (*Macro-mechanism*). In composite laminates, plies that are closer to the metal part tend to cool down/heat up more quickly (due to high thermal conductivity of the metal tool) and solidify faster, while plies from the other side that are closer to the mold (compatibility layer) remain at higher temperature and experience a phase change later. Figure 2.11 shows a heat transfer model, where the top plies tend to heat up quicker than the bottom due to the addition of extra mate-

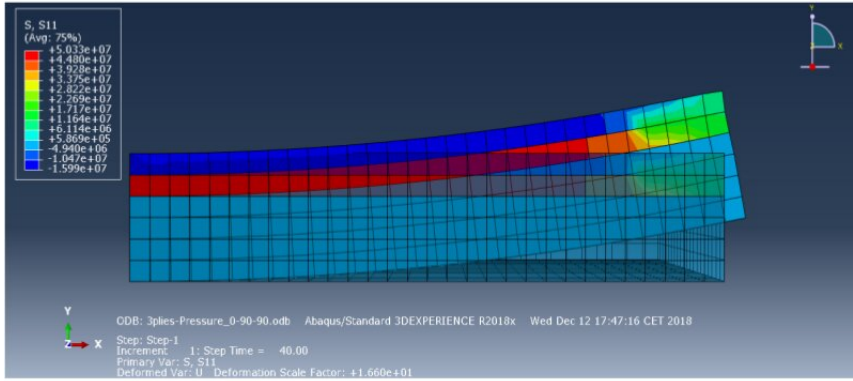


Figure 2.8: Abaqus CAE simulation of [0,90,90] with a tensile stress  $\sigma = 10\text{MPa}$ .

rial (compatibility layer sheet - used for simulation purposes) on the bottom of the laminate, introducing a temperature delay. The specific model was built up for the sake of visualization of the temperature gradient in the material (the dimensional scaling is not correct). Concerning the friction interaction between the interface of the tool and the adjacent composite ply [27], this phenomenon arises from different CTE of the tool (usually higher) and the composite which causes the bottom layers to deform as they will follow the expansion of the tool. This creates different morphology on both sides, which will eventually introduce a bending moment and warpage [5]. Figure 2.12 shows the deformation when the composite is subjected to pressure.

The next sections introduce analytical models describing *heat transfer* in the press, *calculating residual stresses with linear elasticity and viscoelasticity* and also *tool-part interaction* model. Note that there are many more parameters that can cause residual stresses that are not analyzed herein, such as **fiber misalignment**, **imperfections/voids** in the material, **fiber volume fraction**, **lamination sequence**, etc. [20]. Given the lack of knowledge of the microstructural details of the material in this thesis, these effects are neglected henceforth.

## 2.3. PREDICTING RESIDUAL STRESSES IN THERMOFORMING

Thermoforming involves heat transfer, mechanical deformation at high pressure and tool-part interactions. Computational predictions of the process need to address these three aspects. In this work, the multi-scale nature of composite laminates is neglected, and only continuum-level modeling strategies are discussed.

### 2.3.1. HEAT TRANSFER ANALYSIS

The link between temperature gradients and residual stresses implies a need to predict how heat transfers during the manufacturing process of composites [28]. The fast manufacturing processes for thermoplastics mean that there is short consolidation time, therefore the heat transfer processes are expected to be **transient** (as opposed to steady state). Analytical models provide simple closed-form solutions to practical heat transfer problems such as the one of interest in this thesis. Since the material is introduced in the press

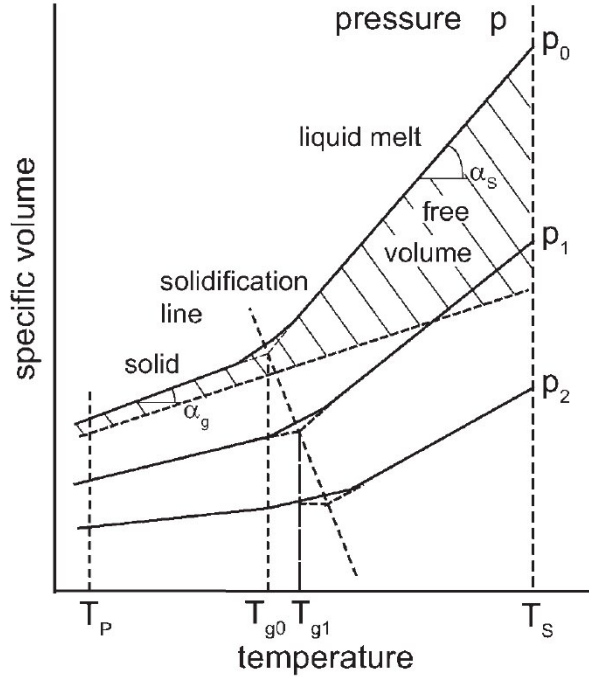


Figure 2.9: Temperature dependence of the specific volume of an amorphous thermoplastic for various pressures (isobaric cooling) [13].

and heat is transferred from both sides, the analytical model presented in [29] is selected herein, which is written as a function of the Dimensionless Fourier number:

$$\frac{T_m - T_o}{T_i - T_o} = F_o = \frac{kt}{\rho \cdot (C_p) \cdot (x_m)^2} \quad (2.3)$$

where  $T_m$  = desirable temperature at the mid-plane ( $^{\circ}C$ ),  $T_o$  = imposed surface Temperature ( $^{\circ}C$ ),  $T_i$  = initial material's Temperature ( $^{\circ}C$ ),  $F_o$  = Fourier number,  $k$  = thermal conductivity ( $\frac{W}{m \cdot ^{\circ}C}$ ),  $\rho$  = density ( $\frac{kg}{m^3}$ ),  $C_p$  = specific heat ( $\frac{J}{kg \cdot ^{\circ}C}$ ),  $x_m$  = distance from the surface to the center ( $m$ ),  $t$  = time needed for the center to be heated at  $T_m$  ( $sec$ ). Figure 2.13 can be used for practical predictions.

These classical results are useful to establish a baseline comparison with finite element models. When first learning a commercial finite element software such as Abaqus, I ensured that the predictions were correct by comparing with this analytical model using two different homogeneous materials (Copper and respective values for Composite CFRP). The simulation results are shown in Figure 2.14, and correspond to the input properties shown in Table 2.1 chosen just for illustration purposes as an average from the literature [30], and for the boundary conditions described in Table 2.2. The simulations agree with the analytical model and predict that the time needed to heat the middle of the material

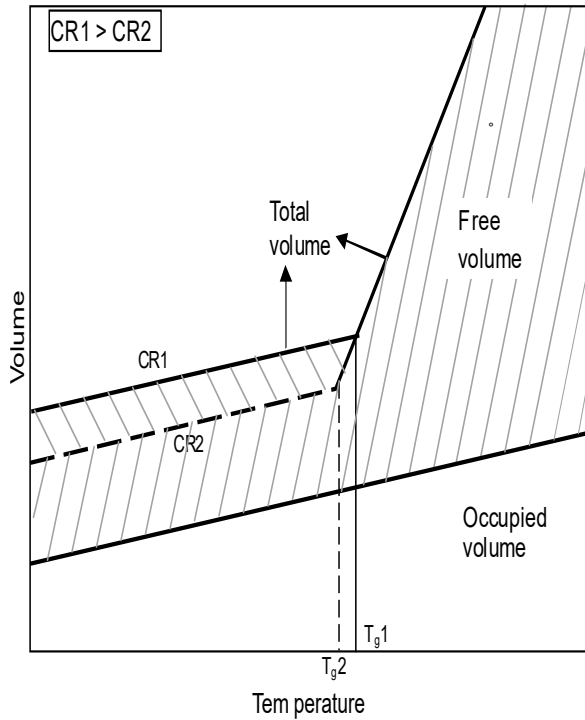


Figure 2.10: Effects of the cooling rate (CR) on the free and occupied volume of the material [21].

is  $t = 35s$  for the Copper and  $t = 381s$  for the Composite.

### 2.3.2. CONSTITUTIVE MODELING

A key aspect in accurately predicting the thermoforming process is the quality of the constitutive models used in the analysis. In the literature there are investigations that simply assume linear elastic behavior of the composite, while others consider their viscoelastic properties. One work that analyzes and compares both behaviors is Ghayoor's et. al [12, 31]. In the work, an automated placement laminate process was used for analyzing the residual stresses that are developed in the laminates during placement. The corresponding process is similar to thermoforming processes, as it is also using temperature to make the laminates pliable and also pressure for consolidation. Also, the consolidation times are small for the same reason that the material used is a thermoplastic. Moreover, the metal plate that the laminates were positioned was assumed to be the tool of this specific process, introducing residual stresses through tool-part interaction (as a thermal gradient or mechanical). Both elastic and viscoelastic behaviors were highlighted, comparing how the internal stresses were developed through the thickness of the material for each material model. Next sections will introduce the mathematical models for each constitutive model separately.

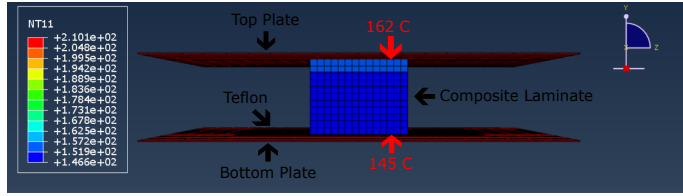


Figure 2.11: Abaqus CAE Heat transfer simulation.

Table 2.1: Reference Properties

Properties	Copper	CFRP
$k \sim \frac{W}{m \cdot ^\circ C}$	380	10
$C_p \sim \frac{J}{kg \cdot ^\circ C}$	385	919
$\rho \sim \frac{kg}{m^3}$	8940	1390
$x_m \sim m$	0.075	0.075

### LINEAR ELASTICITY

From the previous section, the thermal strains due to the temperature difference can be calculated from equation 2.2. Assuming that the material has an amorphous structure, that moisture absorption is negligible, and that the composite only experiences small strains as a result of the applied pressure on the top and bottom surfaces, the effects of elasticity can be predicted at two different levels: micro-mechanical and meso-mechanical level [4, 19, 32].

Calculating these stresses at the **micro-mechanical level** follows the linear elastic law [27]:

$$\sigma_{residual} = S \cdot \varepsilon_{thermal} \quad (2.4)$$

where  $S$  is the material's stiffness matrix and the deformation is uniquely associated to thermal strains. However, in composite materials the stiffness matrix in equation 2.4 depends on the stiffness of the fibers and of the matrix, so that equation can be rewritten as [27]:

Table 2.2: Reference Temperature

Parameters	Values
$T_o(^{\circ}C)$	200
$T_i(^{\circ}C)$	20
$T_m(^{\circ}C)$	150

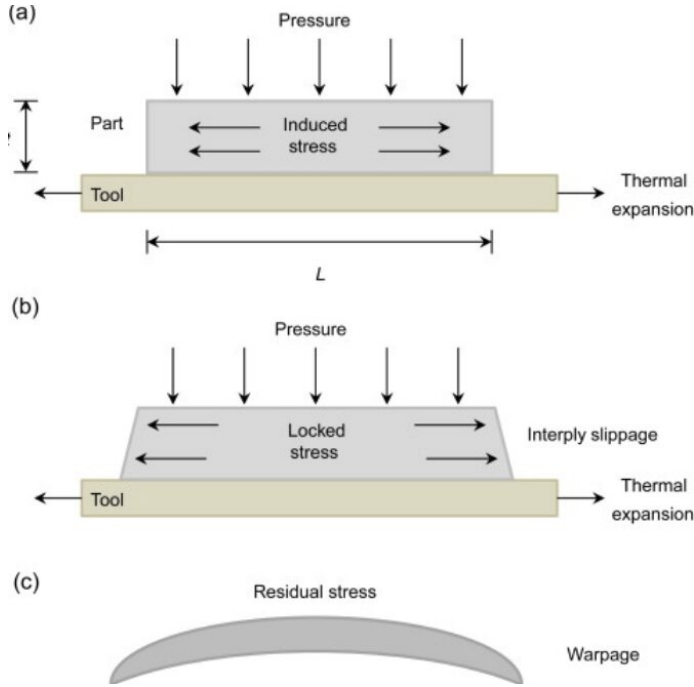


Figure 2.12: The generation of the concave shape due to the interaction between tool-part [20].

$$\sigma_{residual} = \frac{V_f E_f E_m \varepsilon_{thermal}}{E} \quad (2.5)$$

where  $V_f$  is the fiber's volume fraction,  $E_f$  is the fiber's Young's modulus,  $E_m$  is the matrix's Young's modulus and  $E$  is the total modulus [27]. This is an elementary result when calculating residual stresses from simplified models at the **Micro-mechanical level** (confront section 2.2).

At the **Meso-Mechanical level**, the simplest model to predict residual stresses follows from Classical Lamination Theory (CLT) [27, 33]. This follows from the calculation of the ABD matrix as explained in introductory books on the subject [4]:

$$A_{ij} = \sum_{k=1}^n (Q_{ij}^{(k)})(z_k - z_{k-1}) \quad (2.6)$$

$$B_{ij} = \frac{1}{2} \sum_{k=1}^k (Q_{ij}^{(n)})(z_k^2 - z_{k-1}^2) \quad (2.7)$$

$$D_{ij} = \frac{1}{3} \sum_{k=1}^k (Q_{ij}^{(n)})(z_k^3 - z_{k-1}^3) \quad (2.8)$$



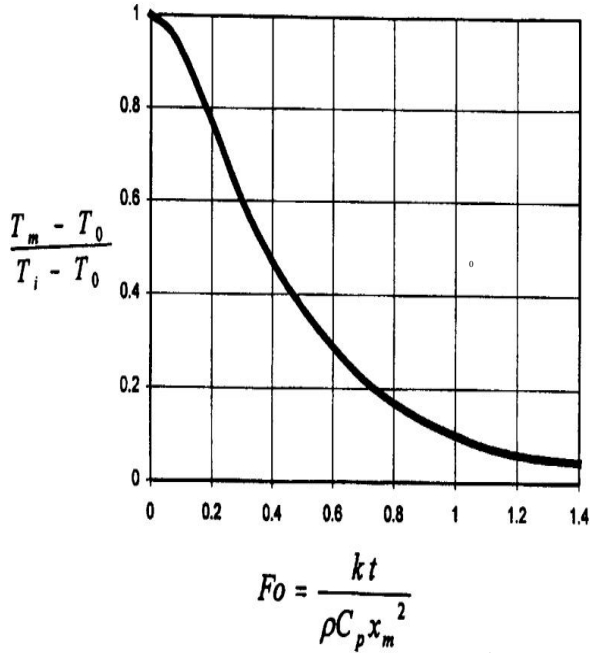


Figure 2.13: Plot for calculating the temperature  $T_m$  at the midplane of a plate as a function of time after the two surfaces are suddenly raised to  $T_o$  [29].

where  $Q_{ij}^{(k)}$  is the stiffness matrix of ply  $k$  and  $z_k$  is the distance of the  $k$ -ply from the center of the laminate. For additional details on CLT, the reader is referred to Isaac et.al [4]. The assembly of the ABD matrix enables to predict strains and curvatures/warpage of the composite laminate under mechanical or thermal loads. In the case of thermal deformation, the result becomes:

$$\begin{bmatrix} N_{thermal} \\ M_{thermal} \end{bmatrix} = \begin{bmatrix} A & B \\ B & D \end{bmatrix} \begin{bmatrix} \varepsilon_{thermal} \\ \kappa_{thermal} \end{bmatrix}$$

where  $N_{thermal}$  and  $M_{thermal}$  are the force and moment per unit length, and  $\varepsilon_{thermal}$  and  $\kappa_{thermal}$  are the strains and curvatures of the midplane of the laminate.

Linear elastic predictions for small strains are trivial predictions, but often they are unsatisfactory because polymers are viscoelastic which cause the composite to behave viscoelastically as well.

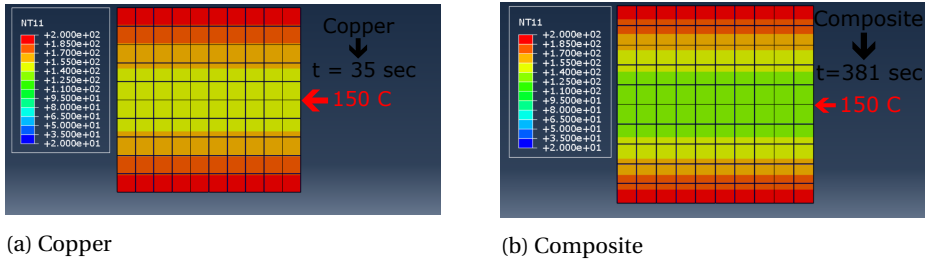


Figure 2.14: Heat transfer simulations of two materials to predict the time needed to heat their center up to  $150^{\circ}\text{C}$

### 2.3.3. VISCOELASTICITY

Most polymers exhibit viscoelastic behaviour under mechanical and thermal loads, instead of being purely linear elastic. Not accounting for viscoelastic effects can severely affect the prediction of residual stresses originated after thermoforming [12, 34–36].

Viscoelasticity is when the material exhibits both viscous and elastic characteristics under stress and deformation. These kind of properties can be found in almost all polymers, due to chain relaxation after an applied stress is removed which imposes a time-dependency to the mechanical response that is a function of the applied strain rate [37]. Viscoelasticity implies energy dissipation, unlike elastic deformation [38]. Since viscosity is the resistance to thermally activated plastic deformation, a viscous material will lose energy after a loading cycle. Moreover, when stress is applied to a viscoelastic polymer, parts of the long polymer chain change positions. This movement or rearrangement is called creep. Polymers remain a solid material even when their chains re-arrange themselves in order to accompany the stresses, and during this accommodation, it creates a back stress in the material [37].

As mentioned, viscoelastic materials experience rate-dependent behavior, i.e. their internal stresses depend of strain rate and time. Viscoelasticity can be linear or non-linear. The simplest theories assume linear elasticity and small strains [34]. If a model is only a function of the degree of cure (only valid for thermosets) and temperature it is labeled pseudo-viscoelastic and can be written as:

$$\sigma(t) = \int_0^t E(T, a) \frac{d\varepsilon}{dt} dt \quad (2.9)$$

where  $E$  is the Young's modulus as a function of temperature and  $a$  is the degree of curing (which is relevant only for thermosets).

Models that take into account the contribution of time-dependency are written as:

$$\sigma(t) = \int_0^t E(t - \tau, T, a) \frac{d\varepsilon}{dt} dt \quad (2.10)$$

Figure 2.15 shows a computational comparison between these two types of linear viscoelastic models [39], comparing computational speed and accuracy when capturing resid-

ual stresses.

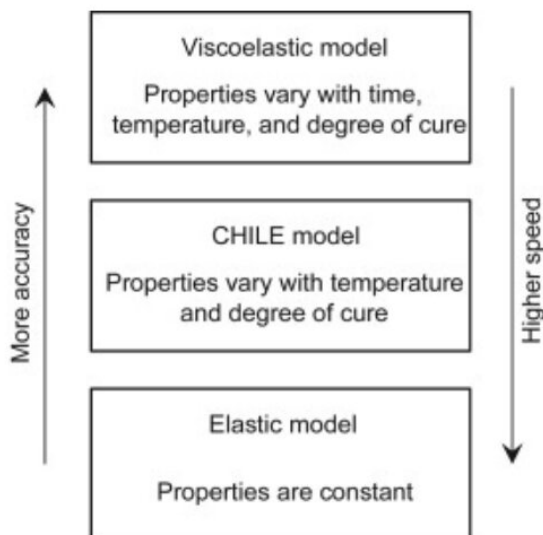


Figure 2.15: Different material constitutive models to predict residual stresses in composites [39].

One important factor about viscoelasticity is the glass transition temperature  $T_g$ . This temperature can discriminate the behaviour of the material from rubbery to glassy, although there is a transformation regime that can be called leathery or viscoelastic (Figure 2.16).

At temperatures well below  $T_g$ , only elastic bonds can be deformed, so polymers exhibit high modulus and can be assumed as glassy. When the temperature increases, the stiffness of the material will drop dramatically due to the movement of polymer chains when energy is obtained (see Figure 2.17). For thermoset polymers, stresses can be calculated from the crosslink density. If the material is not crosslinked such as thermoplastic composites, the stiffness exhibits a short plateau due to the ability of molecular entanglements to act as network junctions, but in the end the stiffness modulus will decrease to zero, as the material will eventually disassemble and melt.

#### VISCOELASTICITY MODELS FOR COMPOSITE MATERIALS

Thermoplastic composites are in the viscoelastic state between  $T_g$  and a lower temperature which is different for each polymer ( $\approx 60 - 80^\circ\text{C}$ ) [12]. This state implies that stresses that were induced due to thermal shrinkage of the composite can be relaxed as a function of time. This is possible because molecular chains of the polymer matrix have enough energy to re-entangle and move, causing relaxation of the loads in order to adapt with the stresses. Moreover, viscoelasticity is a time- and temperature- dependent parameter, so cooling rate is the most important factor that affect the generation of stresses. As an example, lower cooling rates give more time to the chains to move and relax and lead to smaller warpage. For cross ply laminates, the residual stresses between the  $0^\circ$  and  $90^\circ$  are discontinuous, which can cause delamination and fracture in the material.

2

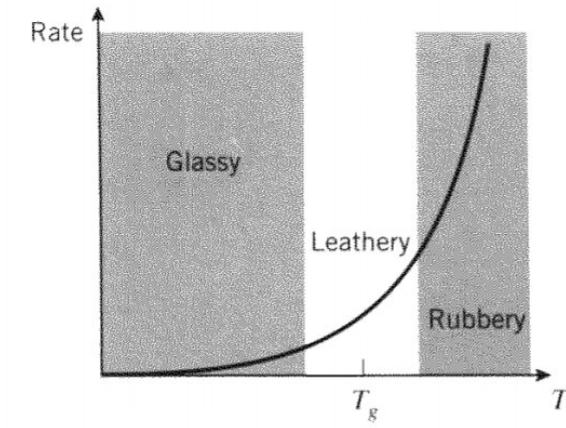


Figure 2.16: Temperature dependence of rate [40].

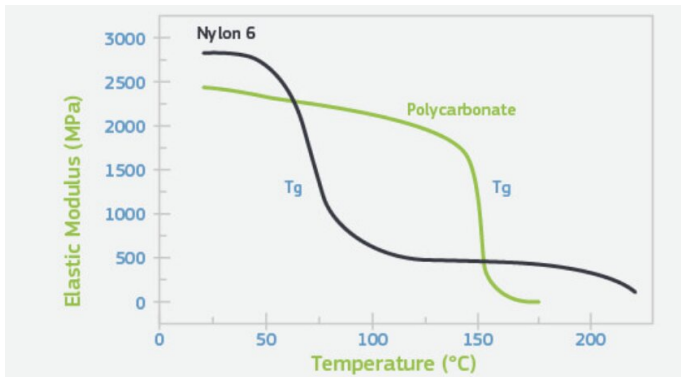


Figure 2.17: Temperature dependence of Young's modulus of amorphous PC and semi-crystalline Nylon [41].

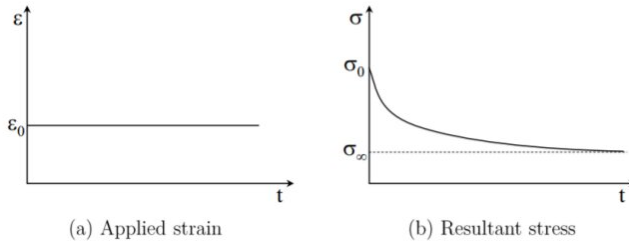


Figure 2.18: Applied strain and the stress relaxation through time [12].

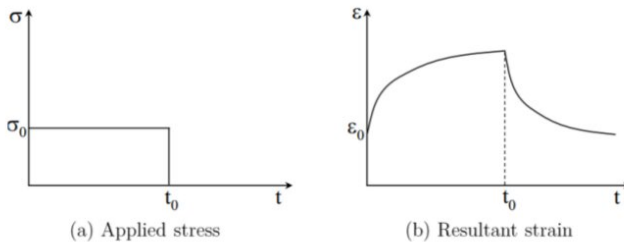


Figure 2.19: Applied constant stress and the resultant strain, especially at time  $t_0$  when the step stress is zero (creep recovery) [12].

There are three concepts that are important to consider in viscoelasticity: hysteresis, which reflects the dependency of the system on its loading and unloading history [37]; stress relaxation, occurring when the material is under a constant applied strain  $\varepsilon_o$  (Figure 2.18); and creep, which is the reverse case, i.e. a constant stress  $\sigma_o$  is applied to the material up to time  $t_o$  as the material deforms.

For stress relaxation, the Young's modulus can be calculated as:

$$E(t) = \frac{\sigma(t)}{\varepsilon_o} \quad (2.11)$$

In the case of creep, the strain starts increasing but after the removal of stress it tends to exponentially decrease (Figure 2.19). As with stress relaxation, the creep compliance is:

$$D(t) = \frac{\varepsilon(t)}{\sigma_o} \quad (2.12)$$

The two elementary mechanical models describing the viscoelastic response of polymers (Figure 2.20 are the **Maxwell model** and the **Kelvin model** [12]). The spring represents the elastic behaviour of the material (instantaneous bond deformation [40]) which is the Young's modulus  $E$  and the dashpot shows how the material behaves under viscous conditions where  $\mu$  represents the viscosity. For the viscous part, the stress can be calculated by the following equation:

$$\sigma = \mu \frac{d\varepsilon}{dt} \quad (2.13)$$

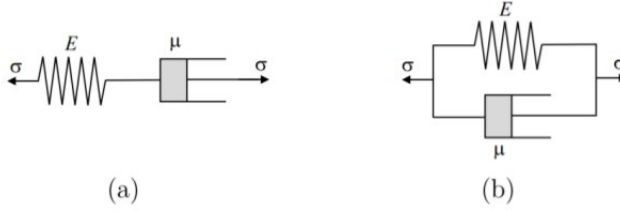


Figure 2.20: a) Maxwell model, b) Kelvin model [12].

Each model captures different behaviours. The Maxwell model is more adequate to capture stress relaxation as opposed to creep due the constraints that the dashpot apply to the spring during deformation.

Maxwell model assumes that:

$$\sigma = \sigma_s = \sigma_d$$

and

$$\varepsilon = \varepsilon_s + \varepsilon_d$$

where the subscript  $s$  refers to spring and  $d$  to dashpot.

Therefore, the basic relation for the Maxwell model is:

$$E \frac{d\varepsilon}{dt} = \frac{d\sigma}{dt} + \left(\frac{1}{t}\right) \cdot \sigma \quad (2.14)$$

Due to the time derivatives, it is difficult to calculate the respective quantities, so experimental data is important. Expanding more, the **relaxed** Young's modulus can be calculated ([12, 40]) as:

$$E_{rel}(t) = k \exp\left(\frac{-t}{\tau}\right) \quad (2.15)$$

where  $\tau = \frac{\mu}{E}$  is the relaxation time, an important parameter to consider in order to perfectly calculate the respective parameters [40].

The **Kelvin-Voigt** model is exactly the opposite. Due to the assumption that the spring and the dashpot are in parallel mode the strains can be assumed equal:

$$\varepsilon = \varepsilon_s = \varepsilon_d$$

and

$$\sigma = \sigma_s + \sigma_d$$

After calculations, the basic equation is:

$$\sigma = E\varepsilon + \mu \frac{d\varepsilon}{dt} \quad (2.16)$$

This model is adequate to capture creep since the strains are assumed equal. The model is governed by the spring and not by the dashpot which gives no stress relaxation.

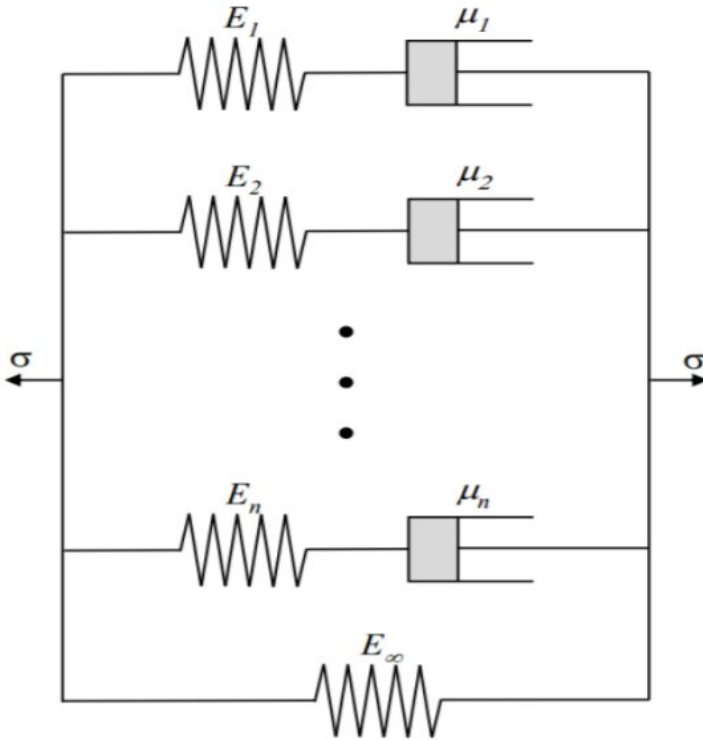


Figure 16: Weichert model [6].

Figure 2.21: Weichert model [12].

The creep compliance (time-dependent creep strain) can be calculated as:

$$J(t) = \frac{1}{E} (1 - \exp(-\frac{t}{\tau})) \quad (2.17)$$

where  $\tau$  is the retardation time for creep strains [42].

More complicated models are needed due to the complexity of the polymer chains. Models such as the **Three elements model** which capture the phenomenon using a combination of one elementary model (Maxwell or Kelvin) and one additional spring or dashpot. These models are called Standard models and they are separated in those suitable for solids and those suitable for fluids (an example is given later) [42].

A more generalized model about viscoelasticity is the **Weichert model**, which is a combination of many parallel Maxwell models. This model is good for stress relaxation calculations and can be used when the highlight of the project is to capture the stresses on a material with time dependency (Figure 2.21).

The constitutive equation now is:

$$\sigma(t) = \varepsilon_o (\sum_{i=1}^n E_i \exp(-\frac{t}{\tau}) + E_{\infty}) \quad (2.18)$$

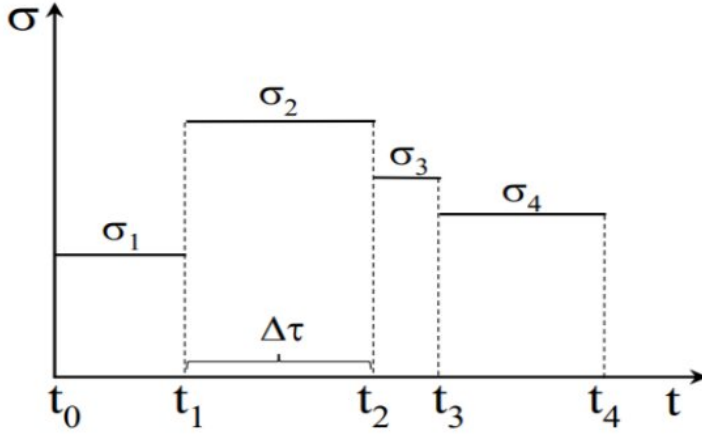


Figure 2.22: Stress vs Time diagram [12].

where  $i$  is for each spring and damper set up in the model. Moreover,  $E_\infty$  is the equilibrium modulus which explain the minimum stress after relaxation [12].

In practical implementations of viscoelastic models in finite element simulations, considering the stress variation with time is important, i.e. where every cycle has different applied load. For that, the concept of Boltzmann superposition should be introduced (Figure 2.22). In that case, the constitutive equation becomes:

$$\sigma(t) = \int_0^t \left( \sum_{i=1}^n E_i \exp\left(\frac{-t}{\tau}\right) + E_\infty \right) \frac{d\varepsilon(t)}{dt} dt \quad (2.19)$$

This equation can be used in finite element analysis simulations, provided that appropriate experimental data is available. Reference [43] details a three-dimensional implementation using tensorial notation. Lastly the Young's modulus as a function of time is written as:

$$E(t) = \sum_{i=1}^n E_i \exp\left(\frac{-t}{\tau}\right) + E_\infty \quad (2.20)$$

This equation is called the **Prony Series**, and represents a basic input of most viscoelastic models used in finite element simulations.

However, composite materials are not isotropic, which means that it is not sufficient to express one Young's modulus as a function of time. Current commercial finite element software do not have implementations for orthotropic viscoelastic models, which introduces practical difficulties in analyzing composite viscoelasticity in a practical setting. The interested reader in more advanced viscoelastic models is referred to references [42, 44]. In this thesis, the focus is on finding practical solutions that are sufficiently simple to quickly implement and use in a practical (industrial) setting. In a recent work, Martynenko [44] proposed a new method in which he merges two finite element models with independent meshes where one is an isotropic viscoelastic model and the other an orthotropic elastic one (Figure 2.23).



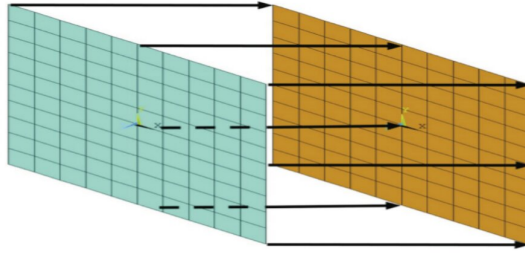


Figure 2.23: Nodes merging [44]

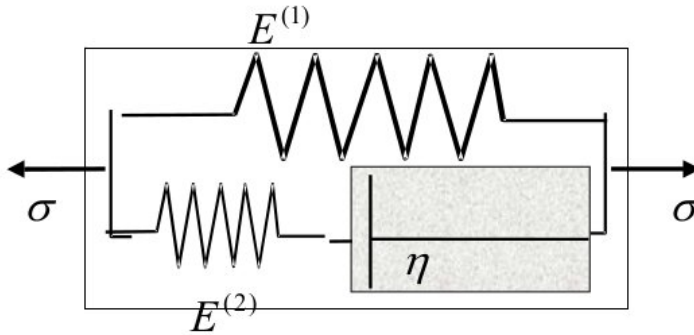


Figure 2.24: Standard Solid II [34].

This modeling strategy of merging the nodes of two material models provides a simple pathway to exhibit both elastic and viscoelastic properties [44]. If the viscoelastic model is the standard Maxwell model, then this modeling strategy is equivalent to the Standard Solid II model [34] shown in Figure 2.24 where the additional spring ( $E^{(1)}$ ) represents a solid with orthotropic elasticity, due to the superposition principle.

The stress can be calculated as:

$$\sigma + \frac{\eta}{E_2} \dot{\sigma} = E_1 \epsilon + \frac{\eta(E_1 + E_2)}{E_2} \dot{\epsilon} \quad (2.21)$$

where  $\dot{\sigma}$  and  $\dot{\epsilon}$  indicate the stress and strain rate that the material undergo and  $\eta$  is the viscosity. This modeling strategy is adopted in this thesis, and additional details are provided in section 5.2.

A final note is included herein concerning the modeling of temperature-dependent viscoelastic properties. A simple strategy that is widely used [12, 45] is to define a master curve. In essence many measurements at different temperatures are considered, and then the shifting of the responses is captured via the Williams-Landel-Ferry (WLF) [46, 47]:

$$\log(a_T) = \frac{-C_1(T - T_0)}{C_2 + (T - T_0)} \quad (2.22)$$

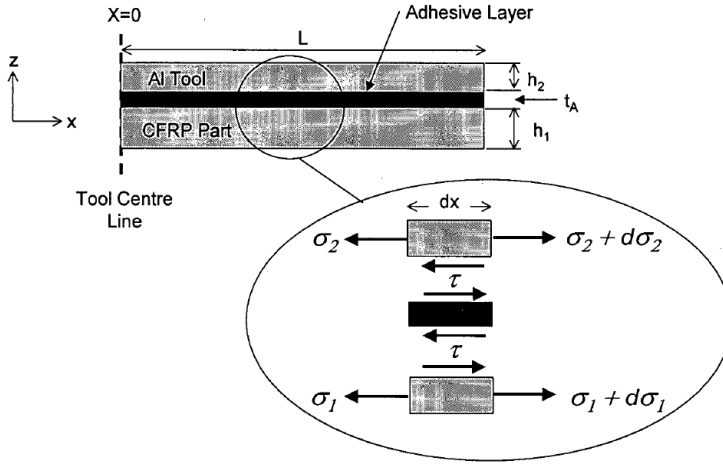


Figure 2.25: Interply/Interface stresses due to slippage [48].

where  $a_T$  is the time-based shift factor,  $T$  is the measured temperature,  $T_0$  is the reference temperature and  $C_1$ ,  $C_2$  are material parameters.

### 2.3.4. FRICTION MODEL

Completing the essential models for simulating the thermoforming of composites is the selection of an appropriate friction model. Interaction between the composite and the tool is important because it imposes transversal deformation to the composite (see Figure 2.12). For example, if a metallic tool imposes pressure on the top surface of the composite laminate and the material does not allow slippage, it will create shear stresses at the top and induces bending moments that create a stress gradient between the plies, which can cause undesirable deformation and damage. Twigg et.al [5] proposed analytical models and conducted experiments to confirm the influence of friction. In his master thesis [48], he extensively analyzed all the effects of friction with different parameters such as the **applied pressure, material dimensions** and **different tooling**. He assumed that the stress gradient is only developed between the first layer that is in touch with the tool, instead of through the entire thickness of the material (Figure 2.25). With this assumption, the stress can be obtained as [5]:

$$\sigma = \frac{\tau_{Net}(L-x)}{t_{ply}} \quad (2.23)$$

where  $\tau_{Net} = \tau_{interface} - \tau_{interply}$ , with  $\tau_{interface}$  being the shear stress between the first and the second ply. The other parameters can be seen in Figure 2.25.

The interested reader is referred to the original reference for better understanding about the analytical model proposed. As will be investigated in Chapter 4, the interaction between the laminates and the compatibility layer is found to be very important due to the no-slip conditions that occur in practice.

# 3

## INFLUENCE OF THE THERMAL GRADIENT

**A**UTOMATING the computational analysis of laminates manufactured by the thermoforming process (Falcon production line) is achieved by creating parametric finite element models for the thermal and mechanical interactions that the laminates undergo. The codes for the simulations of this Chapter are provided in Appendix A.

In this chapter, the focus is solely on the thermal analysis and corresponding influence on laminate warpage, in an attempt to isolate different effects. The chapter starts with section 3.1 defining the various material properties required for these simulations, section 3.2.1 presents the the different consolidation cycles to be simulated via a commercial finite element software (Abaqus), section 3.2.2 includes experimental results of warpage that can be used to establish a baseline comparison with the predictions, and section 3.3 concerns the predictions of warpage by finite element analysis.

### 3.1. MATERIAL PROPERTIES

The composite laminates are pressed under high temperature. In a first stage, understanding the influence of the heat transfer process without considering mechanical deformation provides important information on whether the laminates experience a significant temperature gradient through their thickness which would cause warpage. The essential parameters for these simulations are the **thermal conductivity** of the constituents and the **thermal conductance** (GAPCON). The latter explains how the thermal energy is conducted between materials that are in contact [49]. Contact between two materials or systems is not ideal, instead there are microgaps of air called asperities that lower the thermal conductivity (or equivalently, the thermal conductance, which is the thermal conductivity per unit thickness multiplied by the contact area). High thermal conductance indicates quick transfer of the thermal energy from one material to the other, which implies that more "surface points" are in contact. Simulations and experiments from many authors have been conducted to establish qualitatively the thermal conductance [50].

Table 3.1: Carbon Fibers: Type AS4 (High strength) [4]

Parameters	Values
Longitudinal Young's Modulus $E_{f1}$ (GPa)	230
Transverse Young's Modulus $E_{f2}$ (GPa)	15
Poison Ratio	0.2
Flexural Modulus $G_{12f}$ (GPa)	27
Linear Thermal Expansion coefficient (longitudinal) $a_{1f}$ ( $\frac{1}{K}$ )	$-0.5 \times 10^{-6}$
Linear Thermal Expansion coefficient (transverse) $a_{2f}$ ( $\frac{1}{K}$ )	$15 \times 10^{-6}$

Table 3.2: Sabic's Polycarbonate: Type ALS01 (medium-low flow rate) [8]

Parameters	Values
Young's Modulus $E$ (GPa)	2.35
Poison Ratio	0.37
Flexural Modulus $G_m$ (GPa)	2.3
Linear Thermal Expansion coefficient $a_m$ ( $\frac{1}{K}$ )	$70 \times 10^{-6}$
Thermal Conductivity $k_m$ ( $\frac{W}{mK}$ )	0.2

Due to practical constraints and confidentiality issues, determining the properties of the specific composite laminates of interest is not possible. Instead, this thesis focuses on automating the simulation process and the input material properties were estimated with appropriate literature, as referenced throughout [51–59]. Unquestionably, not measuring the properties directly invalidates a rigorous validation of the simulations since there is significant scatter in the literature for the different properties. Table 3.1 provides the properties of AS4 carbon fibers (high strength fibers) obtained by Isaac et. al [4], while Table 3.2 includes the properties for polycarbonate ALS01 provided by **Sabic** [8]. Moreover, due to the lack of some important properties, articles were used to fill the missing values (from the main references provided above).

### 3.1.1. COMPOSITE PROPERTIES

Composite's **Density** is calculated by the rule of mixtures assuming a fiber volume fraction of  $V_f = 55\%$ :

$$\rho_{composite} = \rho_{matrix} V_m + \rho_{fibers} V_f = 1390 \left( \frac{kg}{m^3} \right) \quad (3.1)$$

The composite elastic properties are estimated from elementary micromechanical models thoroughly explained in appropriate textbooks, e.g. [4]. More accurate models can be considered, without loss of generality of the automated finite element analysis. Con-

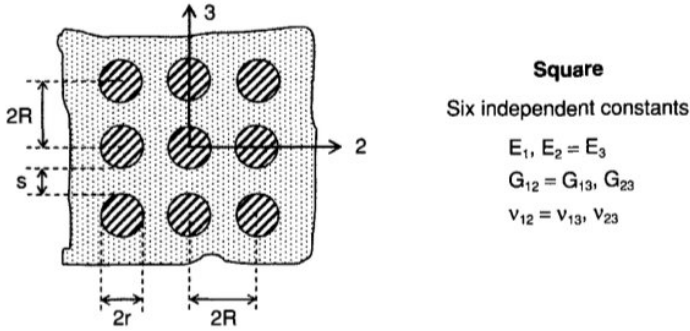


Figure 3.1: Square Properties of a composite laminate [4].

Considering the laminate transversely isotropic, which means that there are 6 independent elastic constants as shown in Figure 3.1, the elementary micromechanical models predict the following properties [4, 60, 61]:

$$E_1 = V_f E_f + V_m E_m \quad (3.2)$$

$$E_2 = E_3 = \frac{E_{2f}}{V_f + V_m \frac{E_{2f}}{E_m}} = \frac{E_{2f} E_m}{V_f E_m' + E_{2f} V_m} \quad (3.3)$$

$$G_{12} = G_{13} = \frac{1}{\frac{V_f}{G_{12f}} + \frac{V_m}{G_m}} = \frac{G_{12f} G_m}{V_f G_m + V_m G_{12f}} \quad (3.4)$$

$$G_{23} = \frac{E_f}{2(1 + \mu_{23})} \quad (3.5)$$

$$\mu_{12} = V_f \mu_{12f} + V_m \mu_m \quad (3.6)$$

$$\mu_{23} = 1 - \mu_{21} - \frac{E_2}{3K} = 1 - \frac{E_2}{2K} - 2\mu_{12}^2 \frac{E_2}{E_1} \quad (3.7)$$

where  $V_f$  and  $V_m$  are the fiber and matrix volume fractions, respectively,  $G_{12f} = \frac{E_f}{2(1+\mu_f)}$ ,  $G_m = \frac{E_m}{2(1+\mu_m)}$ ,  $\mu_{21} = \frac{E_2}{E_1} \mu_{12}$  and  $K = (\frac{V_f}{K_f} + \frac{V_m}{K_m})^{-1}$  which  $K$  being the bulk modulus. The numbering of 1,2 and 3 correspond to the local ply coordinates (1 is the fiber orientation and 2,3 are the transverse directions for a Unidirectional laminate).

Note that the elastic properties of the material are strongly dependent on temperature. As previously discussed (Figure 2.17), the elastic modulus of polycarbonate decreases with the increase of temperature, especially above its glass transition temperature  $T_g = 150^\circ C$ .

Table 3.3: Composite's elastic properties as a function of temperature (GPa)

T (°C)	$E_{11}$	$E_{22}$	$E_{33}$	$G_{12}$	$G_{13}$	$G_{23}$	$\mu_{12}$	$\mu_{13}$	$\mu_{23}$
20	130.47	4.95	4.95	4.62	4.62	1.65	0.276	0.276	0.51
70	130.34	4.51	4.51	4.40	4.40	1.48	0.276	0.276	0.52
120	130.24	4.15	4.15	4.00	4.00	1.36	0.276	0.276	0.53
170	129.90	2.88	2.88	2.50	2.50	0.92	0.276	0.276	0.55
210	129.51	1.23	1.23	0.3	0.3	0.1	0.276	0.276	0.58

According to references [41, 62, 63], and from the previously discussed micromechanical predictions, the composite elastic properties as a function of temperature are calculated and shown in Table 3.3. In these predictions, the properties of the carbon fibers are considered temperature independent.

The composite thermal properties are predicted according to models proposed in [52, 54]. The **coefficients of thermal expansion CTE** and **Specific Heat** are estimated as,

$$a_{11} = \frac{E_f a_f V_f + E_m a_m V_m}{E_f V_f + E_m V_m} \quad (3.8)$$

$$a_{22} = a_{33} = a_{2f} V_f (1 + \mu_{12f} \frac{a_{1f}}{a_{2f}}) + a_m V_m (1 + \mu_m) - (\mu_{12f} V_f + \mu_m V_m) a_{11} \quad (3.9)$$

leading to the values in Table 3.4 based on the constituent properties in [4, 8, 54, 64]). When the material undergoes phase transformations, the specific heat exhibits a peak due to the heat absorption or extraction (so, the experimental points need to be refined around that region).

**Thermal conductivity** in the longitudinal and transverse directions is also estimated according to elementary micromechanical models,

$$k_{11} = V_m k_m + V_f k_f \quad (3.10)$$

$$\frac{1}{k_{22}} = \frac{1}{k_{33}} = \frac{V_m}{k_m} + \frac{V_f}{k_f} \quad (3.11)$$

from which the estimated values are summarized in Table 3.5.

### 3.1.2. TOOL PROPERTIES

The steel plates that were used for the simulations are stainless steels type 304 (Table 3.6).

Table 3.4: Composite's Volume Thermal Expansion and Specific Heat

T ( $^{\circ}\text{C}$ )	$a_{11}(\frac{\mu\text{m}}{\text{mK}})$	$a_{22}(\frac{\mu\text{m}}{\text{mK}})$	$a_{33}(\frac{\mu\text{m}}{\text{mK}})$	$C(\frac{\text{J}}{\text{kgK}})$
20	0.4	39	39	919
70	0.42	40	40	938.4
120	0.39	41	41	996.7
170	0.36	41.5	41.5	1035.5
210	0.33	42	42	1105

Table 3.5: Composite's Thermal Conductivity

T ( $^{\circ}\text{C}$ )	$k_{11}(\frac{\text{W}}{\text{mK}})$	$k_{22}(\frac{\text{W}}{\text{mK}})$	$k_{33}(\frac{\text{W}}{\text{mK}})$
20	20	1.2	1.2
70	21	1.5	1.5
120	22	2	2
170	24	2.5	2.5
210	25	3	3

Table 3.6: Stainless Steel Properties

Parameters	Values
Young's Modulus (GPa)	200
Poison Ratio	0.28
Yield Strength (MPa)	215
Thermal Conductivity ( $\frac{\text{W}}{\text{mK}}$ )	16.2
Volume Thermal Expansion ( $\frac{\mu\text{m}}{\text{mK}}$ )	17.55
Density ( $\frac{\text{kg}}{\text{m}^3}$ )	8000

Table 3.7: Compatibility layer sheet Properties for the computational work [65]

Parameters	Values
Young's Modulus ( <i>GPa</i> )	2
Poison Ratio	0.4
Yield Strength ( <i>MPa</i> )	30
Thermal Conductivity ( $\frac{W}{mK}$ )	0.25
Volume Thermal Expansion ( $\frac{\mu m}{mK}$ )	120
Density ( $\frac{kg}{m^3}$ )	2200

The bottom part of the laminate is in contact with a compatibility layer for which the properties could only be estimated roughly due to confidentiality issues. Table 3.7 summarizes the properties of the material [65]. The main reference for obtaining these properties is [65], and the material was assumed to be isotropic. In Chapter 4, this additional sheet is considered orthotropic (a composite) due to its influence on the mechanical deformation.

## 3.2. HEAT TRANSFER ANALYSIS MODULE

Before any experimental result was available, the heat transfer analysis were conducted to provide a qualitative assessment on whether thermal gradients could be responsible for the warpage of the composite laminate. Subsection 3.2.1 details how these simulations were defined, while subsection 3.2.2 presents experimental results (subsequent to the simulations).

### 3.2.1. HEAT TRANSFER SIMULATIONS

When compared to the material properties discussed in the previous section, the thermal conductance is particularly challenging to estimate, as this property changes not only with the applied pressure and temperature but it is also dependent on the different material interfaces that are in contact. For the process and materials under analysis, typical values can range from 500 to more than 3000  $JT^{-1}L^{-2}\Theta^{-1}$  (typically thermal conductance is a measure in Watts per Kelvin) [66, 67]. Recall that the process under analysis involves different material interfaces that have different thermal conductance.

Nevertheless, since the finite element simulations are parameterized (Appendix A), analyzing the thermoforming process assuming different thermal conductance values between different materials is straightforward. A commercial finite element software is used (Abaqus), and transient **heat Transfer** analysis are conducted to obtain the temperature profiles considering convection and conduction.

For these simulations, two stainless steel 304 plates, a compatibility layer sheet and the composite laminate are considered, as seen in Figure 3.2 and Figure 3.3. A complete simulations involves 6 heat transfer steps, three heating cycles and each of them followed by a cooling cycle as the material is transferred from one press to another (confront with



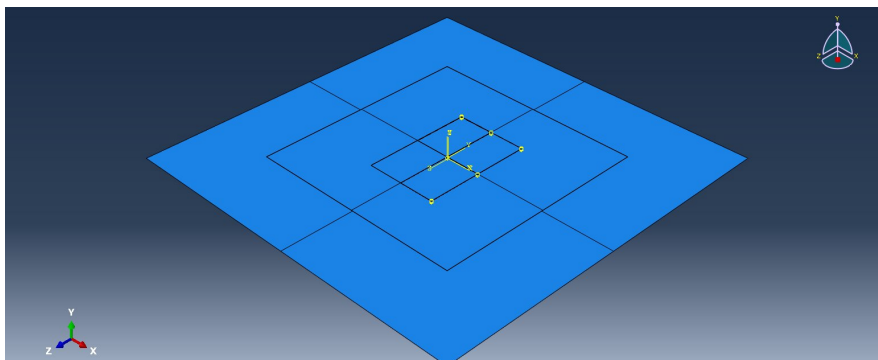


Figure 3.2: Assembly on Abaqus CAE

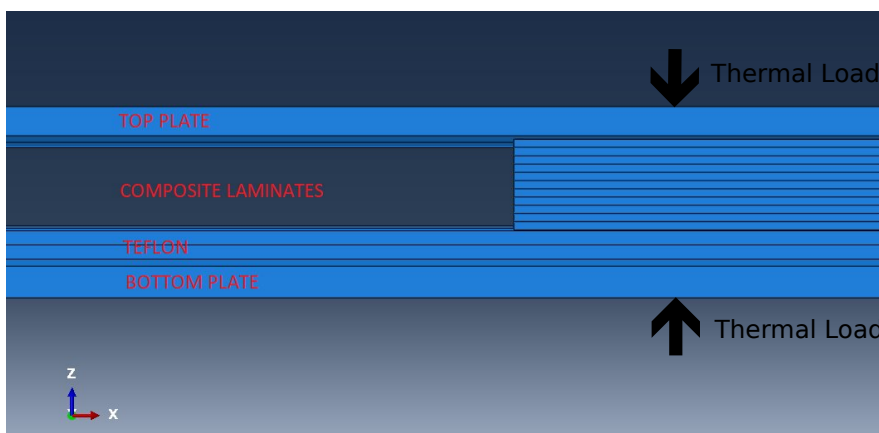


Figure 3.3: Structure layup of the Assembly

Figure 1.1). The cooling mechanism was assumed to be *Natural Convection*, which is applied on the top and bottom of the stainless steel's faces with a value of  $7 \frac{W}{m^2K}$ , given past experience with the process.

Thermal conductance (GAPCON) is assumed to be higher at interfaces between stainless steel and each polymer composite (steel with compatibility layer sheet composite, or steel with composite laminate) when compared to the value between the two composites (compatibility layer sheet and laminate). This assumption follows from the smoothness and higher thermal conductivity of the steel plates compared to the compatibility layer sheet and the Laminate. Also in the literature, compatibility layer sheet and PC have GAPCON values in the range of  $370\text{-}1300 \text{ JT}^{-1}\text{L}^{-2}\Theta^{-1}$  depending of the applied temperature, pressure and the materials that they are in contact with. For the stainless steel, it is on the range of  $1000\text{-}2500 \text{ JT}^{-1}\text{L}^{-2}\Theta^{-1}$  [66–68].

Each simulation of the complete process using different GAPCON values leads to different predictions of the temperature profile that can be assessed at different locations of the laminate. Figures 3.4 and 3.5 assumed  $GAPCON_{T-C} = 500 \text{ JT}^{-1}\text{L}^{-2}\Theta^{-1}$ , i.e. the thermal

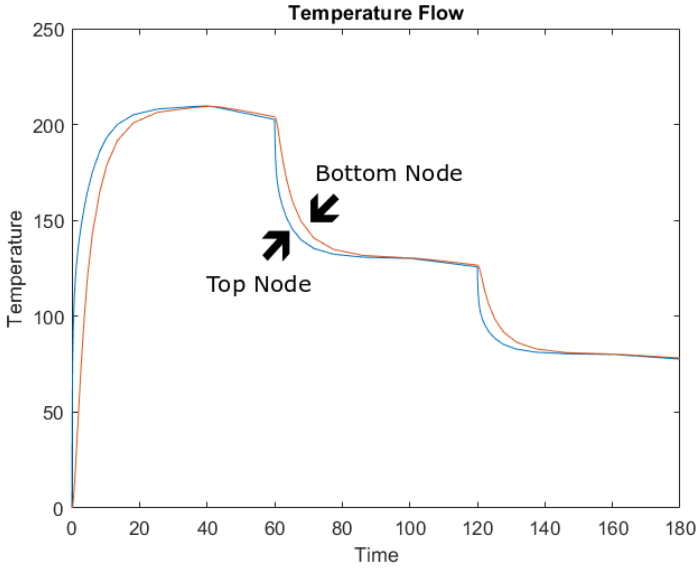


Figure 3.4: Temperature vs Time from the top and the bottom node of the laminate for  $GAPCON_{T-C} = 500$  and  $GAPCON_{SS-T-C} = 1500$

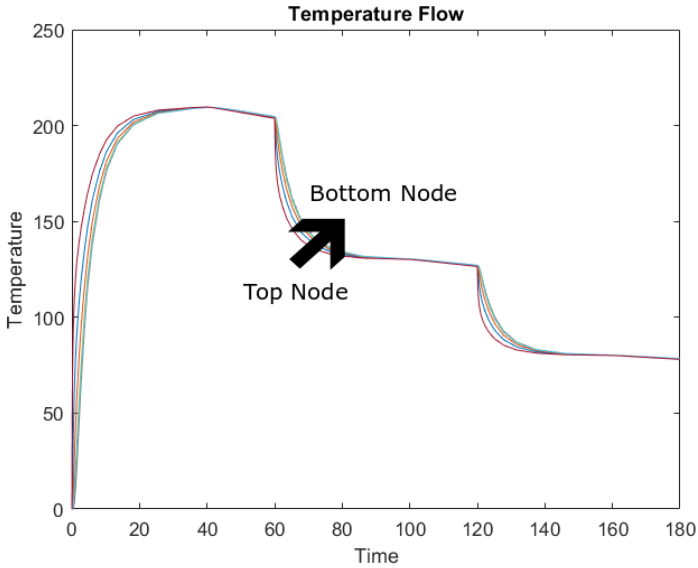


Figure 3.5: Temperature vs Time, nodes through all the laminate's thickness for  $GAPCON_{T-C} = 500$  and  $GAPCON_{SS-T-C} = 1500$

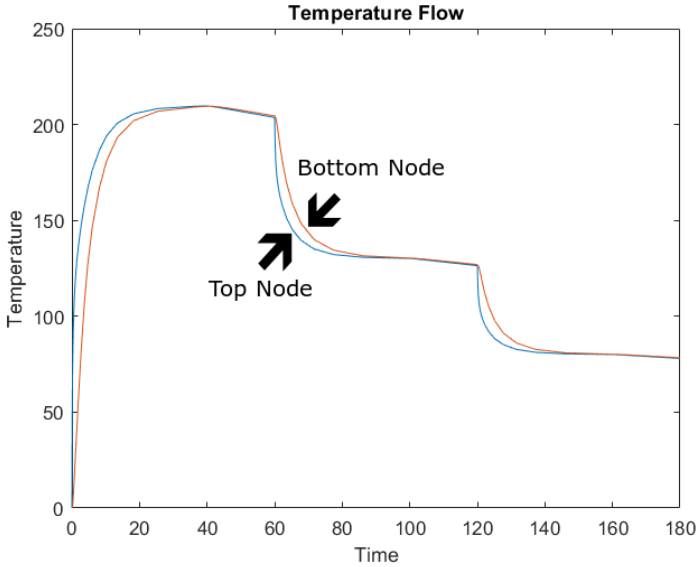


Figure 3.6: Temperature vs Time for  $GAPCON_{T-C} = 1000$  and  $GAPCON_{SS-T-C} = 1500$

conductance between the compatibility layer sheet and the Laminate is  $500JT^{-1}L^{-2}\Theta^{-1}$ , and  $GAPCON_{SS-T-C} = 1500JT^{-1}L^{-2}\Theta^{-1}$  as the thermal conductance between the stainless steel plates with the compatibility layer sheet and with the Laminate (assumption that due to their polymeric nature, they have the same GAPCON with the stainless steel sides). Figure 3.4 shows the temperature values as the laminate goes through the cycles, where the blue line corresponds to the temperature at the top surface of the laminate (the assigned node is the one at the very top of the laminate which is in contact with the top plate), and the orange line is the first node of the laminate from the bottom, showing how the temperature changes from the compatibility layer sheet side. Figure 3.5 shows similar information, but including more nodes through the thickness of the laminate (a node is assigned from every two plies).

For illustrative purposes, two other simulations are shown where the influence of different thermal conductance values on the temperature profile can be seen. Figure 3.6 presents the heat flow for a different thermal conductance between the compatibility layer sheet composite sheet and the composite laminate  $GAPCON_{T-C} = 1000JT^{-1}L^{-2}\Theta^{-1}$  while maintaining  $GAPCON_{SS-T-C} = 1500JT^{-1}L^{-2}\Theta^{-1}$ . Figure 3.7 shows the heat flow for  $GAPCON_{T-C} = 500JT^{-1}L^{-2}\Theta^{-1}$  while considering different  $GAPCON_{SS-T-C} = 2000JT^{-1}L^{-2}\Theta^{-1}$ . These figures illustrate how the thermal conductance delays the heating and cooling of the laminate, especially when the material is close to its glass transition temperature (recall that PC's  $T_g \approx 150^\circ C$ ). From Figure 3.4, the top surface cooled down from its  $T_g$  in 63 seconds, but the bottom one only achieves the same temperature after 67 sec. The other two figures show similar heating and cooling times (62-63 sec for the top surface and 67-68 for the bottom). Therefore, the lack of precise values for the thermal conductance does not seem to be a significant issue.

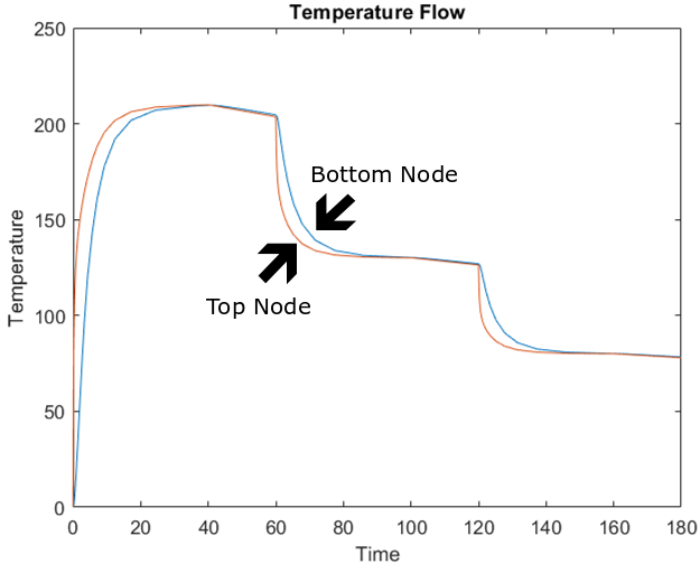


Figure 3.7: Temperature vs Time for  $GAPCON_{T-C} = 500$  and  $GAPCON_{SS-T-C} = 2000$

### 3.2.2. HEAT TRANSFER EXPERIMENTS

The qualitative computational investigation pointed towards an asymmetric temperature profile of the laminate, especially around the glass transition temperature. Therefore, an experimental investigation is conducted to determine the temperature at the top and bottom of the laminate during the thermoforming process. The laminates before and after the process are shown in Figure 3.8.

In order to measure temperatures during the process, thermocouples are placed in various locations through the laminate's thickness. Figure 3.9 shows a Temperature vs Time measurement, where the 2 thermocouples are on the top surface of the laminate (between the last laminate ply and the top stainless steel plate) and one at the bottom (between the last laminate ply and the compatibility layer). Figure 3.10 shows result for two thermocouples at other positions through the thickness of the laminate (one between ply 3 and ply 4, and one between ply 8 and 9). Figure 3.11 is similar to Figure 3.9, but where the process is conducted at lower pressure configurations.

Warpage of twelve laminates are analyzed after going through the manufacturing process. Nine laminates with the following stacking sequence  $[0_2/90/0/90_2]_s$ , and three consisting with a similar stacking sequence but only 7 plies with stacking sequence  $[0_2/90/0]_s$ . The warpage measurements were manually conducted by measuring the height for each edge (displacement in the out-of-plane dimension; z-axis). The measurements include an offset of 1.4 – 1.5 mm due to the thickness of the laminates. Only 3 out of 4 laminates that were extracted from each run were used for measurement due to fracture conditions of one of the laminates caused by the presence of the thermocouples (can be seen from Figure 3.8). Tables 3.8, 3.9, 3.10 and 3.11 summarize the measurements.

The Temperature vs Time figures demonstrate that there is negligible temperature differ-

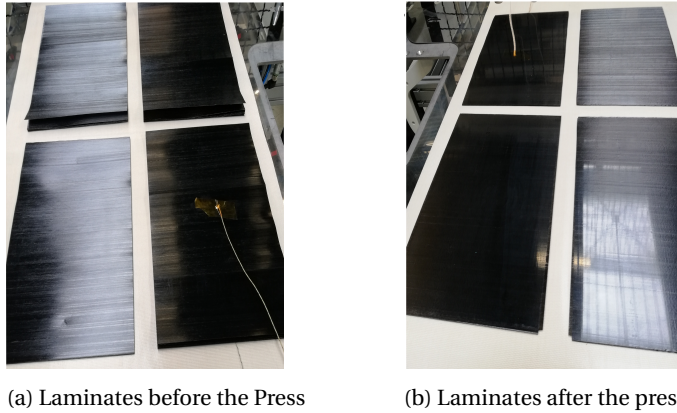


Figure 3.8: Airborne configuration of Laminates

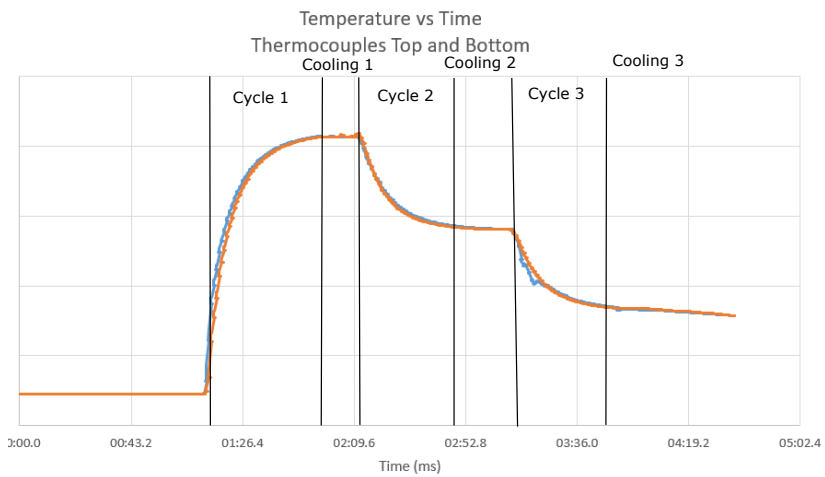


Figure 3.9: Temperature vs time obtained from thermocouples at the top and the bottom of the laminate (laminate has 11 plies).

Table 3.8: First Run with High applied Pressure and 11 plies

First Run	Edge 1	Edge 2	Edge 3	Edge 4
Laminate 1 (mm)	1.6	1.05	0.6	1.3
Laminate 2 (mm)	1.7	0.25	1.25	0.55
Laminate 3 (mm)	1.1	1.2	0.4	1

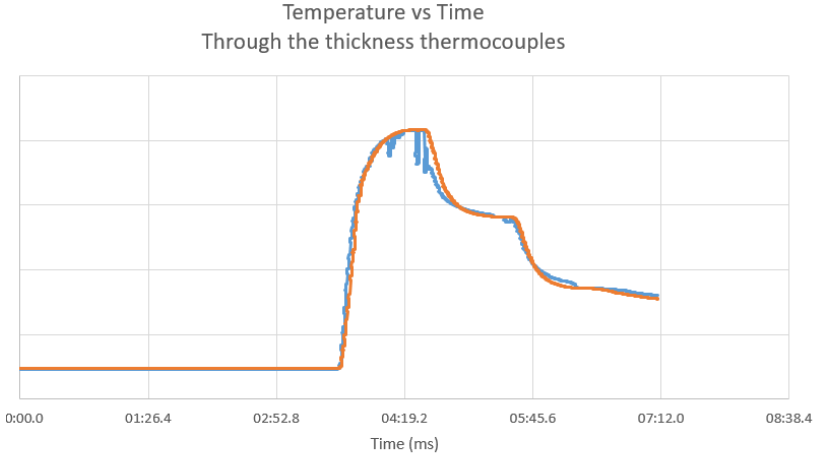


Figure 3.10: Temperature vs time obtained from thermocouples within the laminate (plies 3 and 4, and between 8 and 9).

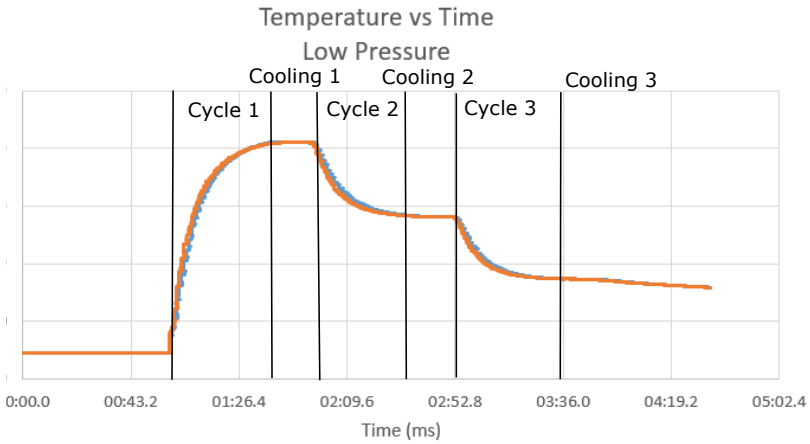


Figure 3.11: Temperature vs time obtained from thermocouples at the top and bottom of the laminate, but using lower pressure.

Table 3.9: Second Run with High applied Pressure and 11 plies

Second Run	Edge 1	Edge 2	Edge 3	Edge 4
Laminate 1 (mm)	1.9	1.7	0.9	1
Laminate 2 (mm)	0.8	1.5	0.7	1
Laminate 3 (mm)	0.9	0.5	1.6	1.4

Table 3.10: Third Run with High applied Pressure and 11 plies

Third Run	Edge 1	Edge 2	Edge 3	Edge 4
Laminate 1 (mm)	1.55	2.1	1.5	1.7
Laminate 2 (mm)	1.65	2	1.2	1.5
Laminate 3 (mm)	1.4	1.4	1.3	0.6

Table 3.11: Fourth Run with High applied Pressure and 7 plies

Fourth Run	Edge 1	Edge 2	Edge 3	Edge 4
Laminate 1 (mm)	0.9	0.85	0.3	0.4
Laminate 2 (mm)	0.2	0.3	0.3	0.2
Laminate 3 (mm)	0.2	0.3	0.5	0.5

ence between the top and bottom of the laminates, i.e. there is no significant temperature gradient. In addition, the temperature is stable for several seconds before each pressing cycle (cooling stages of approximately 40 seconds). In some cases, one of the thermocouples showed some measurement errors (fluctuations in Figure 3.10), but the results are consistent through different measurements. Therefore, the presence of a temperature gradient and the subsequent asymmetric buildup of residual stresses is ruled out as the source of warpage. This is explained by the small thickness of the laminates and the compatibility layer sheet. However, Tables 3.8, 3.9, 3.10 and 3.11 also clearly show that the laminates are warped. Therefore, the probable cause for this phenomenon remains unclear at this point (motivating the subsequent investigations of this thesis).

### 3.2.3. CONCLUSIONS FROM HEAT TRANSFER ANALYSIS

The heat transfer simulations demonstrate that there is a negligible thermal gradient occurring due to the presence of the composite compatibility layer sheet at the bottom of the laminate during the thermoforming process. This conclusion is merely qualitative, as a good estimation of material properties was not possible. However, an experimental verification led to the same conclusion (even less temperature difference is observed).

Figures 3.12 and 3.13 show finite element predictions when the composite compatibility layer sheet is present or not during the manufacturing process, in order to highlight the small thermal asymmetry induced by the composite compatibility layer sheet. If this difference was larger, the top part of the laminate would solidify faster than the bottom which would lead to residual stresses that cause undesirable deformation.

Therefore, the laminate warpage that is observed experimentally cannot be explained by the heat transfer process. Instead, the focus should be on the mechanical deformation and the tool-part interactions. Yet, before analyzing the mechanical deformation, the next section 3.3 includes Coupled Temperature Displacement simulations to illustrate the effect of the small temperature differences when the laminate temperature is around the glass transition temperature.

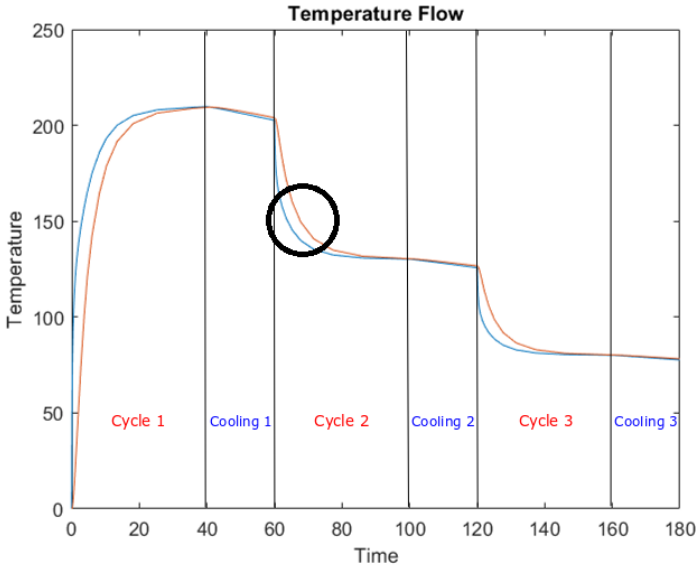


Figure 3.12: Temperature gradient with the use of compatibility layer sheet

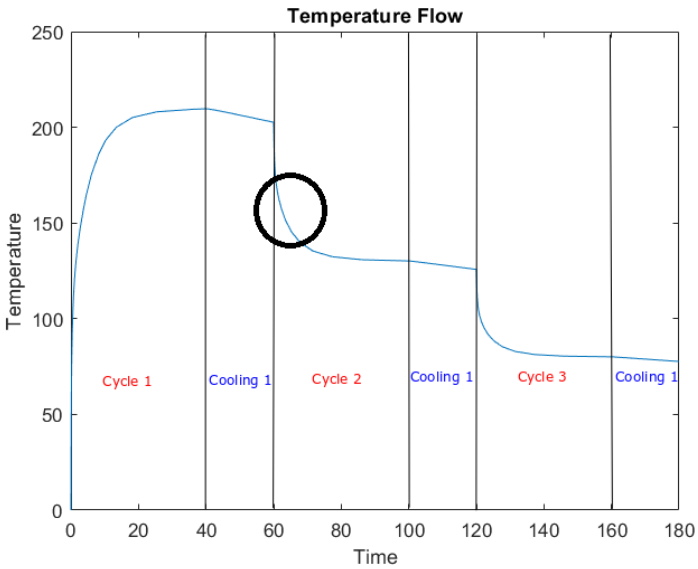


Figure 3.13: Temperature gradient without the use of compatibility layer sheet



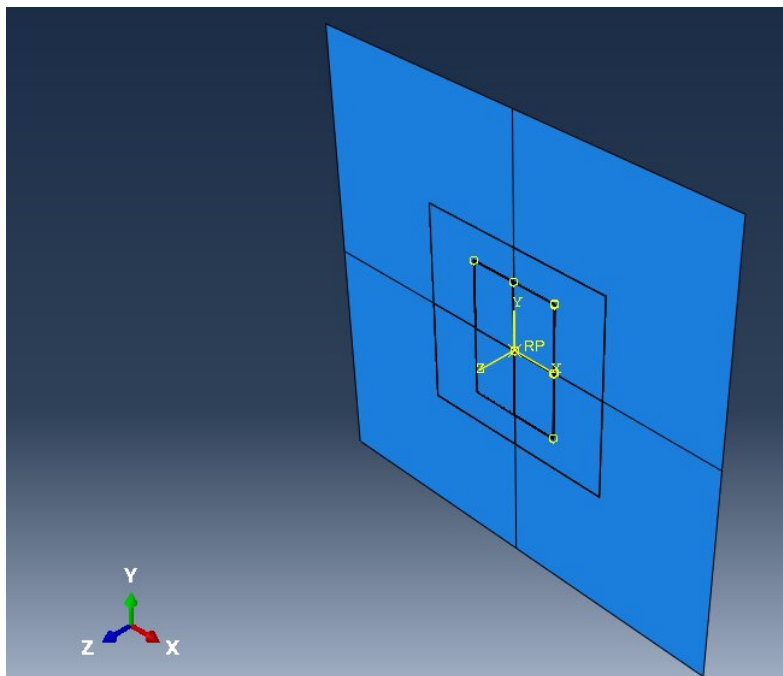


Figure 3.14: Assembly for Coupled Temperature-Displacement simulation

### 3.3. COUPLED TEMPERATURE-DISPLACEMENT SIMULATIONS

The temperature difference in the beginning of cycle 2 occurs during the glass transition, where the material goes from rubbery to glassy. At this stage, the material closer to the top would become more rigid and constrain the bottom material, introducing residual stresses. Considering coupled temperature-displacement simulations it is possible to assess what is the distortion caused at the moment when the temperature difference is highest. The top steel plate is omitted in order to let the laminate deform freely. Figure 3.14 shows the setup assembly, and the simulation steps are summarized as follows:

1. The simulations lasts for 20-60 sec (several tries to observe the difference).
2. Surface interactions between the materials are considered, where the tangential and normal behavior is specified, as well as the Thermal conductance (Table 3.12). The values for the tangential behavior are estimated from the literature [69]. The friction between compatibility layer sheet and steel is small compared to the friction between compatibility layer sheet and laminate. For the latter, no-slippage condition is considered [69].
3. The boundary conditions of the problem include a fixed bottom steel plate and a fixed node at the top surface of the laminate (to hold the material in place during deformation).
4. From the heat transfer simulation it is possible to pre-define a temperature profile at the time the material transitioned from a rubbery to solid form, defined here

Table 3.12: Interaction properties

	SS to compatibility layer sheet	compatibility layer sheet to Lamina
Tangential Behaviour (Penalty)	0.04	0.4
Normal Behaviour	Hard contact	Hard contact
GAPCON	1500	500

as the time when the top layers reach a percentage of the glass transition temperature. Looking at figure 3.12 and with the well-said assumption that  $T_g \approx 150^\circ C$ , the time the top ply is reaching  $T_g$  is different than the bottom ply. This can be illustrated with the circle at figure 3.12, where there is a delay from the bottom side. This specific moment is captured in Abaqus, which represent the temperature gradient. This temperature gradient is super-imposed as the initial condition/state of the compatibility layer sheet and laminate.

5. Surface Convection at the top surface of the laminate and at the bottom of the composite compatibility layer sheet's surface is considered, in order to cool the materials.
6. Meshing of the 2 materials (rigid plates cannot be meshed) with 8-node thermally coupled brick elements (C3D8T elements in Abaqus, suitable for thermo-mechanical analysis).

The Tangential behavior [69] was implemented by a Penalty method that approximates contact without introducing Lagrange multipliers (that can lead to convergence issues [70]). The Normal behavior was used as a Hard contact, which does not let any nodes penetrate the surface. Moreover, Thermal conductance was used with the same values as in the Heat Transfer module.

For comparison, simulations with homogeneous temperature profile as a predefined step were also conducted. Figures 3.15 and 3.16 illustrates the pre and post analysis when an initial thermal gradient is applied.

Unsurprisingly, the temperature gradient would cause warpage of the laminate. Since the central node of the top surface is fixed, all four edges warp outwards with similar values, approximately around 0.9 to 1.2 mm depending the step time, where for 60 seconds, maximum warpage was observed. After that (if the step is bigger than 60 seconds), the material tend to return to its original non-deformed shape due to its elastic nature. Evidently, if there is no temperature gradient, then there is no warpage of the composite laminate – see Figure 3.17.

Note that these simulations are significant simplifications of reality, but they illustrate how the temperature gradient can lead to warpage by creating local stress imbalances at the time when the plies are becoming glassy. However, these simulations do not include viscoelastic effects, neither phase transformations, nor mechanical loads. There-

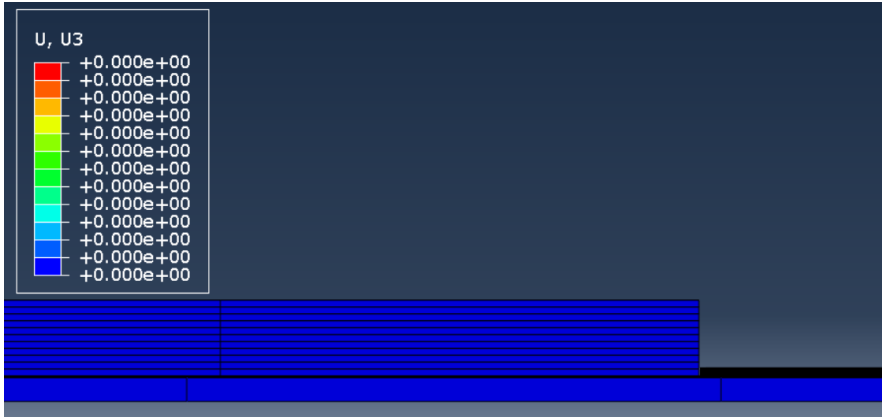


Figure 3.15: Pre-analysis

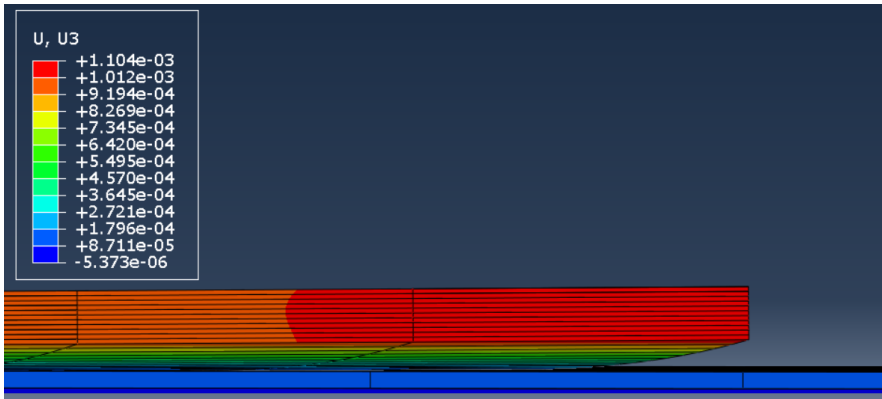


Figure 3.16: Post-analysis with temperature initial gradient

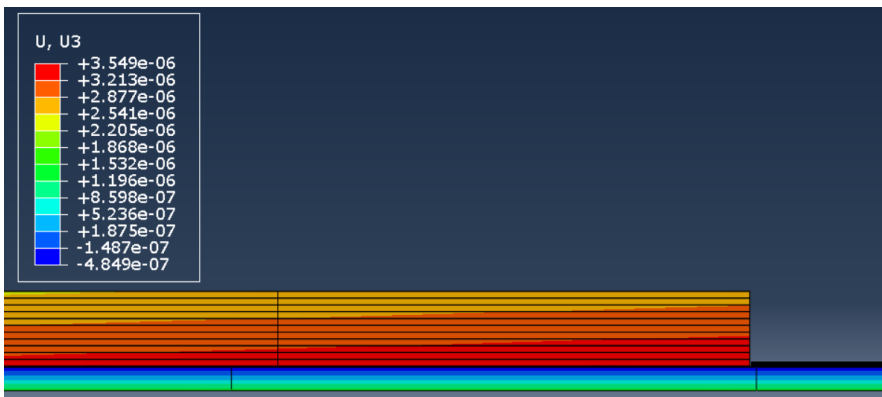


Figure 3.17: Post-analysis with uniform temperature initial profile

fore, these simulations just provide a preliminary estimation about the influence of temperature gradients through the thickness on the warpage of the laminate. Nevertheless, as repeatedly mentioned, this effect is concluded to be small in practice, excluding heat transfer effects as the main cause for warpage.

# 4

## TOOL-PART INTERACTION

**H**EAT transfer analyses and temperature profile measurements have demonstrated that temperature gradients are unlikely to be the cause of significant laminate warpage in the practical thermoforming process under analysis (Chapter 3).

For reminder, placing a tool in one side will introduce several effects:

1. Different heating and also cooling rate comparing both sides that it will introduce a significant Temperature Gradient (Chapter 3).
2. Different friction coefficients between both sides that it will introduce constraints and eventually a stress gradient profile.
3. Introduction of imperfections and fiber misalignment due to the interaction of the laminate with the tool and most important,
4. The compatibility layer will expand due to its higher thermal expansion coefficient, letting the bottom layers expand with it.

Therefore, this Chapter focuses on the mechanical tool-part interaction and its possible effect on warpage. Similarly to the previous Chapter, the main goal is to automate the analysis process by creating parametric finite element models that can be used for future design and analysis tasks. The reason of that is due to the several input properties of the laminates, compatibility layer (compatibility layer sheet for the simulations) and also the system's configurations that can influence the stress development. The codes for the simulations of this Chapter are provided in Appendix B.

As discussed in Chapter 2 and illustrated in Figure 2.12, in general if the part being formed is subjected to pressure on the top surface and there is a tool at the bottom surface that constrains deformation, when the part cools down it can lock the induced stress state which has a through the thickness gradient. This creates asymmetrical residual stresses that lead to warpage.

The process under analysis has two similar press plates at the top and bottom of the laminate, but there is an additional composite compatibility layer sheet placed in be-

tween the bottom press plate and the laminate which can potentially introduce a similar effect because there are different friction coefficients between the different surfaces, and the composite compatibility layer sheet has a higher coefficient of thermal expansion (CTE) compared to the laminate. In addition, warpage could also be caused by manufacturing or microstructural imperfections such as fiber misalignment.

Section 4.1 details the parametric simulations for the tool-part interaction predictions, while Section 4.2 includes additional experiments of the manufacturing process conducted at different pressure cycles to assess the influence of the mechanical load in warpage.

#### 4.1. TOOL-PART FINITE ELEMENT ANALYSES

As discussed in Chapters 2 and 3, most residual stresses in the laminate are arrested when the material stiffness steeply increases after the part is cooled below the glass transition temperature. In the process under analysis, this occurs at the second pressure cycle (see for example Figure 3.12). The first pressure cycle heats up both the laminate and the composite compatibility layer sheet to high temperatures where the laminate is in a viscous state but the sheet is not. In this cycle, the stress build-up at the laminate is expected to be negligible, but the deformation of the bottom layers is larger due to the higher thermal expansion of the sheet compared to the top press plate (metal). During cool down, the laminate transforms from a rubbery state into a solid state and higher stresses start to develop (Cycle 2), so capturing the stress gradient at this moment is expected to be of critical importance for predicting warpage.

The parametric finite element analyses undergo three steps to simulate Cycle 1, Cycle 2 and the warping effect. Each step enables to create appropriate Predefined fields for the subsequent step. Note that the laminate's geometry changes due to mechanical interactions between the laminate closer to the composite compatibility layer sheet but also between the plies themselves [5]. As discussed in Section 2.3.4 and shown in Figure 2.12, the bottom plies of the laminate "slide" as the tool expands (here, the composite compatibility layer sheet).

The 1<sup>st</sup> step (Cycle 1) is simulated with top and bottom stainless steel plates as Rigid surfaces and assuming frictionless interaction between the plate and the laminate and a very small friction with the composite compatibility layer sheet. Assuming rigid surfaces reduces the computational time and facilitates convergence. This finite element analysis is summarized as follows:

1. Laminate and composite compatibility layer sheet are modeled as 3D solids and the stainless steel plates as Rigid Surfaces.
2. Abaqus Implicit analyses are used, despite potential convergence issues arising from contact conditions, because larger time steps can be considered when compared to Explicit analyses. Nonetheless, convergence issues can occur for some of the automated simulations, depending on the input parameters chosen. It was noticed that by considering smaller simulation time when compared to the real time of the process, convergence of the simulations improved. A second difficulty when pre-processing these analyses pertains the contact heating condition. Rigid surfaces cannot transfer heat (by nature of Abaqus), so in this case, heating conditions are applied on the surfaces of the composite laminate and the compatibility layer sheet

Table 4.1: Interaction properties

	Compatibility layer sheet-BP	Composite-TP
Tangential Behaviour	0.04	Frictionless
Normal Behaviour	Hard contact	Hard contact
GAPCON	1500	1500

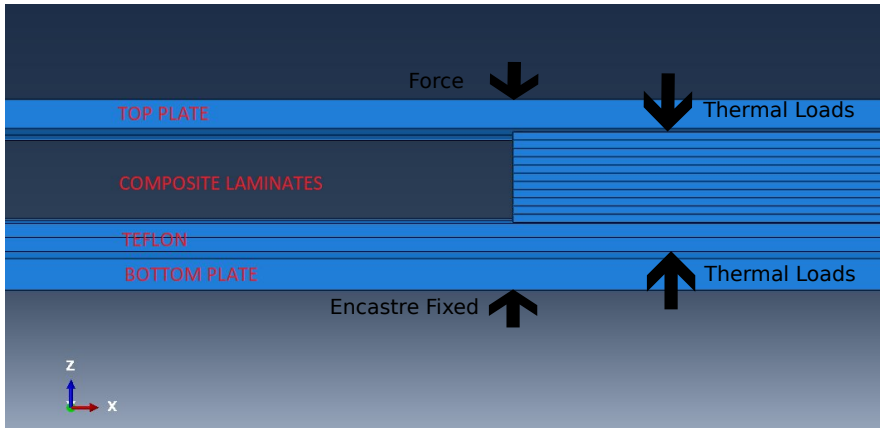


Figure 4.1: Structure layup of the Assembly

(so the heating is faster comparing to the heat transfer simulations from Chapter 3). When imposing the total simulation time, the main condition is to ensure that the material is heated well above its  $T_g$ . As in Chapter 3, **Coupled Temperature Displacement** simulations are considered, using thermo-mechanical finite elements to predict both the temperature distributions as well as the deformation of the laminate. Laminate and composite compatibility layer sheet are meshed with 8-node thermally coupled brick elements (C3D8T in Abaqus).

3. Contact interactions between the top plate and the laminate, and between the composite compatibility layer sheet and the bottom plate are imposed according to Table 4.1. For the interaction between the Laminate and the compatibility layer sheet a no-slip condition is considered (as if they are perfectly bonded, which corresponds to a Tie constraint in Abaqus). Viscous damping is assumed in the contact areas, in order to stabilize the model [71].
4. Boundary conditions are defined by a concentrated mechanical load at the top plate applied in a reference point of the rigid surface. The bottom plate is fixed. Temperature is applied on top of the Laminate's surface and on the bottom of compatibility layer sheet's surface. The analyses start with the Laminate and compatibility layer sheet at room temperature using a Predefined Temperature Field. Figure 4.1 shows the assembly of the complete model. The same simulation strategy is used for Cycle 2 but with different input conditions.

Once Cycle 1 is simulated, warpage can be predicted by removing the plates and applying

Table 4.2: Compatibility layer sheet Isotropic Properties

T ( $^{\circ}\text{C}$ )	E (GPa)	$\mu$	$a(\frac{\mu\text{m}}{\text{mK}})$	$k(\frac{\text{W}}{\text{mK}})$	$C(\frac{\text{J}}{\text{kgK}})$
20	2	0.4	120	0.25	970
70	2	0.4	125	0.27	980
120	1.9	0.4	150	0.3	1000
170	1.8	0.4	177	0.32	1100
210	1.78	0.4	200	0.33	1200

a stress gradient created at the end of Cycle 1 as an initial step for the whole assembly (same procedure as the warpage model for the heat transfer module, but this time with stress gradient rather than thermal). Moreover, the Tie condition was also replaced by a friction interaction, in order to let the laminate warp. The cooling simulation is an implicit static analyses where the only applied load in the structure is the stress gradient. The boundary conditions are defined by fixing the center node of the laminate's top surface and also the center node of the bottom surface of the composite compatibility layer sheet. This allows the material to deform according to the stress gradient, causing warpage due to its unbalanced profile. This step is only for comparison with the stress profile that is generated through Cycle 2.

Cycle 2 is simulated similarly to Cycle 1, but considering different input conditions. Following the work of Ghayoor [12], Cycle 2 starts with an undeformed part but defining two predefined fields (temperature and stress) according to the end of the analysis of Cycle 1. These predefined fields are superimposed in the structure and then the loads are applied according to the specified cycle conditions. Implementing Cycle 1 and Cycle 2 in the same simulation leads to convergence issues; therefore, this strategy is adopted instead. A different strategy was also attempted, where Cycle 2 starts with a deformed structure, but where the thermal loads were implemented differently (convection cooling instead of an assigned temperature), and similar predictions were obtained.

The computational analysis are conducted considering different materials as the bottom sheet in the process. This illustrates the influence of this added material in the process. Therefore, a composite compatibility layer sheet with properties outlined in Table 4.3 is used, as well as an isotropic sheet of pure compatibility layer sheet (Table 4.2). Note that the composite compatibility layer sheet is a cross-ply laminate with two layers (0 and 90 degrees).

#### 4.1.1. SIMULATION RESULTS

##### CYCLE 1

The choice of pure compatibility layer sheet (isotropic) or composite compatibility layer sheet should affect significantly the warpage of the composite laminate because the coefficients of thermal expansion are significantly higher for the pure polymer. Figure 4.2 shows the undeformed configuration of the analyses, while Figure 4.3 shows the deformed configuration at the end of Cycle 1 when using only pure compatibility layer sheet at the



Table 4.3: Compatibility layer sheet Composite Properties

T ( $^{\circ}C$ )	20	70	120	170	210
$E_{11}(GPa)$	20.37	20.20	20	19.8	19.1
$E_{22}(GPa)$	6.65	6.5	6.2	6	5.9
$E_{33}(GPa)$	6.65	6.5	6.2	6	5.9
$G_{12}(GPa)$	4.4	4.3	4	3.50	3.4
$G_{13}(GPa)$	4.4	4.3	4	3.50	3.4
$G_{23}(GPa)$	3	2.8	2.6	2.5	2.4
$\mu_{12}$	0.35	0.35	0.35	0.35	0.35
$\mu_{13}$	0.35	0.35	0.35	0.35	0.35
$\mu_{23}$	0.4	0.4	0.4	0.4	0.4
$a_{11}(\frac{\mu m}{mK})$	2.7	2.8	3	3.1	3
$a_{22}(\frac{\mu m}{mK})$	126	127	200	210	250
$a_{33}(\frac{\mu m}{mK})$	126	127	200	210	250
$C(\frac{J}{kgK})$	1000	1050	1100	1150	1200
$k_{11}(\frac{W}{mK})$	0.49	0.5	0.52	0.55	0.6
$k_{22}(\frac{W}{mK})$	0.31	0.32	0.33	0.35	0.4
$k_{33}(\frac{W}{mK})$	0.31	0.32	0.33	0.35	0.4

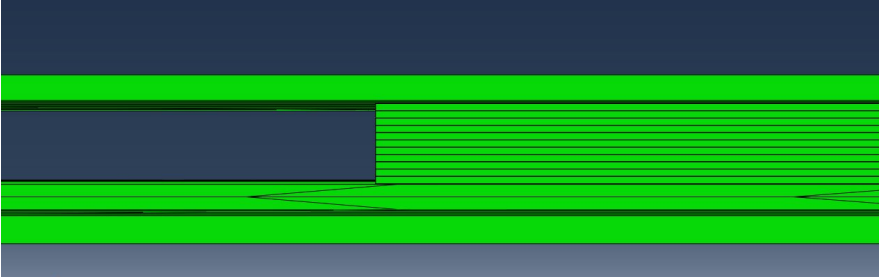


Figure 4.2: Undeformed configuration

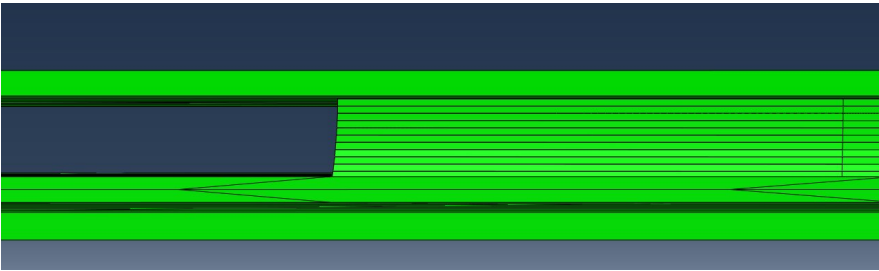


Figure 4.3: Deformed configuration with Isotropic compatibility layer sheet

bottom of the laminate. The deformation of the laminate is clearly visible, as compared with Figure 2.12. Figure 4.4 shows the deformed configuration when a composite compatibility layer sheet is used instead of the pure polymer. In this case, the deformation also exists but it is significantly less pronounced.

The displacement on the x-direction (sliding/dragging of the laminate due to the compatibility layer sheet expansion) is  $1.26\text{ mm}$  for the simulation with pure compatibility layer sheet and  $0.09\text{ mm}$  for the simulation with composite compatibility layer sheet. These values are indicative because, as discussed previously, the input material properties have not been accurately characterized. Figures 4.5 and 4.6 show the stresses along the fibers di-

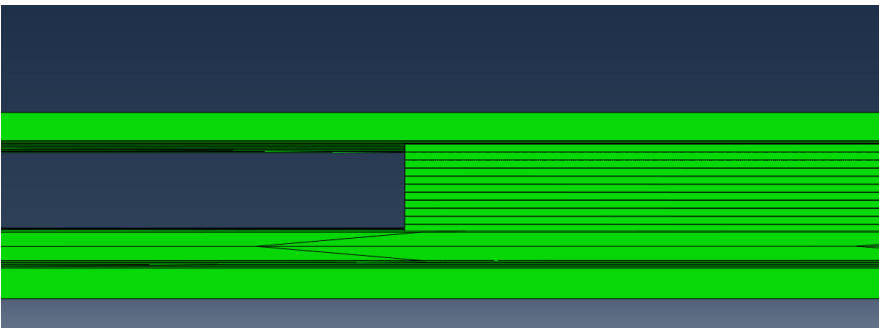


Figure 4.4: Deformed configuration with Composite compatibility layer sheet

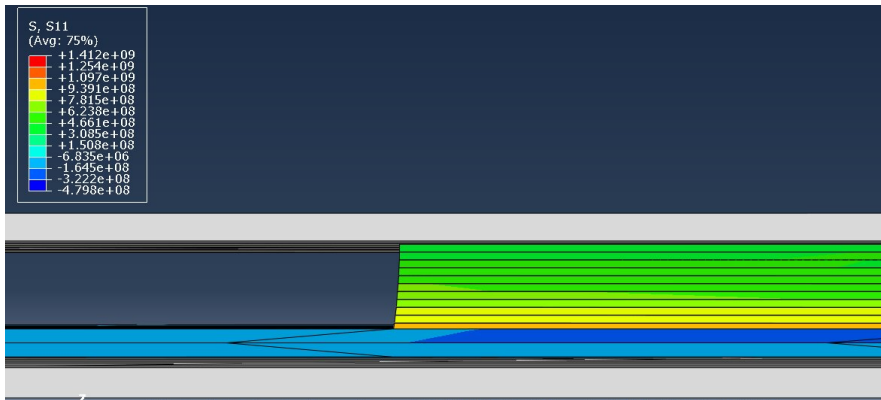


Figure 4.5: Stresses along the fibers direction ( $\sigma_{11} \equiv S11$ ) when using a compatibility layer sheet at the bottom.

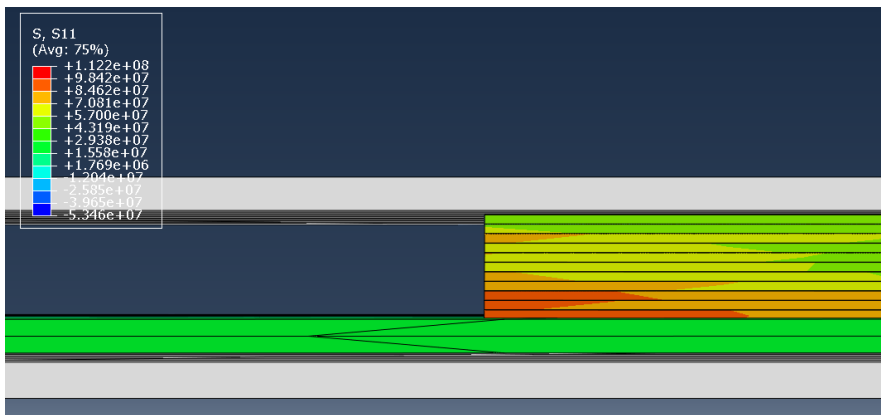


Figure 4.6: Stresses along the fibers direction ( $\sigma_{11} \equiv S11$ ) when using a composite compatibility layer sheet at the bottom.

rection through the thickness of the laminate when considering pure compatibility layer sheet or composite compatibility layer sheet. Note that showing the stresses along the fibers directions ( $\sigma_{11} \equiv S11$ ) can be misleading in the sense that  $0^\circ$  plies correspond to stresses along the horizontal (left to right) direction, while  $90^\circ$  plies correspond to stresses aligned perpendicular to the paper plane (coming towards the reader). However, since the laminate is rectangular, the strains in the two directions are the same which implies that the stresses  $\sigma_{11}$  become continuous. Moreover, Figure 4.9 shows the stress gradient through the global x-direction which is discontinuous. However, the point of showing the stress gradient on the local coordinates (S11) is to strongly pinpoint the steep increase of the stresses through thickness, so, the subsequent analyses will only show the local stress gradients.

Note that the stress components are very large, which is unphysical because unlike the simulations, in reality the material during Cycle 1 is in a viscous state and has very limited

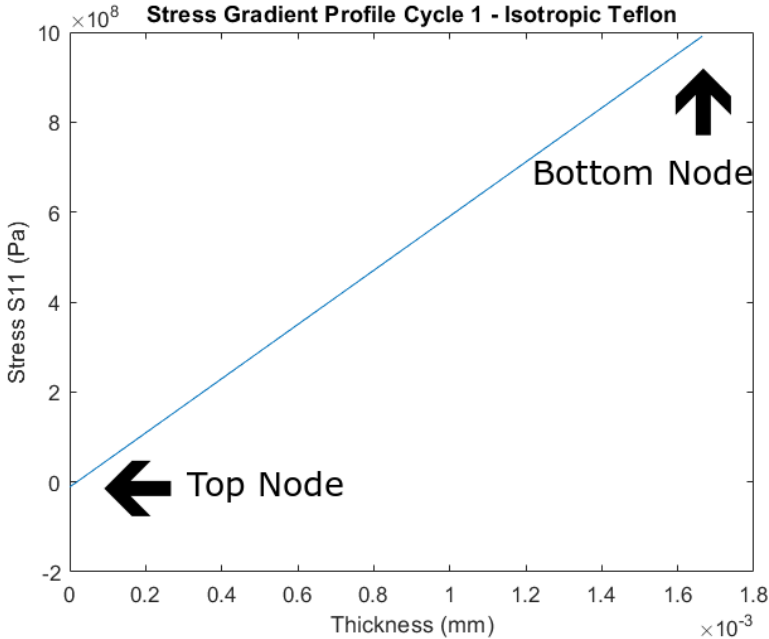


Figure 4.7: Stress S11 through the thickness for a laminate on top of a pure compatibility layer sheet.

ability to hold stresses. This is confirmed by plotting the stress S11 variation along the thickness of the laminate, in Figures 4.7 and 4.8. Obviously, the induced stresses are higher when using pure compatibility layer sheet instead of the composite compatibility layer sheet.

One way to visualize the effects of the stress gradients introduced by the expansion of the compatibility layer sheet, is to create a new simulation where the plates are released and the laminate is allowed to relax in the presence of the residual stresses. For the pure compatibility layer sheet, Figure 4.10 shows how the laminate warps reaching a maximum displacement of **0.54 mm**. For the Composite compatibility layer sheet, Figure 4.11 shows a value of warpage that is one order of magnitude lower, around **0.03 mm**. The laminate warps in the same way as shown in Figure 2.12, i.e. bending outwards (the edges stayed in contact with the compatibility layer sheet).

## CYCLE 2

Simulations of Cycle 2 are conducted only considering a pure compatibility layer sheet, given that this exaggerates the warping effect (although other conditions can easily be considered, as the simulations are parameterized). Cycle 2 is influenced by the stresses of Cycle 1, so the loads are applied similarly as in Cycle 1 but not with the same value (Temperature below the  $T_g$  and Pressure of several kN). Also, as already explained in section 4.1, the structures are undeformed initially and the simulation starts by predefining temperature and stresses. Figure 4.12 shows the deformation of the laminate, where the horizontal displacement U2 is 0.3 mm. The stress S11 through the thickness is shown in

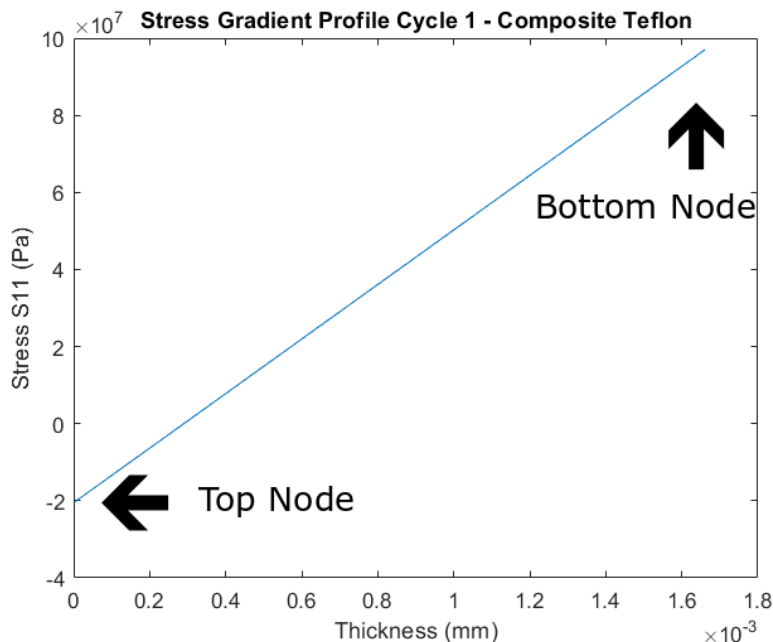


Figure 4.8: Stress S11 through the thickness for a laminate on top of a composite compatibility layer sheet.

Figure 4.13.

The next step is to show how the material warps. First, the stress gradient at the end of the step (when the temperature of the material is  $130^{\circ}\text{C}$  through the thickness) is predicted (Figure 4.14). The second stress gradient that was used is during the solidification temperature range, where part of the laminate is under its  $T_g = 150^{\circ}\text{C}$  and part of it over the glass transition (so half of it is solid and the other half still at rubbery stage). Figures 4.14, 4.15 and 4.16 show the calculated warpage at each Temperature. Using the stress gradient at the end of Cycle 2, the warpage is small and around **0.3 mm**. However, when the stress gradient was captured around its  $T_g$ , the warpage deformation is higher, since the maximum displacement reaches **1 mm** which is very close to the real experimental results. The second case is higher due to the additional effect of the temperature gradient discussed in Chapter 3, which is sufficient to enhance warpage.

#### 4.1.2. SIMULATION CONCLUSIONS

The presence of a compatibility layer sheet (pure or composite) is concluded to induce non-negligible warpage into the laminates after manufacturing. During Cycle 1, the compatibility layer sheet expands due to the increase of temperature, so the laminate deforms with it. However, since the temperature is above the glass transition, the internal stresses should not be large (contrary to linear elastic predictions). Then, in Cycle 2 there is cooling below the glass transition and there the stresses are locked. Since the compatibility layer sheet contracts significantly it drags the laminate with it and leads to the final

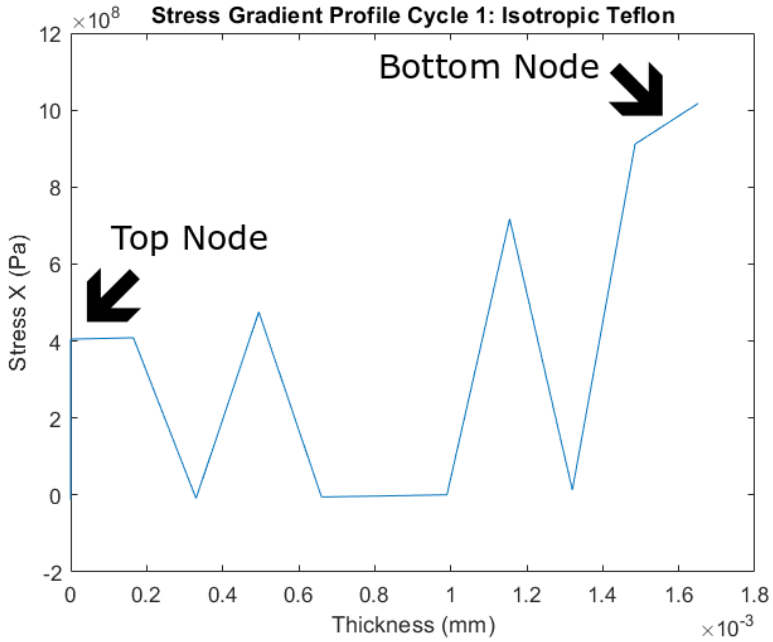


Figure 4.9: Stress x-direction through the thickness for a laminate on top of a pure compatibility layer sheet.

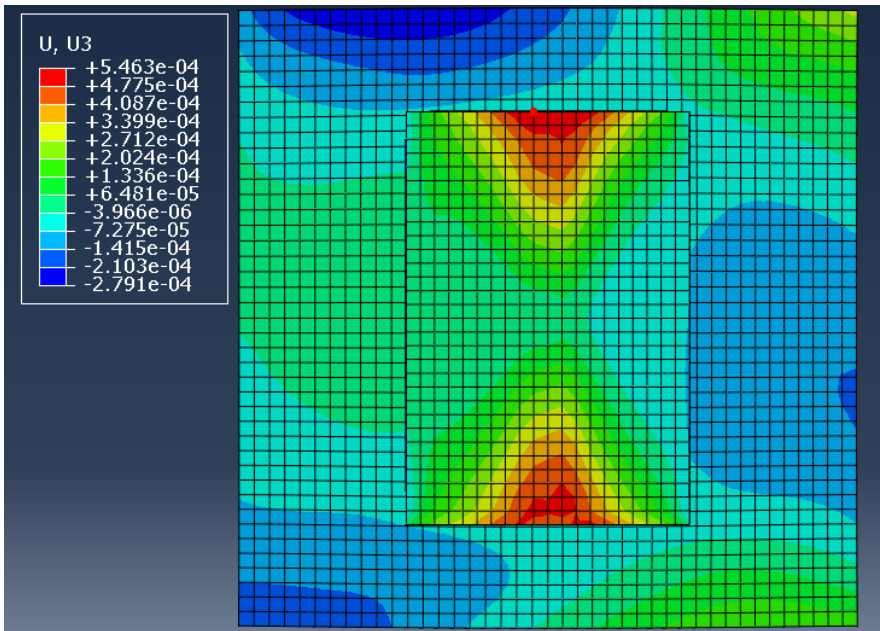


Figure 4.10: Top view warpage from Isotropic compatibility layer sheet Simulation

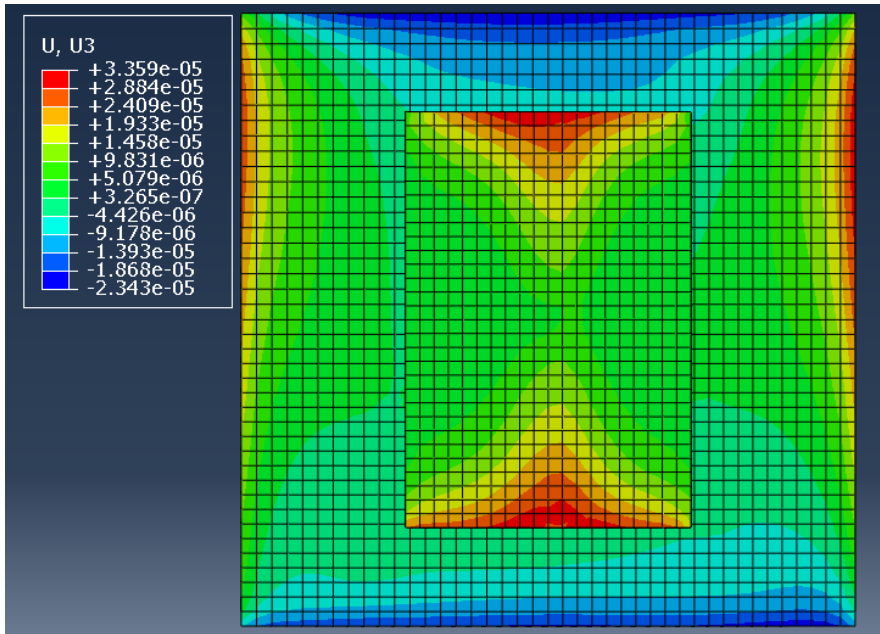


Figure 4.11: Top view warpage from Composite compatibility layer sheet Simulation

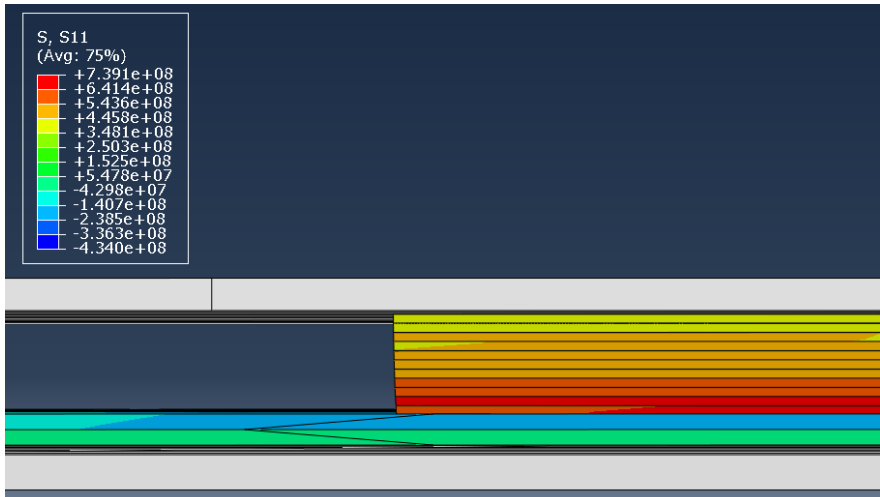


Figure 4.12: Stress S11 through the thickness for laminate on top of pure compatibility layer sheet for Cycle 2

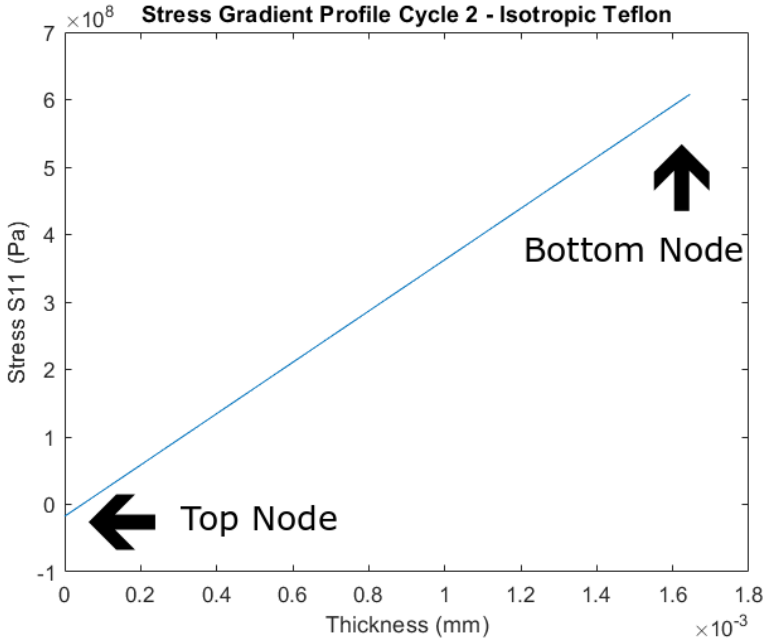


Figure 4.13: Stress S11 through the thickness for laminate on top of pure compatibility layer sheet for Cycle 2

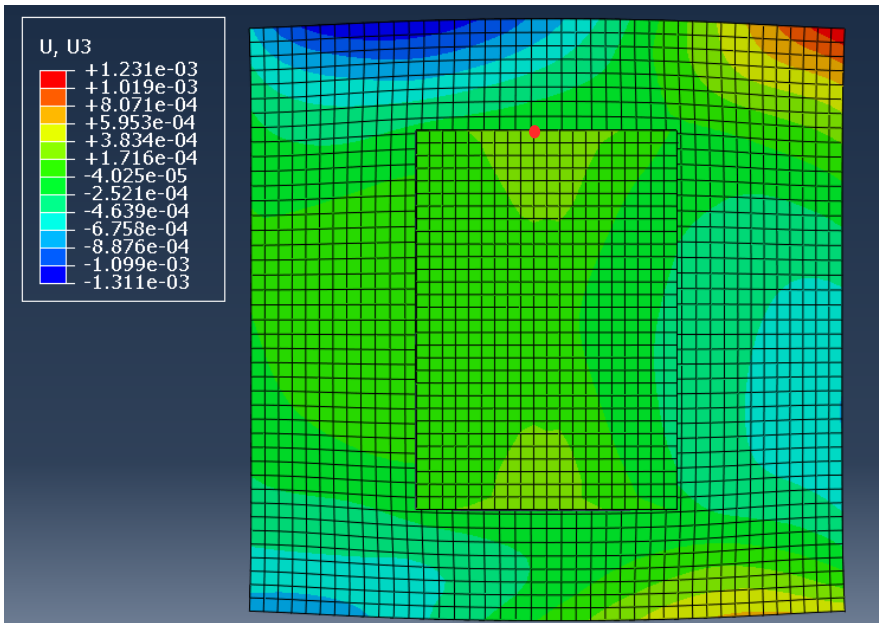


Figure 4.14: Cycle 2 warpage at the end of the step  $T = 130^{\circ}\text{C}$



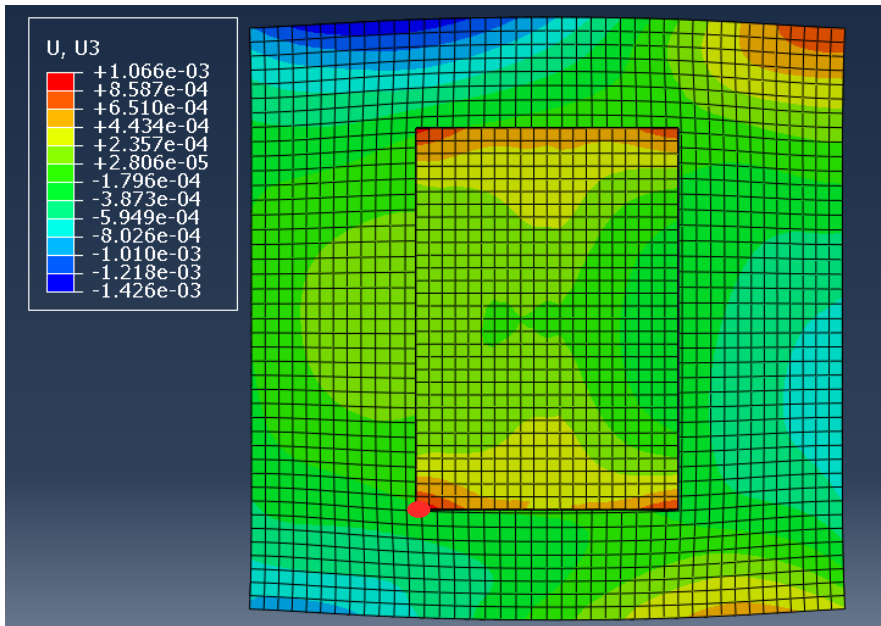


Figure 4.15: Cycle 2 warpage at the solidification  $T \sim 150^{\circ}\text{C}$

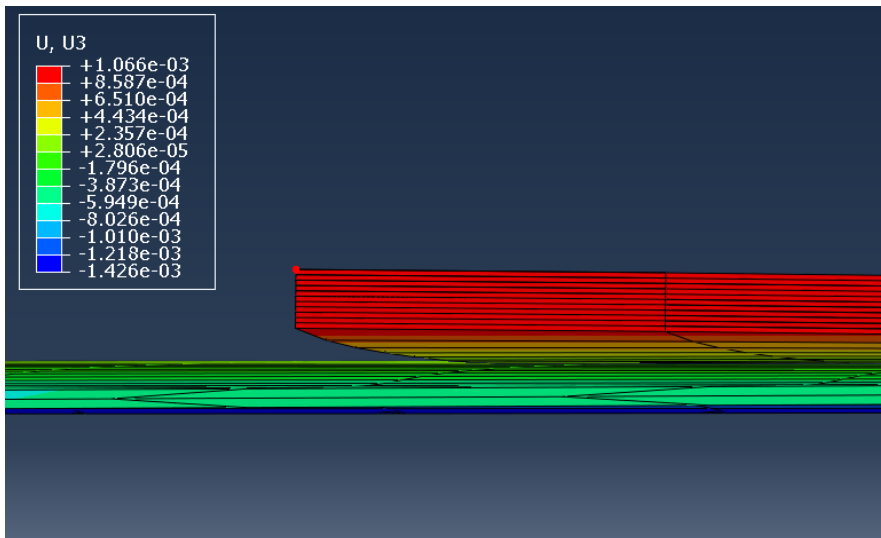


Figure 4.16: Cycle 2 edge warpage at the solidification  $T \sim 150^{\circ}\text{C}$

warpage.

Figures 4.7 and 4.13 show a steep stress gradient for the first cycle, but an almost uniform temperature across the thickness ( $\sim 180^\circ\text{C}$ ). For Cycle 2, the stress gradient is similar but there is also a temperature gradient during the time when stresses are arrested, which imposes extra constraints and deforms the material further.

## 4.2. TOOL-PART EXPERIMENTS

Subsequently to the simulations, a simple experimental investigation was conducted to assess the impact of the presence of the compatibility layer sheet on the warpage of the laminate. Three pressure configurations were used, ranking from Low to High. For these 3 configurations, 6 total runs were conducted where 3 of them used the compatibility layer sheet and the other 3 without it. Moreover, 3 more tests with different compatibility layer sheet and laminate sequence were done for the sake of comparison. The temperatures for each cycle were the same for each pressure configuration.

1. Low Pressure Configuration: Cycle 1: 100kN, Cycle 2: 100kN, Cycle 3: 50kN
2. Medium Pressure Configuration: Cycle 1: 200kN, Cycle 2: 200kN, Cycle 3: 50kN
3. High Pressure Configuration: Cycle 1: 300kN, Cycle 2: 300kN, Cycle 3: 50kN

Figure 4.17 shows the configuration of the laminates before the press. To make the data collection easier and also to observe if there is any correlation or warpage pattern, the laminates were numbered, where 1 is the top left, 2 is the top right, 3 is the bottom left and 4 is the bottom right. Also, the edges of each laminate were numbered in the same way (1 is the top left edge and so on). The compatibility layer has thickness of  $500\mu\text{m}$ .

After the runs, manual measurements were conducted using a metallic handling tool for every edge of all the laminates. Tables 4.4 and 4.5 show the results from the measurements with the standard 11 layers  $[\text{0}_2, \text{90}, \text{0}, \text{90}_2]_s$  lamination sequence with and without the compatibility layer respectively.

To check if the lamination sequence affects the warpage initiation, one extra experiment was conducted with different layup sequence  $[\text{0}_4, \text{90}_2]_s$  (Table 4.6). It was decided for the Pressure configuration to be High due to the assumption that the higher the Pressure, the better the consolidation of the laminates.

The last experiment was with the use of a different compatibility layer sheet, which was thinner with value of  $230\mu\text{m}$  and also of smaller strength (Table 4.7).

### 4.2.1. EXPERIMENTAL CONCLUSIONS

The experiments clearly demonstrate that the use of compatibility layer sheet introduces significant deformation in the laminates. The warpage was in the range of **1.3-1.8 mm** on average with the use of compatibility layer sheet and for all the pressure configurations. So probably, the pressure does not affect significantly the warpage initiation, but it is possible that the extracted laminates may have different properties depending of the consolidation pressure cycle that was used. Without compatibility layer sheet, the warpage was minimal since there is no asymmetry introduced by the top and bottom press plates. When thinner compatibility layer sheet was used, it does not seem to affect the warpage differently than



Figure 4.17: Laminate Configuration before the press

Table 4.4: Warpage measurements with the use of regular Airborne's compatibility layer sheet

<b>Low Pressure</b>				
	Edge 1	Edge 2	Edge 3	Edge 4
Laminate 1 (mm)	1.44	1.9	2	1.4
Laminate 2 (mm)	1.35	1.4	1	0.9
Laminate 3 (mm)	1.4	1.4	1.5	1
Laminate 4 (mm)	1	1.2	1.3	1
<b>Medium Pressure</b>				
	Edge 1	Edge 2	Edge 3	Edge 4
Laminate 1 (mm)	1.2	1.3	1.1	1.45
Laminate 2 (mm)	0.7	2.3	2	1.1
Laminate 3 (mm)	1.3	0.6	0.8	0.8
Laminate 4 (mm)	1.45	1.25	1.1	1.8
<b>High Pressure</b>				
	Edge 1	Edge 2	Edge 3	Edge 4
Laminate 1 (mm)	1.5	2.1	1.5	1.9
Laminate 2 (mm)	0.6	2.4	1.5	1
Laminate 3 (mm)	1.1	1.7	1.4	1.3
Laminate 4 (mm)	1.5	1.2	0.8	1.5

Table 4.5: Warpage measurements without the use of compatibility layer sheet

<b>Low Pressure</b>				
	Edge 1	Edge 2	Edge 3	Edge 4
Laminate 1 (mm)	0.5	0.4	0.5	0.3
Laminate 2 (mm)	0.3	0.7	0.8	0.6
Laminate 3 (mm)	1	0.6	1.1	0.1
Laminate 4 (mm)	0.1	0.3	0.1	0
<b>Medium Pressure</b>				
	Edge 1	Edge 2	Edge 3	Edge 4
Laminate 1 (mm)	0.5	0.2	0.55	0.7
Laminate 2 (mm)	0.1	0.65	0.9	0.7
Laminate 3 (mm)	0.4	0.6	0.8	0.3
Laminate 4 (mm)	1	0.6	0.5	0.7
<b>High Pressure</b>				
	Edge 1	Edge 2	Edge 3	Edge 4
Laminate 1 (mm)	0.4	0.1	0.3	0.1
Laminate 2 (mm)	0.1	0.2	0.1	0.1
Laminate 3 (mm)	0.2	0.1	0.5	0.1
Laminate 4 (mm)	0.2	0.1	0.1	0.4

Table 4.6: Warpage measurements with the use of the regular compatibility layer sheet and different layup sequence

<b>High Pressure with compatibility layer sheet</b>				
	Edge 1	Edge 2	Edge 3	Edge 4
Laminate 1 (mm)	2.5	1.4	2.1	2.5
Laminate 2 (mm)	0.5	2.4	4.1	3.7
Laminate 3 (mm)	1.8	2	2.45	1.7
Laminate 4 (mm)	2.1	1.6	3.1	3.2
<b>High Pressure without compatibility layer sheet</b>				
	Edge 1	Edge 2	Edge 3	Edge 4
Laminate 1 (mm)	0.5	0.6	1.5	1.4
Laminate 2 (mm)	2	2.5	2.4	1.6
Laminate 3 (mm)	4.6	4.6	5.6	5.4
Laminate 4 (mm)	0.5	0.4	0.3	0.3

Table 4.7: Warpage measurements with the use of thinner compatibility layer sheet

<b>High Pressure</b>				
	Edge 1	Edge 2	Edge 3	Edge 4
Laminate 1 (mm)	2	0.7	0.9	1.6
Laminate 2 (mm)	1.6	1.8	0.6	0.8
Laminate 3 (mm)	1.6	1.4	1.6	0.7
Laminate 4 (mm)	0.9	0.7	1.1	1.7

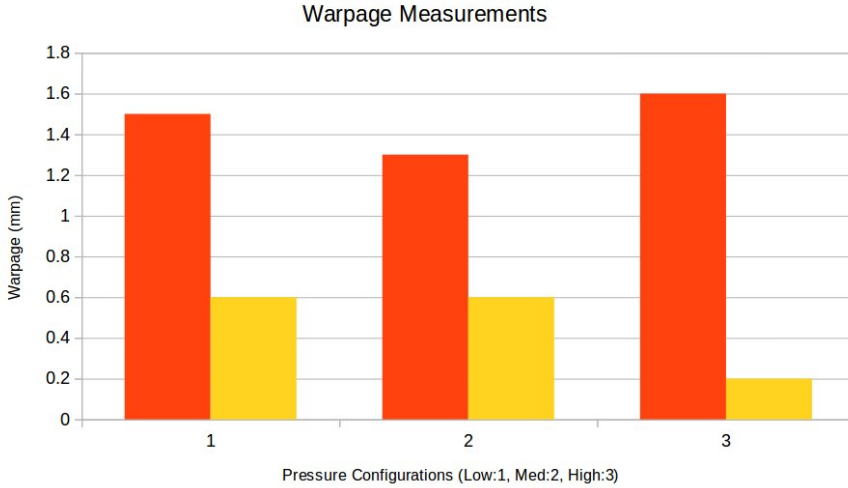


Figure 4.18: Average Warpage Measurements with (red) and without (yellow) compatibility layer sheet.

the regular one. It should be noted that the laminates adhered well to the compatibility layer sheet, i.e. the compatibility layer sheet was not as effective in facilitating extraction as intended. Concerning the experiments with different laminates, it was evident that due to the block effect (high number of consequent layers with the same direction) the interlaminar stresses would have been high enough to bend the laminate in higher values concerning the regular laminate (see Figure 2.5 and section 2.2). Figure 4.18 illustrates an average of the warpage measurements for the 3 pressure configurations for the sake of visualization (for the meaning of low, medium and high pressures, you can refer to the start of this section).

As an overall conclusion, simulations showed that the compatibility layer sheet affects the warpage initiation, where the experiments validate this result. However, the input properties and constitutive models that were considered in this Chapter are not truly representative of reality. In addition, manufacturing imperfections such as fiber misalignments were not taken into account.

# 5

## VISCOELASTICITY

**P**OLYMERS are viscoelastic, i.e. their elastic behavior is time-dependent. This has implications for residual stresses because the material can relax with time. Therefore, this chapter follows a simple modeling strategy to predict viscoelasticity of composite laminates using commercial finite element software.

### 5.1. IMPLEMENTATION IN FINITE ELEMENT ANALYSIS

The commercial finite element software used herein, Abaqus, does not have orthotropic viscoelastic material models implemented. However, a simple strategy [44] is to merge two separate material models to as shown in Figure 5.1. In practice, this is achieved as follows:

1. Create two materials and assign the corresponding constitutive laws having exactly the same part dimensions: one with an isotropic viscoelastic law, and one with an elastic orthotropic law.
2. Mesh the parts with the same element configuration.
3. Merge the 2 parts as one, such that they occupy the same location (perfect superposition). Note that this merge operation should be a "node" merge, not a "geometry" merge.

This simple strategy is equivalent to having a parallel model between the elastic response (that is orthotropic) and an isotropic viscoelastic response. Due to the parallel addition of an extra elastic element (spring), the stiffness of the material will be stiffer comparing to the one with only one elastic part (see equation 2.21 and Figure 2.24).

After merging the two models, the Teflon sheet and the two plates are added into the assembly with the proper assignment of interactions and loads, as discussed previously in Chapter 4. There are different viscoelastic models that can be considered. Typically, their properties can be assigned using three types of time dependencies:

1. Relaxation data (time dependent shear modulus vs time)

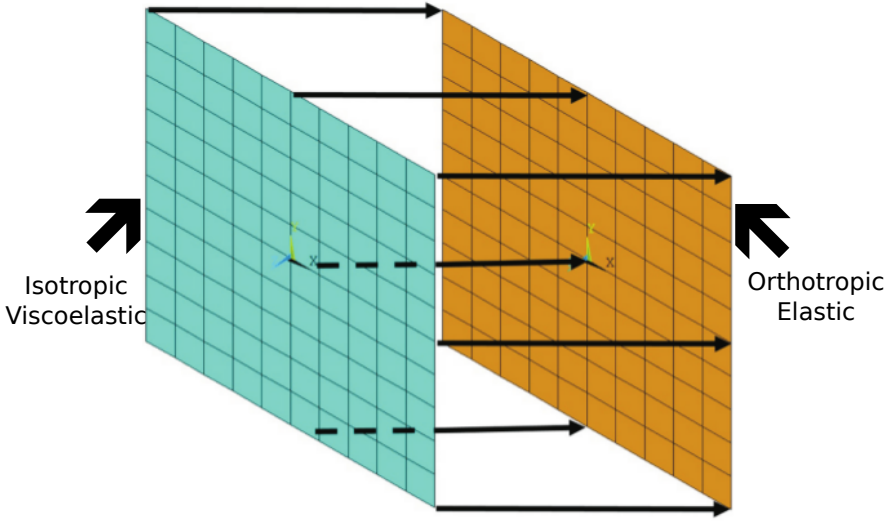


Figure 5.1: Merging of coincident nodes for elastic (orange) and viscoelastic (blue) finite element models [44]

2. Creep data (time dependent creep compliance vs time)
3. Prony series

The Prony series can be defined directly or calculated from the relaxation or creep data. Moreover, they can be implemented as shear relaxation tensor ( $G$ ) or/and bulk relaxation function ( $K$ ) with the equations:

$$\hat{G}_t = \hat{G}_o [E_\infty^G + \sum_i^n E_i^G \exp(-\frac{t}{\tau_i^G})] \quad (5.1)$$

$$K_t = K_o [E_\infty^K + \sum_i^n E_i^K \exp(-\frac{t}{\tau_i^K})] \quad (5.2)$$

where the same notation of Section 2.3.3 is used.

For this thesis, the material properties are selected from Jazouli et al. [35], who report on creep data for polycarbonate. The creep compliance must be normalized according to Figure 5.2. As highlighted in the figure, the data associated to creep at higher applied stress is considered herein, as the manufacturing process occurs at high pressure. Figures 5.3 and 5.4 show the corresponding viscoelastic data implemented in the finite element code. After the generation of the Figures 5.3 and 5.4, Abaqus also provide a way to evaluate the viscoelastic model. What it does is to calculate the Prony series using the equations 5.1 and 5.2 with all the data properties that the user provided to the software. The extracted Prony series is then defined by the coefficients listed in table 5.1. The user can



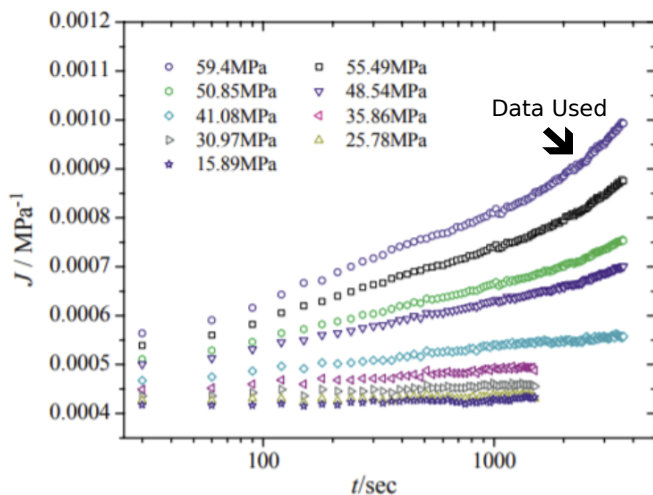


Figure 5.2: Creep compliance curves of PC for various stress levels [35]

Table 5.1: Prony series from Abaqus evaluation from data [35]

Linear	Isotropic	Prony Series	
I	G(I)	K(I)	TAU(I)
1	-2.23E-02	0.0	5.19E-03
2	0.25	0.0	156.3

also define the Prony series immediately, if they are known through numerical analysis and experimental results.

## 5.2. COMPUTATIONAL PREDICTIONS WITH VISCOELASTICITY

### CYCLE 1

The simulations are similar to Chapter 4, but now using the merged finite element meshes as described in the previous section. Recall that during Cycle 1 the temperature is 210 °C and the force is 400 kN. Figures 5.5 and 5.6 show the pre- and post-deformation of the material after the applied loads (only the laminate for better illustration). Figure 5.7 illustrates the overall stresses and also the residual stresses along the direction of the fibers.

Concerning the deformed laminate, the displacement on the x-axis is small, about 0.4 mm of horizontal dragging. However, the deformed shape of the laminate is different to the one observed for the purely elastic case seen in Chapter 4. The laminate's top layers are more deformed than the bottom ones – the opposite of what was observed in the previous Chapter. The stress gradient is also smaller, as expected due to relaxation (Figure 5.8).

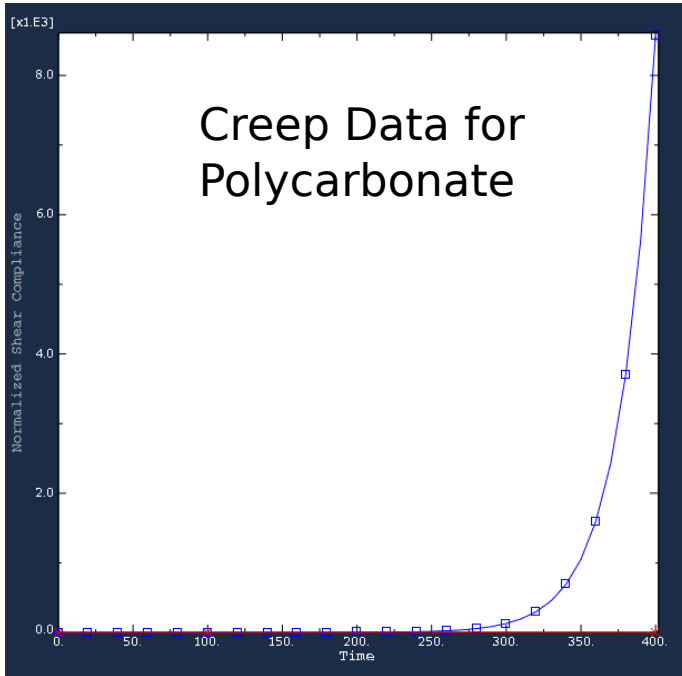


Figure 5.3: Creep compliance vs Time from ABAQUS CAE evaluation

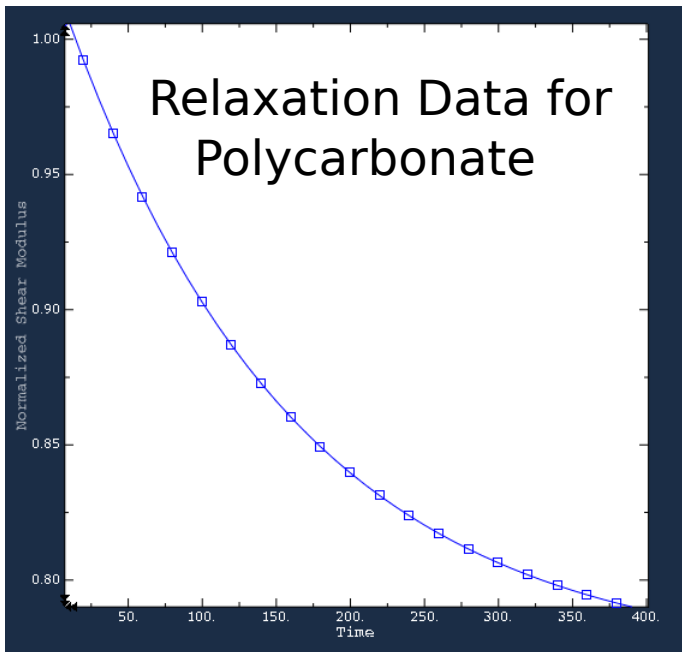


Figure 5.4: Time Dependent Shear Modulus vs Time from ABAQUS CAE evaluation

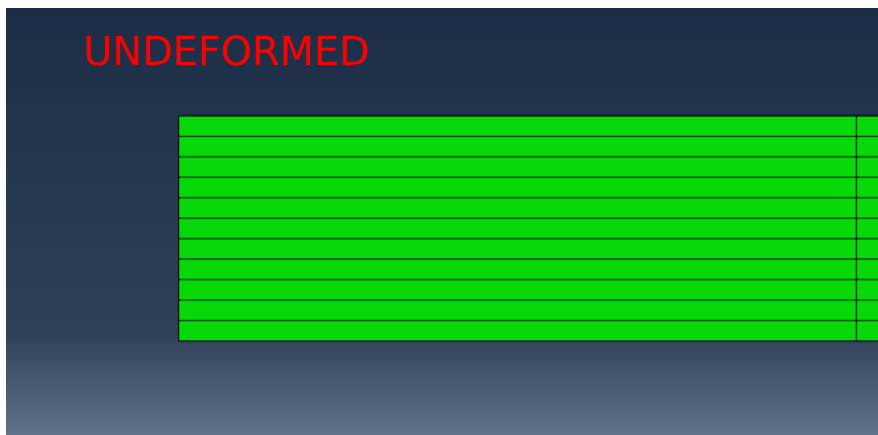


Figure 5.5: Undeformed configuration of the viscoelastic laminate

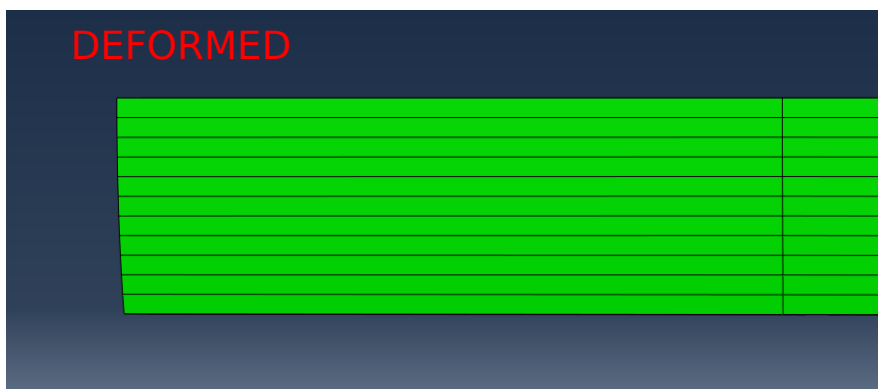


Figure 5.6: Deformed configuration of the viscoelastic laminate for Cycle 1

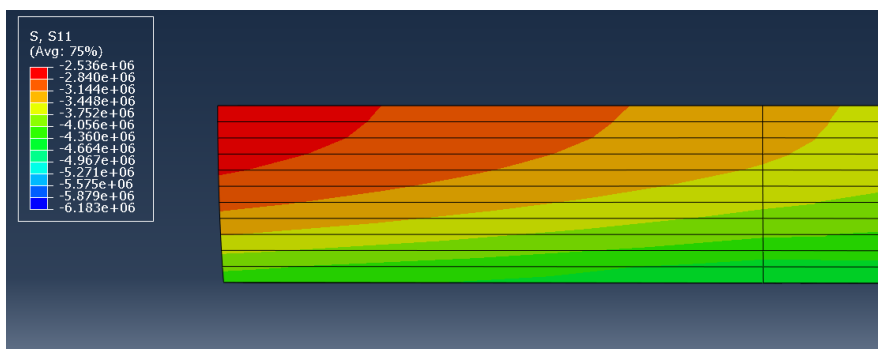


Figure 5.7: Stress profile along the fibers direction for Cycle 1

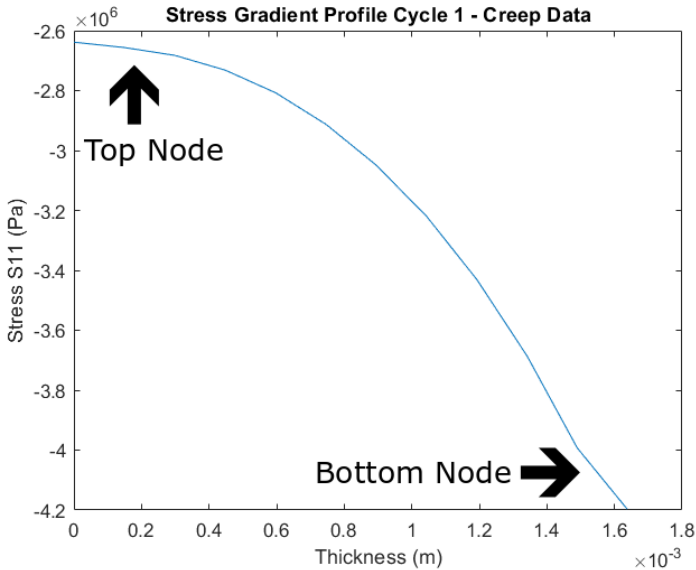


Figure 5.8: Stress profile along the fibers direction for Cycle 1 graph

After the stress gradient was obtained at the end of the cycle, it was used as a predefined field for the warpage simulation. Figure 5.9 illustrates how the material warped. As can be seen, the warpage is very small compared to the purely elastic material. The value is approximately 0.06 mm. The reason of the limited warpage is associated to the low residual stresses due to relaxation.

## CYCLE 2

In Cycle 2 recall that the stress and temperature profiles are predefined from the last increment of Cycle 1, and then the loads of Cycle 2 are applied. Figure 5.10 shows the deformed configuration and Figure 5.11 illustrates the stress profile along the fibers direction.

The horizontal displacement along the x-axis is very small, approximately 0.056 mm. Also, the stress gradient in this case is not what was expected. As can be seen from Figure 5.11, there are fluctuations of the stresses between the layers, where the middle layers have negative residual stresses comparing with the top layers (tensile forces are applied on top layers and compressive stresses of the same magnitude on the middle layers). The bottom layers have smaller compressive stresses than the middle layers and in general, the residual stresses are small. Figure 5.12 shows a top view of the laminate and the corresponding vertical displacement. The warpage of the laminate is higher than the one obtained from Cycle 1, achieving a value around 0.1 mm. However, this value is small compared to experimental results.

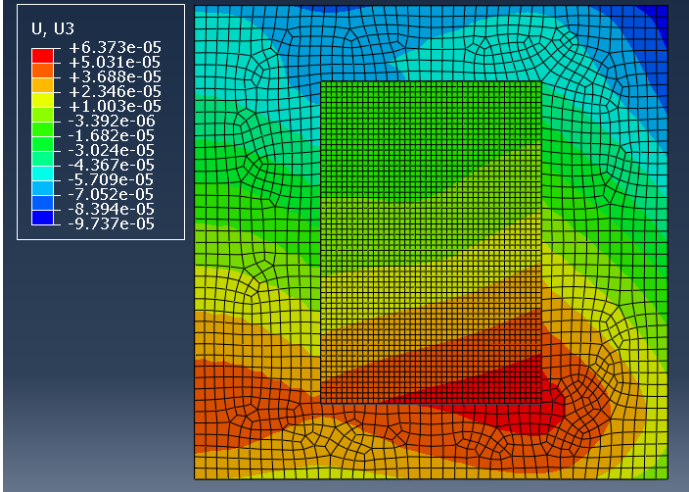


Figure 5.9: Warpage from stress gradient from Cycle 1

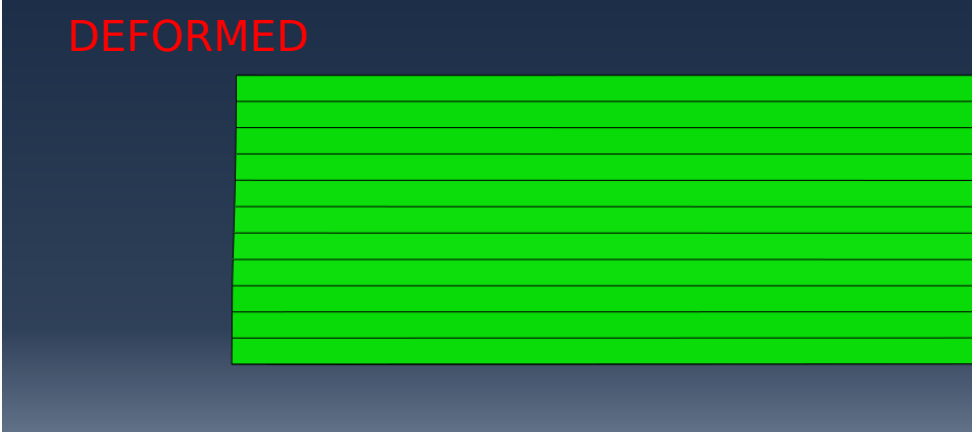


Figure 5.10: Deformed configuration of the viscoelastic laminate for Cycle 2

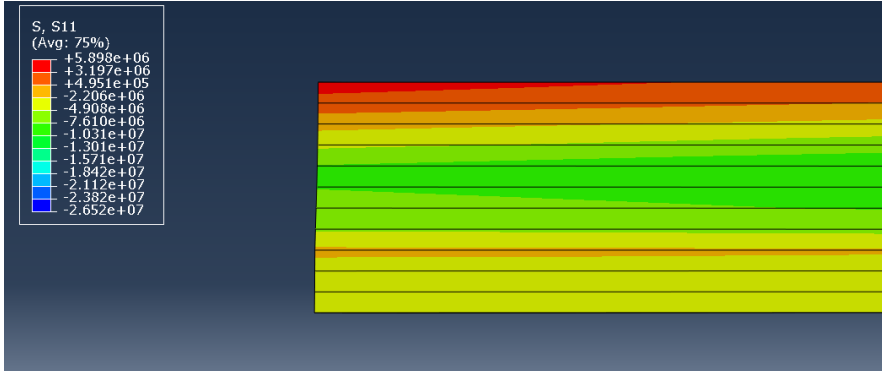


Figure 5.11: Stress gradient on the x-direction for Cycle 2

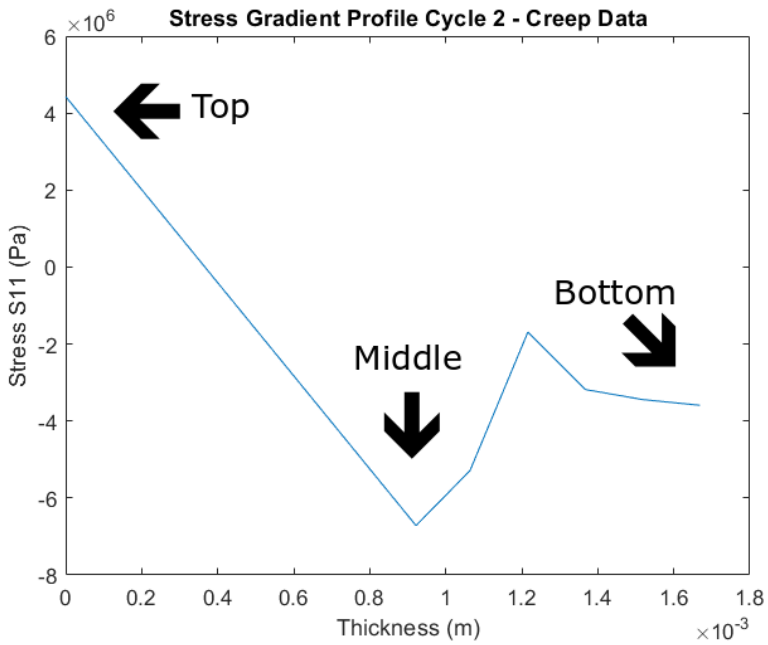


Figure 5.12: Stress gradient on the x-direction for Cycle 2 graph

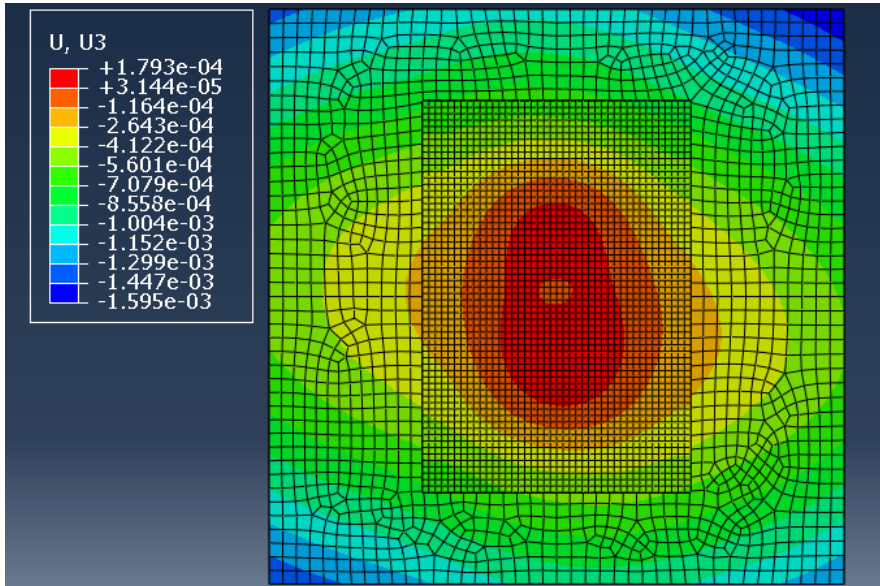


Figure 5.13: Warpage from stress gradient from Cycle 2

### 5.3. VISCOELASTICITY CONCLUSION

Due to time constraints in performing this work, the viscoelasticity simulations can only be considered preliminary. However, the modeling strategy is implemented and future work can be developed to improve the quality of the predictions by including adequate material properties and experimentally validating them. Nevertheless, the effect of relaxation mechanisms is demonstrated where the residual stresses become lower when compared to an elastic material, leading to less warpage.





# 6

## DISCUSSION

**T**HIS work aims at understanding warpage of thermoformed composite laminates. Although this investigation focused on a particular manufacturing line, the codes developed herein are parametric and applicable to other thermoforming processes with different conditions.

Concerning the particular thermoforming process under analysis, it was observed that the laminates at the end of the process were undesirably warped. The literature on the subject offers several origins for the residual stresses that explain this behavior: from micro-scale to macro-scale phenomena. This thesis concentrates on simulating the main macro-scale phenomena.

In Chapter 3, finite element analyses have demonstrated that thermal gradients are not significant, so they cannot explain the formation of residual stresses because heat transfers sufficiently quickly in each press cycle of the process. The simulations can still be improved significantly:

1. Input material properties have not been experimentally determined. This is a major limitation of this work because the properties found in the literature cannot be representative of the particular material under analysis, which severely affects the quality of the simulations;
2. Viscous/rubbery phases of the composite laminate have not been simulated;
3. The temperature profile is obtained without considering mechanical loads (pressure)
4. Few simulations have been conducted, only providing qualitative information, instead of determining the dependency of warpage on the input material properties and process conditions.

Notwithstanding the above stated, the computational analyses of Chapter 3 enabled an estimation of the influence of thermal conductance and contact conditions on the thermal profile, and excluded thermal effects as being the only ones responsible for residual

stresses.

In Chapter 4, the interaction with the tool is shown to significantly affect warpage by introducing a stress gradient due to the expansion of a Teflon sheet at the bottom of the composite laminate. If that sheet is itself a composite with Teflon matrix, then warpage decreases significantly, although still being observed. Nevertheless, appreciable limitations in the developed models should be taken into consideration:

1. Again, reliable input material properties have not been used;
2. Elastic material laws are used, so the rubbery and viscous phases are not properly modeled;
3. Cycle 2 is modeled from an undeformed configuration and by importing the thermal and stress profiles at the end of Cycle 1 as predefined fields;
4. Similar issue when simulating warpage after Cycle 2;
5. No microstructural defects have been considered.

Finally, Chapter 5 introduced a practical strategy to predict viscoelastic behavior in composite laminates where two finite element models are merged into one by superimposing orthotropic elasticity with isotropic viscoelasticity. These simulations show that the relaxation of the polymer matrix leads to lower residual stresses and less warpage, as compared to a purely elastic material (Chapter 4). However, simulating orthotropic viscoelasticity with this strategy involves important simplifications:

1. The elastic and viscoelastic model are in parallel. In micromechanics, parallel models provide a lower bound for composite properties (and series models an upper bound). Therefore, this modeling strategy should be validated appropriately by comparing against other modeling strategies, and especially against experimental results;
2. Once again, experimental input should be carefully determined to enhance the predictive capabilities of the model;

# 7

## CONCLUSION

This thesis provides basic knowledge about thermoforming of thermoplastics and the role of residual stresses in warping composite laminates. This is intended to be a modest first step towards automating the simulation process such that more in depth investigations can be conducted, including sensitivity analysis, machine learning, and optimization. Sensitivity analyses can help understand what are the input material properties and process parameters that affect more significantly the properties of interest (e.g. warpage), while machine learning can map the input-output relationship. Yet, these techniques can only be used after automating the analyses process, which is the main focus of this thesis.

The macro-scale models created showed that the presence of a Teflon sheet in between the bottom press and the composite laminate leads to non-negligible warpage of the material. This warpage was identified to arise from a mechanical interaction between the Teflon and the laminate, due to a higher thermal expansion of the first when compared to the latter. This stretches the bottom part of the laminate while the temperatures are above the glass transition temperature, i.e. when the laminate is in a viscous/rubbery state and offers little resistance to deformation. Yet, after cooling, there is a stress build-up and these residual stresses are arrested, causing the subsequent warpage when the laminate is released from the press. The finite element simulations also excluded the possibility of the residual stresses arising from a thermal gradient through the thickness of the laminate. In summary, the computational predictions showed that warpage can be predicted, and assisted in isolating the causes behind this warpage.

Due to the limited duration of a masters research project, a vast parametric study was not possible. However, the parametric finite element models developed herein are shared in the Appendix of this work for assisting future investigations. A future investigation should start by carefully characterizing the material properties and developing adequate constitutive models that include viscoelasticity and phase transformations. Predicting the viscous/rubbery state of the material may involve different modeling techniques, such as Arbitrary Lagrangian-Eulerian finite element methods, meshfree methods, or even Computational Fluid Dynamics.



# REFERENCES

- [1] G. K. Jeyakodi, *Finite Element Simulation of the In - Situ AFP process for Thermoplastic Composites using Abaqus*, Master's thesis, TU Delft (2016).
- [2] I. Zewi, I. Daniel, and J. Gotro, *Residual stresses and warpage in woven-glass/epoxy laminates*, *Experimental mechanics* **27**, 44 (1987).
- [3] G. Fernlund, A. Poursartip, G. Twigg, and C. Albert, *Residual stress, spring-in and warpage in autoclaved composite parts*, TECHNICAL PAPERS-SOCIETY OF MANUFACTURING ENGINEERS-ALL SERIES- (2003).
- [4] I. M. Daniel, O. Ishai, I. M. Daniel, and I. Daniel, *Engineering mechanics of composite materials*, Vol. 3 (Oxford university press New York, 1994).
- [5] G. Twigg, A. Poursartip, and G. Fernlund, *Tool-part interaction in composites processing. part i: experimental investigation and analytical model*, *Composites Part A: Applied Science and Manufacturing* **35**, 121 (2004).
- [6] T. E. of Encyclopaedia Britannica, *Van der waals forces chemistry and physics*, (2019).
- [7] M. Mayer, *What is a thermoplastic polymer?* (2018).
- [8] Sabic, *Sabic® pc resin*, (2019).
- [9] E. Britannica, *Amorphous solid*, (2019).
- [10] A. Van der Vegt, *From polymers to plastics* (VSSD Delft, The Netherlands, 2006).
- [11] P. S. L. Center, *The glass transition*, (2019).
- [12] H. G. Karimiani, *Analysis of Residual Stresses in Thermoplastic Composites Manufactured by Automated Fiber Placement*, Master's thesis, Concordia University (2015).
- [13] N. Rudolph, I. Kühnert, E. Schmachtenberg, and G. Ehrenstein, *Pressure solidification of amorphous thermoplastics*, *Polymer Engineering & Science* **49**, 154 (2009).
- [14] A. Jungmeier, W. Wildner, D. Drummer, and I. Kühnert, *Compression-induced solidification: A novel processing technique for precise thermoplastic optical components with negligible internal stresses*, *ISRN Optics* **2012** (2012).
- [15] formlabs, *Guide to manufacturing processes for plastics*, (2019).
- [16] S. Faris, *Four primary types of manufacturing processes*, (2018).
- [17] R. M. Stack and F. Lai, *Development in thermoforming thermoplastic composites*, (2018).

- [18] F. Saraiva, *Development of press forming techniques for thermoplastic composites*, Master's thesis, TU Delft (2017).
- [19] M. Shokrieh and A. G. Mohammadi, *The importance of measuring residual stresses in composite materials*, in *Residual Stresses in Composite Materials* (Elsevier, 2014) pp. 3–14.
- [20] N. Zobeiry and A. Poursartip, *The origins of residual stress and its evaluation in composite materials*, in *Structural integrity and durability of advanced composites* (Elsevier, 2015) pp. 43–72.
- [21] P. P. Parlevliet, H. E. Bersee, and A. Beukers, *Residual stresses in thermoplastic composites—a study of the literature—part i: Formation of residual stresses*, *Composites Part A: Applied Science and Manufacturing* **37**, 1847 (2006).
- [22] D. Plastics, *How engineering plastics expand with temperature*, (2013).
- [23] N. K. MacVarish, *The difference between amorphous and semi crystalline polymers*, (2017).
- [24] B. Lotz, *Phase Transitions and Structure Of Crystalline Polymers*, Tech. Rep. (Institut Charles Sadron).
- [25] Y. Guo, Y. Wang, G. Guo, and Y. Xie, *Finite element analysis of the thermal residual stress distribution in the interphase of unidirectional fiber-reinforced resin matrix composites*, *Composite Interfaces* **25**, 823 (2018).
- [26] F. Teixeira-Dias and L. Menezes, *Numerical aspects of finite element simulations of residual stresses in metal matrix composites*, *International Journal for Numerical Methods in Engineering* **50**, 629 (2001).
- [27] C. Ridgard, *Accuracy and distortion of composite parts and tools: causes and solutions*, TECHNICAL PAPERS-SOCIETY OF MANUFACTURING ENGINEERS-ALL SERIES- (1993).
- [28] Autodesk, *The causes of warpage*, (2019).
- [29] J. Vlachopoulos and D. Strutt, *Basic heat transfer and some applications in polymer processing*, *Plastics Technician's Toolbox* **2**, 21 (2002).
- [30] A. Ferrous and N.-F. M. Stockist, *Copper - specifications, properties, classifications and classes*, (2005).
- [31] H. Ghayoor, F. Shadmehri, and S. Van Hoa, *Development of experimental technique for measuring strain and deformation in manufacturing of thermoplastic composites using automated fiber placement (afp)*, .
- [32] Bergsma, *Design of lightweight materials*, (2018).
- [33] G. Jeronimidis and A. Parkyn, *Residual stresses in carbon fibre-thermoplastic matrix laminates*, *Journal of Composite Materials* **22**, 401 (1988).
- [34] P. Kelly, *Solid mechanics lecture notes*, Reological Models (2013).

- [35] S. Jazouli, W. Luo, F. Bremand, and T. Vu-Khanh, *Application of time-stress equivalence to nonlinear creep of polycarbonate*, *Polymer testing* **24**, 463 (2005).
- [36] Sorbothane, *The difference between elastic materials and viscoelastic materials*, (2019).
- [37] A. Y. Malkin and A. I. Isayev, *Rheology: concepts, methods, and applications* (Elsevier, 2017).
- [38] Sorbothane, *The difference between elastic materials and viscoelastic materials*, .
- [39] Zobeiry and Nima, *iscoelastic constitutive models for evaluation of residual stresses in thermoset composites during cure*, Ph.D. thesis, Diss. University of British Columbia (2006).
- [40] D. Roylance, *ENGINEERING VISCOELASTICITY*, Tech. Rep. (Department of Materials Science and Engineering Massachusetts Institute of Technology, 2001).
- [41] D. S. C. Shit, *Approach for ascertaining service temperature of plastics based on heat deflection temperature*, (2019).
- [42] Kelly, *Rheological models*, in *Solid Mechanics Part I*.
- [43] A. Ding, S. Li, J. Sun, J. Wang, and L. Zu, *A thermo-viscoelastic model of process-induced residual stresses in composite structures with considering thermal dependence*, *Composite Structures* **136**, 34 (2016).
- [44] V. G. Martynenko, *An original technique for modeling of anisotropic viscoelasticity of orthotropic materials in finite element codes applied to the mechanics of plates and shells*, *Mechanics and Mechanical Engineering* **21**, 389 (2017).
- [45] T. Sakai and S. Somiya, *Estimating creep deformation of glass-fiber-reinforced polycarbonate*, *Mechanics of Time-Dependent Materials* **10**, 185 (2006).
- [46] P. P. Database, *Temperature dependence of polymer viscosity*, (2015).
- [47] T. Instruments, *Thermal Analysis Application Brief*, Tech. Rep. (Thermal Analysis and Rheology, 2019).
- [48] G. Twigg, *TOOL-PART INTERACTION IN COMPOSITES PROCESSING*, Master's thesis, BA.Sc. (Materials and Metallurgical Engineering), Queen's University (1997).
- [49] A. Aleksandrov, Archer and Azzopardi, *Thermal contact resistance*, (2011).
- [50] K. N. Babu, *Thermal Contact Resistance: Experiments and Simulation*, Master's thesis, Department of Applied Mechanics CHALMERS UNIVERSITY OF TECHNOLOGY (2015).
- [51] C. Demerchant, *Thermal conductivity of carbon fiber, and other carbon based materials*, (2019).
- [52] R. Progelhof, J. Throne, and R. Ruetsch, *Methods for predicting the thermal conductivity of composite systems: a review*, *Polymer Engineering & Science* **16**, 615 (1976).

- [53] E. System, *Parameters of polycarbonate*, .
- [54] M. Velea and S. Lache, *Thermal expansion of composite laminates*, Bulletin of the Transilvania University of Brasov. Engineering Sciences. Series I **8**, 25 (2015).
- [55] C. Demerchant, *Youngs modulus is a measure of stiffness*, (2019).
- [56] D. Edie, *The effect of processing on the structure and properties of carbon fibers*, Carbon **36**, 345 (1998).
- [57] P. C. LTD, *Mechanical properties of carbon fibre composite materials, fibre / epoxy resin (120°C cure)*, (2009).
- [58] AZoM, *Polycarbonate ( pc ) - conductive polycarbonate - properties - supplier data by goodfellow*, .
- [59] M. MINus and S. Kumar, *The processing, properties, and structure of carbon fibers*, Jom **57**, 52 (2005).
- [60] N. Morton, *Design and Manufacture of an Advanced Composite*, Master's thesis, University of Glasgow, Meng in Mechanical Engineering with Aeronautics (2010-2011).
- [61] C. C. Chamis, *Mechanics of composite materials: past, present, and future*, Journal of Composites, Technology and Research **11**, 3 (1989).
- [62] G. B. Media, *The effects of temperature*, (2011).
- [63] S. Krop, *Constitutive modeling of rate and temperature dependent strain hardening in polycarbonate*, Master's thesis, Eindhoven University of Technology (2011).
- [64] NETZSCH, *Polycarbonate — thermal conductivity*, (2019).
- [65] DuPont, *Teflon ptfe, properties handbook*, .
- [66] S. M. Wahid and C. Madhusudana, *Gap conductance in contact heat transfer*, International Journal of Heat and Mass Transfer **43**, 4483 (2000).
- [67] S. Song, M. Yovanovich, and F. Goodman, *Thermal gap conductance of conforming surfaces in contact*, Journal of Heat Transfer **115**, 533 (1993).
- [68] E. Marotta and L. Fletcher, *Thermal contact conductance of selected polymeric materials*, Journal of Thermophysics and Heat Transfer **10**, 334 (1996).
- [69] E. ToolBox, *Friction and friction coefficients*, (2004).
- [70] R. Weyler, J. Oliver, T. Sain, and J. Cante, *On the contact domain method: A comparison of penalty and lagrange multiplier implementations*, Computer methods in applied mechanics and engineering **205**, 68 (2012).
- [71] A. 6.14, *Contact controls*, (2019).
- [72] J. HERMAN, *Running sobol sensitivity analysis using salib*, (2017).
- [73] N. Hsieh, *Sensitivity analysis by python salib*, (2017).



# A

## APPENDIX A

In the Appendix A, some basic Python scripts for simulating the Heat Transfer simulation from Chapter 3 will be provided. The basic structural code will be given, which will be the same for simulations of Chapters 4 and 5. Off course, for each Chapter, extra structural coding will be needed (such as the simulation of the plates as rigid or deformable). The interactions, boundary conditions and mesh of the elements will be given in each Chapter individually. Moreover, for display methods, the viewer can't copy and paste the codes, as the need of splitting them in order to be fully displayed in the document. But, the code is fully automated if correctly displayed in Python programming. There are two ways to run the scripts. One is to use the "Run Script" command in Abaqus, where you can choose the desirable file and the second one is to run script by script in Abaqus GUI (this is better if the user wants to add different scripts and also using the tools from the interface in conjunction).

For better understanding, comments will be given in the script (the comments are illustrated in Python with "hash-tag"). The code is one big script, but each smaller script can be used to simulate separate needs.

### A.1. HEAT TRANSFER SIMULATION

```
1  ## Heat Transfer
2
3  from abaqus import *
4  from abaqusConstants import *
5  from caeModules import *
6  from driverUtils import executeOnCaeStartup
7  executeOnCaeStartup()
8  import os
9  #os.chdir(r"C:\temp")
10 os.chdir(r"E:\HDD_BACKUP_03.09.19\temp")
11
12 # Import important modulus
```

```
13 from part import *
14 from material import *
15 from section import *
16 from assembly import *
17 from step import *
18 from interaction import *
19 from load import *
20 from mesh import *
21 from job import *
22 from sketch import *
23 from visualization import *
24 from connectorBehavior import *
25
26 session.journalOptions.setValues(replayGeometry=COORDINATE,
27     recoverGeometry=COORDINATE)
28
29 Grid = 0.04
30 ## Composite Parameters
31 #Dimensions and laminate sequence,
32 sheet_Size = 1 #If i want to change parameters
33 Length = 0.3
34 Width = 0.2
35
36 Width_=Width/2.0
37 Length_=Length/2.0
38
39 thick_ply=0.00015
40 #Airborne 11 plies composite
41 OrientationPlyes= [ 0, 0, 90, 0, 90, 90, 90, 0, 90, 0, 0 ]
42 #Thickness of the cohesive zone (change it concerning the units)
43 delta=0.00001
44
45 Nplies=(len(OrientationPlyes))-1
46
47 ## Create the laminate with adding the thickness of the plies
48
49 ThicknessPlyes=[]
50
51 for i in range(len(OrientationPlyes)):
52     ThicknessPlyes.append(thick_ply)
53
54 # Calculate the Thickness of the composite
55
56 Thickness_=0.0
57 ThicknessPlyesCumulative=[]
58
59
```

```

60 for i in range(len(ThicknessPlyes)):
61     Thickness_=Thickness_+ThicknessPlyes[i]
62     ThicknessPlyesCumulative.append(Thickness_)
63
64 # Create the cohesive layer (pure matrix material)
65 ThicknessPlyesCohesive=[]
66
67 for i in range(len(ThicknessPlyesCumulative)):
68     ThicknessPlyesCohesive.append(ThicknessPlyesCumulative[i]-delta/2.0)
69     ThicknessPlyesCohesive.append(ThicknessPlyesCumulative[i]+delta/2.0)
70
71 ThicknessPlyesCohesive.remove(Thickness_+delta/2.0)
72
73 # Teflon Parameters
74 Sides = 0.45
75 Sides_=Sides/2.0
76 thickness = 0.0005
77
78 # Heat Transfer Steps
79 time_Heat = 40
80 time_Couling = 20
81
82 # Interaction
83 Thermal_Conductance_Comp_Teflon=500
84 Thermal_Conductance_Plates_Polymers=1500
85 ContactValue = 0.1
86
87 # Convection: Not needed now
88 Convection = 7
89 sink_temperature = 20
90
91 #####
92
93 ## Composite
94 # Sketch and Part
95 mdb.models['Model-1'].ConstrainedSketch(name='__profile__',
96     sheetSize= sheet_Size)
97 mdb.models['Model-1'].sketches['__profile__'].rectangle(point1=(
98     Width_,Length_),
99     point2=( -Width_,-Length_))
100 mdb.models['Model-1'].Part(dimensionality=THREE_D,
101     name='Airborne-Composite', type=
102     DEFORMABLE_BODY)
103 mdb.models['Model-1'].parts['Airborne-Composite'].BaseSolidExtrude(
104     depth=Thickness_, sketch=
105     mdb.models['Model-1'].sketches['__profile__'])
106 del mdb.models['Model-1'].sketches['__profile__']

```

```

107
108 # partition for the edge with cohesive elements
109
110 for i in range(len(ThicknessPlyesCohesive)):
111     # partition of the edge
112     p = mdb.models['Model-1'].parts['Airborne-Composite']
113     e1, v1, d1 = p.edges, p.vertices, p.datums
114     c = p.cells
115     p.DatumPointByCoordinate(coords=(Width_, Length_,
116     ThicknessPlyesCohesive[i]))
117     Datum_1 = p.datums[p.datums.keys()[-1]]
118     p.DatumPointByCoordinate(coords=( Width_, -Length_,
119     ThicknessPlyesCohesive[i]))
120     Datum_2 = p.datums[p.datums.keys()[-1]]
121     p.DatumPointByCoordinate(coords=( -Width_, Length_,
122     ThicknessPlyesCohesive[i]))
123     Datum_3 = p.datums[p.datums.keys()[-1]]
124     p.PartitionCellByPlaneThreePoints(point1=Datum_1, point2=Datum_2,
125     point3=Datum_3, cells=c)
126
127 # Vertical cut (partition) of the top and bottom face
128 p = mdb.models['Model-1'].parts['Airborne-Composite']
129 e1, v1, d1 = p.edges, p.vertices, p.datums
130 c = p.cells
131 p.DatumPointByCoordinate(coords=(0.0, 0.0,0.0))
132 Datum_1 = p.datums[p.datums.keys()[-1]]
133 p.DatumPointByCoordinate(coords=(0.0, Length_,0.0))
134 Datum_2 = p.datums[p.datums.keys()[-1]]
135 p.DatumPointByCoordinate(coords=(0.0, Length_, Thickness_))
136 Datum_3 = p.datums[p.datums.keys()[-1]]
137 p.PartitionCellByPlaneThreePoints(point1=Datum_1, point2=Datum_2,
138 point3=Datum_3, cells=c)
139
140 # Horizontal cut (partition) of the top and bottom face
141 p = mdb.models['Model-1'].parts['Airborne-Composite']
142 e1, v1, d1 = p.edges, p.vertices, p.datums
143 c = p.cells
144 p.DatumPointByCoordinate(coords=(0.0, 0.0,0.0))
145 Datum_1 = p.datums[p.datums.keys()[-1]]
146 p.DatumPointByCoordinate(coords=(Width_, 0.0,0.0))
147 Datum_2 = p.datums[p.datums.keys()[-1]]
148 p.DatumPointByCoordinate(coords=(Width_, 0.0, Thickness_))
149 Datum_3 = p.datums[p.datums.keys()[-1]]
150 p.PartitionCellByPlaneThreePoints(point1=Datum_1, point2=Datum_2,
151 point3=Datum_3, cells=c)
152
153 # Define Lamina for Composite

```

```

154 p = mdb.models[ 'Model-1' ]. parts [ 'Airborne-Composite' ]
155 lamina_Composite=[]
156 for i in range(len(ThicknessPlyesCumulative)):
157     c = p.cells
158     cells = c.findAt(
159         ((Width_)/2.0, (Length_)/2.0,
160         (ThicknessPlyesCumulative[i]-ThicknessPlyes[i]/2.0)
161         ),),
162         ((-(Width_)/2.0, (Length_)/2.0,
163         (ThicknessPlyesCumulative[i]-ThicknessPlyes[i]/2.0)
164         ),),
165         (((Width_)/2.0, -(Length_)/2.0,
166         (ThicknessPlyesCumulative[i]-ThicknessPlyes[i]/2.0)
167         ),),
168         (((-(Width_)/2.0, -(Length_)/2.0,
169         (ThicknessPlyesCumulative[i]-ThicknessPlyes[i]/2.0)
170         ),),),
171     string='Lamina-'+str(i+1)
172     p.Set(cells=cells, name=string)
173     lamina_Composite.append(cells)
174
175 p.Set(cells=lamina_Composite, name='Lamina')
176
177 # Define Lamina for Cohesive
178 p = mdb.models[ 'Model-1' ]. parts [ 'Airborne-Composite' ]
179 lamina_Cohesive=[]
180 for i in range(len(ThicknessPlyesCumulative)):
181     c = p.cells
182     cells = c.findAt(
183         (((Width_)/2.0, (Length_)/2.0,
184         ThicknessPlyesCumulative[i] ),),),
185         (((-(Width_)/2.0, (Length_)/2.0,
186         ThicknessPlyesCumulative[i] ),),),
187         (((Width_)/2.0, -(Length_)/2.0,
188         ThicknessPlyesCumulative[i] ),),),
189         (((-(Width_)/2.0, -(Length_)/2.0,
190         ThicknessPlyesCumulative[i] ),),),),
191     string='Lamina-Cohesive-'+str(i+1)
192     p.Set(cells=cells, name=string)
193     lamina_Cohesive.append(cells)
194
195 p.Set(cells=lamina_Cohesive, name='Lamina-Cohesive')
196
197
198 ## Assign material properties
199 # Airborne-Composite
200 mdb.models[ 'Model-1' ]. Material(name='Airborne-Composite')

```

```

201 mdb.models['Model-1'].materials['Airborne-Composite'].Density(
202     table=((1390,
203           ), ))
204 mdb.models['Model-1'].materials['Airborne-Composite'].Elastic(
205     type=ENGINEERING_CONSTANTS, table=((166010000000.0, 4950000000.0,
206     4950000000.0, 0.3115, 0.3115, 0.0093, 1810000000.0, 1810000000.0,
207     1810000000.0, 20.0), (165990000000.0, 4840000000.0, 4840000000.0,
208     0.3115,
209     0.3115, 0.00908, 1760000000.0, 1760000000.0, 1760000000.0, 70.0),
210     (
211     165900000000.0, 4410000000.0, 4410000000.0, 0.3115, 0.3115, 0.00828,
212     1600000000.0, 1600000000.0, 1600000000.0, 393.0), (165800000000.0,
213     3740000000.0, 3750000000.0, 0.3115, 0.3115, 0.00705, 1370000000.0,
214     1370000000.0, 1370000000.0, 443.0)), temperatureDependency=ON)
215 mdb.models['Model-1'].materials['Airborne-Composite'].Expansion(
216     type=ORTHOTROPIC, table=((4e-07, 3.9e-05, 3.9e-05, 293.0), (4.2e-07,
217     3.9e-05, 3.9e-05,
218     343.0), (3.9e-07, 4e-05, 4e-05, 393.0), (3.36e-07, 4.1e-05, 4.1e-05,
219     433.0)), temperatureDependency=ON)
220 mdb.models['Model-1'].materials['Airborne-Composite'].SpecificHeat(
221     table=((919.0, 293.0), (938.4, 393.0), (996.7,
222     413.0), (1035.5, 433.0), (1074.4, 453.0)), temperatureDependency=ON)
223 mdb.models['Model-1'].materials['Airborne-Composite'].Conductivity(
224     type=ORTHOTROPIC, table=((20.0, 1.0, 1.0, 20.0), (21.0, 2.0,
225     2.0, 393.0), (22.0, 3.0, 3.0, 443.0)), temperatureDependency=ON)
226
227 # Cohesive
228 mdb.models['Model-1'].Material(name='Cohesive')
229 mdb.models['Model-1'].materials['Cohesive'].Density(table=((1200,
230           ), ))
231 mdb.models['Model-1'].materials['Cohesive'].Elastic(
232     type=ISOTROPIC, table=((2250000000.0, 0.3, 293.0), (2200000000.0,
233     0.3, 343.0), (2000000000.0, 0.3, 393.0), (1700000000.0, 0.3, 443.0)),
234     temperatureDependency=ON)
235 mdb.models['Model-1'].materials['Cohesive'].Expansion(
236     type=ISOTROPIC, table=((
237     6.7e-05, 293.0), (7.2e-05, 333.0), (7.4e-05, 353.0), (7.5e-05, 373.0),
238     (
239     7.7e-05, 393.0)), temperatureDependency=ON)
240 mdb.models['Model-1'].materials['Cohesive'].SpecificHeat(table=((1100.0,
241     293.0), (1150.0, 393.0), (1300.0,
242     413.0), (1400.0, 433.0), (1500.0, 453.0)), temperatureDependency=ON)
243 mdb.models['Model-1'].materials['Cohesive'].Conductivity(
244     type=ISOTROPIC, table=((0.2, 293.0), (0.26, 393.0), (0.28,
245     443.0), (0.3, 493.0)), temperatureDependency=ON)
246
247 ## Create material sections (Composite and Cohesive)

```

```
248 mdb.models[ 'Model-1' ].HomogeneousSolidSection(name='Composite-Section',
249     material='Airborne-Composite', thickness=None)
250
251 mdb.models[ 'Model-1' ].HomogeneousSolidSection(name='Cohesive-Section',
252     material='Cohesive', thickness=None)
253
254 # Assign material sections
255 mdb.models[ 'Model-1' ].parts[ 'Airborne-Composite' ].SectionAssignment(
256     offset=0.0, region=
257     mdb.models[ 'Model-1' ].parts[ 'Airborne-Composite' ].sets[ 'Lamina' ],
258     sectionName=
259     'Composite-Section')
260
261 mdb.models[ 'Model-1' ].parts[ 'Airborne-Composite' ].SectionAssignment(
262     offset=0.0, region=
263     mdb.models[ 'Model-1' ].parts[ 'Airborne-Composite' ].
264     sets[ 'Lamina-Cohesive' ], sectionName=
265     'Cohesive-Section')
266
267 ## Define the orientation and assign Orientation for Composite
268
269 mdb.models[ 'Model-1' ].parts[ 'Airborne-Composite' ].DatumCsysByThreePoints(
270     coordSysType=
271     CARTESIAN, line1=(1.0, 0.0, 0.0), line2=(0.0, 1.0, 0.0), name=
272     'Datum_csys-1', origin=(0.0, 0.0, 0.0))
273
274 DatumOrientation_1 = p.datums[p.datums.keys()[-1]]
275
276 for i in range(len(OrientationPlyes)):
277     string='Lamina-'+str(i+1)
278     mdb.models[ 'Model-1' ].parts[ 'Airborne-Composite' ].
279     MaterialOrientation(angle=OrientationPlyes[i], axis=
280         AXIS_3, localCsys=DatumOrientation_1,
281         orientationType=SYSTEM, region=mdb.models[ 'Model-1' ].
282         parts[ 'Airborne-Composite' ].sets[ string])
283
284 ## Teflon
285
286 # Sketch and Part
287 mdb.models[ 'Model-1' ].ConstrainedSketch(name='__profile__',
288     sheetSize=sheet_Size)
289 mdb.models[ 'Model-1' ].sketches[ '__profile__' ].rectangle(point1=
290     (Sides_, Sides_),
291     point2=(-Sides_, -Sides_))
292 mdb.models[ 'Model-1' ].Part(dimensionality=THREE_D, name='Teflon',
293     type=
294     DEFORMABLE_BODY)
```

```

295 mdb.models[ 'Model-1' ].parts[ 'Teflon' ].BaseSolidExtrude( depth=thickness,
296     sketch=
297     mdb.models[ 'Model-1' ].sketches[ '__profile__' ])
298 del mdb.models[ 'Model-1' ].sketches[ '__profile__' ]
299
300 # Partition
301
302 # First Side
303 mdb.models[ 'Model-1' ].ConstrainedSketch( gridSpacing=Grid,
304     name='__profile__',
305     sheetSize=sheet_Size, transform=
306     mdb.models[ 'Model-1' ].parts[ 'Teflon' ].MakeSketchTransform(
307     sketchPlane=mdb.models[ 'Model-1' ].parts[ 'Teflon' ].faces.findAt((
308     Sides/6.0,
309     Sides/6.0, thickness), ), sketchPlaneSide=SIDE1,
310     sketchUpEdge=mdb.models[ 'Model-1' ].parts[ 'Teflon' ].edges.findAt((
311     -Sides/2.0,
312     -Sides/4.0, thickness), ), sketchOrientation=RIGHT, origin=(0.0,
313     0.0, thickness)))
314 mdb.models[ 'Model-1' ].parts[ 'Teflon' ].projectReferencesOntoSketch(
315     filter=
316     COPLANAR_EDGES, sketch=mdb.models[ 'Model-1' ].sketches[ '__profile__' ])
317 mdb.models[ 'Model-1' ].sketches[ '__profile__' ].Line( point1=(0.0,
318     Sides/2.0), point2=
319     (0.0, -Sides/2.0))
320 mdb.models[ 'Model-1' ].sketches[ '__profile__' ].VerticalConstraint(
321     addUndoState=
322     False, entity=
323     mdb.models[ 'Model-1' ].sketches[ '__profile__' ].geometry.findAt((0.0,
324     0.0),
325     ))
326 mdb.models[ 'Model-1' ].sketches[ '__profile__' ].PerpendicularConstraint(
327     addUndoState=False, entity1=
328     mdb.models[ 'Model-1' ].sketches[ '__profile__' ].geometry.findAt((0.0,
329     Sides/2.0),
330     ), entity2=mdb.models[ 'Model-1' ].sketches[ '__profile__' ].geometry.
331     findAt((
332     0.0, 0.0), ))
333 mdb.models[ 'Model-1' ].sketches[ '__profile__' ].CoincidentConstraint(
334     addUndoState=False, entity1=
335     mdb.models[ 'Model-1' ].sketches[ '__profile__' ].vertices.findAt((0.0,
336     Sides/2.0),
337     ), entity2=mdb.models[ 'Model-1' ].sketches[ '__profile__' ].geometry.
338     findAt((
339     0.0, Sides/2.0), ))
340 mdb.models[ 'Model-1' ].sketches[ '__profile__' ].EqualDistanceConstraint(
341     addUndoState=False, entity1=

```



```
342     mdb.models[ 'Model-1' ].sketches[ '__profile__' ].vertices.findAt((
343         -Sides/2.0,
344         Sides/2.0), ), entity2=
345     mdb.models[ 'Model-1' ].sketches[ '__profile__' ].vertices.findAt((
346         Sides/2.0,
347         Sides/2.0), ), midpoint=
348     mdb.models[ 'Model-1' ].sketches[ '__profile__' ].vertices.findAt((0.0,
349         Sides/2.0),
350     ))
351     mdb.models[ 'Model-1' ].sketches[ '__profile__' ].CoincidentConstraint(
352         addUndoState=False, entity1=
353         mdb.models[ 'Model-1' ].sketches[ '__profile__' ].vertices.findAt((0.0,
354         -Sides/2.0), ), entity2=
355         mdb.models[ 'Model-1' ].sketches[ '__profile__' ].geometry.findAt((0.0,
356         -Sides/2.0), ))
357     mdb.models[ 'Model-1' ].sketches[ '__profile__' ].EqualDistanceConstraint(
358         addUndoState=False, entity1=
359         mdb.models[ 'Model-1' ].sketches[ '__profile__' ].vertices.findAt((
360         Sides/2.0,
361         -Sides/2.0), ), entity2=
362         mdb.models[ 'Model-1' ].sketches[ '__profile__' ].vertices.findAt((
363         -Sides/2.0,
364         -Sides/2.0), ), midpoint=
365         mdb.models[ 'Model-1' ].sketches[ '__profile__' ].vertices.findAt((0.0,
366         -Sides/2.0), ))
367     mdb.models[ 'Model-1' ].sketches[ '__profile__' ].Line(point1=(-Sides/2.0,
368         0.0),
369         point2=(Sides/2.0, 0.0))
370     mdb.models[ 'Model-1' ].sketches[ '__profile__' ].HorizontalConstraint(
371         addUndoState=False, entity=
372         mdb.models[ 'Model-1' ].sketches[ '__profile__' ].geometry.findAt((0.0,
373         0.0),
374     ))
375     mdb.models[ 'Model-1' ].sketches[ '__profile__' ].PerpendicularConstraint(
376         addUndoState=False, entity1=
377         mdb.models[ 'Model-1' ].sketches[ '__profile__' ].geometry.findAt((
378         -Sides/2.0,
379         0.0), ), entity2=
380         mdb.models[ 'Model-1' ].sketches[ '__profile__' ].geometry.findAt((0.0,
381         0.0),
382     ))
383     mdb.models[ 'Model-1' ].sketches[ '__profile__' ].CoincidentConstraint(
384         addUndoState=False, entity1=
385         mdb.models[ 'Model-1' ].sketches[ '__profile__' ].vertices.findAt((
386         -Sides/2.0,
387         0.0), ), entity2=
388         mdb.models[ 'Model-1' ].sketches[ '__profile__' ].geometry.findAt((
```

```

389         -Sides/2.0,
390     0.0), ))
391 mdb.models['Model-1'].sketches['__profile__'].EqualDistanceConstraint(
392     addUndoState=False, entity1=
393     mdb.models['Model-1'].sketches['__profile__'].vertices.findAt((
394         -Sides/2.0,
395         -Sides/2.0), ), entity2=
396     mdb.models['Model-1'].sketches['__profile__'].vertices.findAt((
397         -Sides/2.0,
398         Sides/2.0), ), midpoint=
399     mdb.models['Model-1'].sketches['__profile__'].vertices.findAt((
400         -Sides/2.0,
401         0.0), ))
402 mdb.models['Model-1'].sketches['__profile__'].CoincidentConstraint(
403     addUndoState=False, entity1=
404     mdb.models['Model-1'].sketches['__profile__'].vertices.findAt((
405         Sides/2.0, 0.0),
406     ), entity2=mdb.models['Model-1'].sketches['__profile__'].geometry.
407     findAt((
408         Sides/2.0, 0.0), ))
409 mdb.models['Model-1'].sketches['__profile__'].EqualDistanceConstraint(
410     addUndoState=False, entity1=
411     mdb.models['Model-1'].sketches['__profile__'].vertices.findAt((
412         Sides/2.0,
413         Sides/2.0), ), entity2=
414     mdb.models['Model-1'].sketches['__profile__'].vertices.findAt((
415         Sides/2.0,
416         -Sides/2.0), ), midpoint=
417     mdb.models['Model-1'].sketches['__profile__'].vertices.findAt((
418         Sides/2.0, 0.0),
419     ))
420 mdb.models['Model-1'].parts['Teflon'].PartitionFaceBySketch(faces=
421     mdb.models['Model-1'].parts['Teflon'].faces.findAt(((Sides/6.0,
422         Sides/6.0, thickness),
423     ), ), sketch=mdb.models['Model-1'].sketches['__profile__'],
424     sketchUpEdge=
425     mdb.models['Model-1'].parts['Teflon'].edges.findAt((-Sides/2.0,
426         -Sides/4.0,
427         thickness), ))
428 del mdb.models['Model-1'].sketches['__profile__']
429
430 # Second Side
431 mdb.models['Model-1'].ConstrainedSketch(gridSpacing=Grid,
432     name='__profile__',
433     sheetSize=sheet_Size, transform=
434     mdb.models['Model-1'].parts['Teflon'].MakeSketchTransform(
435     sketchPlane=mdb.models['Model-1'].parts['Teflon'].faces.findAt((

```

```
436         -Sides/6.0,
437         Sides/6.0, 0.0), ), sketchPlaneSide=SIDE1,
438         sketchUpEdge=mdb.models['Model-1'].parts['Teflon'].edges.findAt((
439         -Sides/4.0,
440         Sides/2.0, 0.0), ), sketchOrientation=RIGHT, origin=(0.0, 0.0,
441         0.0)))
442 mdb.models['Model-1'].parts['Teflon'].projectReferencesOntoSketch(
443 filter=
444     COPLANAR_EDGES, sketch=mdb.models['Model-1'].sketches['__profile__'])
445 mdb.models['Model-1'].sketches['__profile__'].Line(point1=(0.0,
446     Sides/2.0), point2=
447     (0.0, -Sides/2.0))
448 mdb.models['Model-1'].sketches['__profile__'].VerticalConstraint(
449 addUndoState=
450     False, entity=
451     mdb.models['Model-1'].sketches['__profile__'].geometry.findAt((0.0,
452     0.0),
453     ))
454 mdb.models['Model-1'].sketches['__profile__'].PerpendicularConstraint(
455 addUndoState=False, entity1=
456     mdb.models['Model-1'].sketches['__profile__'].geometry.findAt((
457     Sides/2.0,
458     Sides/2.0), ), entity2=
459     mdb.models['Model-1'].sketches['__profile__'].geometry.findAt((0.0,
460     0.0),
461     ))
462 mdb.models['Model-1'].sketches['__profile__'].CoincidentConstraint(
463 addUndoState=False, entity1=
464     mdb.models['Model-1'].sketches['__profile__'].vertices.findAt((0.0,
465     Sides/2.0),
466     ), entity2=mdb.models['Model-1'].sketches['__profile__'].geometry.
467     findAt((
468     Sides/2.0, Sides/2.0), ))
469 mdb.models['Model-1'].sketches['__profile__'].EqualDistanceConstraint(
470 addUndoState=False, entity1=
471     mdb.models['Model-1'].sketches['__profile__'].vertices.findAt((
472     Sides/2.0,
473     Sides/2.0), ), entity2=
474     mdb.models['Model-1'].sketches['__profile__'].vertices.findAt((
475     -Sides/2.0,
476     Sides/2.0), ), midpoint=
477     mdb.models['Model-1'].sketches['__profile__'].vertices.findAt((0.0,
478     Sides/2.0),
479     ))
480 mdb.models['Model-1'].sketches['__profile__'].geometry.findAt((
481 -Sides/2.0,
482     -Sides/2.0))
```

```

483 mdb.models['Model-1'].sketches['__profile__'].CoincidentConstraint(
484     addUndoState=False, entity1=
485     mdb.models['Model-1'].sketches['__profile__'].vertices.findAt((0.0,
486     -Sides/2.0), ), entity2=
487     mdb.models['Model-1'].sketches['__profile__'].geometry.findAt((
488     -Sides/2.0,
489     -Sides/2.0), ))
490 mdb.models['Model-1'].sketches['__profile__'].EqualDistanceConstraint(
491     addUndoState=False, entity1=
492     mdb.models['Model-1'].sketches['__profile__'].vertices.findAt((
493     -Sides/2.0,
494     -Sides/2.0), ), entity2=
495     mdb.models['Model-1'].sketches['__profile__'].vertices.findAt((
496     Sides/2.0,
497     -Sides/2.0), ), midpoint=
498     mdb.models['Model-1'].sketches['__profile__'].vertices.findAt((0.0,
499     -Sides/2.0), ))
500 mdb.models['Model-1'].sketches['__profile__'].Line(point1=(-Sides/2.0,
501     0.0),
502     point2=(Sides/2.0, 0.0))
503 mdb.models['Model-1'].sketches['__profile__'].HorizontalConstraint(
504     addUndoState=False, entity=
505     mdb.models['Model-1'].sketches['__profile__'].geometry.findAt((
506     -Sides/2.0,
507     0.0), ))
508 mdb.models['Model-1'].sketches['__profile__'].PerpendicularConstraint(
509     addUndoState=False, entity1=
510     mdb.models['Model-1'].sketches['__profile__'].geometry.findAt((
511     -Sides/2.0,
512     Sides/2.0), ), entity2=
513     mdb.models['Model-1'].sketches['__profile__'].geometry.findAt((
514     -Sides/2.0,
515     0.0), ))
516 mdb.models['Model-1'].sketches['__profile__'].CoincidentConstraint(
517     addUndoState=False, entity1=
518     mdb.models['Model-1'].sketches['__profile__'].vertices.findAt((
519     -Sides/2.0,
520     0.0), ), entity2=
521     mdb.models['Model-1'].sketches['__profile__'].geometry.findAt((
522     -Sides/2.0,
523     Sides/2.0), ))
524 mdb.models['Model-1'].sketches['__profile__'].EqualDistanceConstraint(
525     addUndoState=False, entity1=
526     mdb.models['Model-1'].sketches['__profile__'].vertices.findAt((
527     -Sides/2.0,
528     Sides/2.0), ), entity2=
529     mdb.models['Model-1'].sketches['__profile__'].vertices.findAt((

```

```

530         -Sides/2.0,
531     -Sides/2.0), ), midpoint=
532     mdb.models['Model-1'].sketches['__profile__'].vertices.findAt((
533         -Sides/2.0,
534         0.0), ))
535     mdb.models['Model-1'].sketches['__profile__'].CoincidentConstraint(
536         addUndoState=False, entity1=
537         mdb.models['Model-1'].sketches['__profile__'].vertices.findAt((
538             Sides/2.0, 0.0), ), entity2=
539         mdb.models['Model-1'].sketches['__profile__'].geometry.findAt((
540             Sides/2.0,
541             -Sides/2.0), ))
542     mdb.models['Model-1'].sketches['__profile__'].EqualDistanceConstraint(
543         addUndoState=False, entity1=
544         mdb.models['Model-1'].sketches['__profile__'].vertices.findAt((
545             Sides/2.0,
546             -Sides/2.0), ), entity2=
547         mdb.models['Model-1'].sketches['__profile__'].vertices.findAt((
548             Sides/2.0,
549             Sides/2.0), ), midpoint=
550         mdb.models['Model-1'].sketches['__profile__'].vertices.findAt((
551             Sides/2.0, 0.0), ))
552     mdb.models['Model-1'].parts['Teflon'].PartitionFaceBySketch(faces=
553         mdb.models['Model-1'].parts['Teflon'].faces.findAt((( -Sides/6.0,
554             Sides/6.0, 0.0),
555         )), sketch=mdb.models['Model-1'].sketches['__profile__'],
556         sketchUpEdge=
557         mdb.models['Model-1'].parts['Teflon'].edges.findAt((-Sides/4.0,
558             Sides/2.0, 0.0),
559         ))
560     del mdb.models['Model-1'].sketches['__profile__']
561
562     # Teflon Properties
563
564     mdb.models['Model-1'].Material(name='Teflon')
565     mdb.models['Model-1'].materials['Teflon'].Density(table=((2200.0, ), ))
566     mdb.models['Model-1'].materials['Teflon'].Elastic(table=((200000000000.0,
567         0.3), ))
568     mdb.models['Model-1'].materials['Teflon'].Expansion(table=((0.00012, ),
569         ))
570     mdb.models['Model-1'].materials['Teflon'].Conductivity(table=((0.25, ),
571         ))
572     mdb.models['Model-1'].materials['Teflon'].SpecificHeat(table=((970.0, ),
573         ))
574
575     # Section Assigned
576

```

```

577 mdb.models['Model-1'].parts['Teflon'].Set(cells=
578     mdb.models['Model-1'].parts['Teflon'].cells.findAt((( -Sides/6.0,
579         Sides/6.0, 0.0),
580     )), name='Teflon')
581 mdb.models['Model-1'].HomogeneousSolidSection(material='Teflon', name=
582     'Teflon-Section', thickness=None)
583 mdb.models['Model-1'].parts['Teflon'].SectionAssignment(offset=0.0,
584     offsetField='', offsetType=MIDDLE_SURFACE, region=
585     mdb.models['Model-1'].parts['Teflon'].sets['Teflon'], sectionName=
586     'Teflon-Section', thicknessAssignment=FROM_SECTION)
587
588 #Stainless Steels
589 ##### Plates #####
590 # Dimensions
591 Grid = 0.04
592 TopPlate = 0.6
593 TopPlate_ = TopPlate/2.0
594 BottomPlate = 1.0
595 BottomPlate_ = BottomPlate/2.0
596
597 sheet_Size = 1
598 PlatesDepth = 0.0005
599
600
601 ## SS-Top
602
603 # Sketch and Part
604 mdb.models['Model-1'].ConstrainedSketch(name='__profile__',
605     sheetSize=sheet_Size)
606 mdb.models['Model-1'].sketches['__profile__'].rectangle(point1=(
607     TopPlate_, TopPlate_),
608     point2=(-TopPlate_, -TopPlate_))
609 mdb.models['Model-1'].Part(dimensionality=THREE_D, name='SS_Top',
610     type=
611     DEFORMABLE_BODY)
612 mdb.models['Model-1'].parts['SS_Top'].BaseSolidExtrude(depth=PlatesDepth,
613     sketch=
614     mdb.models['Model-1'].sketches['__profile__'])
615 del mdb.models['Model-1'].sketches['__profile__']
616
617 # Partition Top Plate
618 mdb.models['Model-1'].ConstrainedSketch(gridSpacing=Grid,
619     name='__profile__',
620     sheetSize=sheet_Size, transform=
621     mdb.models['Model-1'].parts['SS_Top'].MakeSketchTransform(
622     sketchPlane=mdb.models['Model-1'].parts['SS_Top'].faces.findAt((
623         TopPlate/6.0, TopPlate/6.0,

```

```
624     PlatesDepth), ), sketchPlaneSide=SIDE1,
625     sketchUpEdge=mdb.models['Model-1'].parts['SS_Top'].edges.findAt((
626         -TopPlate/2.0,
627         -TopPlate/4.0, PlatesDepth), ), sketchOrientation=RIGHT, origin=(0.0,
628         0.0, PlatesDepth))
629 mdb.models['Model-1'].parts['SS_Top'].projectReferencesOntoSketch(
630     filter=
631         COPLANAR_EDGES, sketch=mdb.models['Model-1'].sketches['__profile__'])
632 mdb.models['Model-1'].sketches['__profile__'].Line(point1=(0.0,
633     TopPlate/2.0), point2=(
634         0.0, -TopPlate/2.0))
635 mdb.models['Model-1'].sketches['__profile__'].VerticalConstraint(
636     addUndoState=
637         False, entity=
638         mdb.models['Model-1'].sketches['__profile__'].geometry.findAt((0.0,
639         0.0),
640     ))
641 mdb.models['Model-1'].sketches['__profile__'].PerpendicularConstraint(
642     addUndoState=False, entity1=
643     mdb.models['Model-1'].sketches['__profile__'].geometry.findAt((
644         -TopPlate/2.22, TopPlate/2.0),
645     ), entity2=mdb.models['Model-1'].sketches['__profile__'].geometry.
646     findAt((
647         0.0, 0.0), ))
648 mdb.models['Model-1'].sketches['__profile__'].CoincidentConstraint(
649     addUndoState=False, entity1=
650     mdb.models['Model-1'].sketches['__profile__'].vertices.findAt((0.0,
651     TopPlate/2.0), )
652     , entity2=mdb.models['Model-1'].sketches['__profile__'].geometry.
653     findAt((
654         -TopPlate/2.22, TopPlate/2.0), ))
655 mdb.models['Model-1'].sketches['__profile__'].EqualDistanceConstraint(
656     addUndoState=False, entity1=
657     mdb.models['Model-1'].sketches['__profile__'].vertices.findAt((
658         -TopPlate/2.0, TopPlate/2.0),
659     ), entity2=mdb.models['Model-1'].sketches['__profile__'].vertices.
660     findAt((
661         TopPlate/2.0, TopPlate/2.0), ), midpoint=
662     mdb.models['Model-1'].sketches['__profile__'].vertices.findAt((0.0,
663     TopPlate/2.0),
664     ))
665 mdb.models['Model-1'].sketches['__profile__'].CoincidentConstraint(
666     addUndoState=False, entity1=
667     mdb.models['Model-1'].sketches['__profile__'].vertices.findAt((0.0,
668     -TopPlate/2.0),
669     ), entity2=mdb.models['Model-1'].sketches['__profile__'].geometry.
670     findAt((
```

```

671     TopPlate/2.22, -TopPlate/2.0), ))
672 mdb.models['Model-1'].sketches['__profile__'].EqualDistanceConstraint(
673     addUndoState=False, entity1=
674     mdb.models['Model-1'].sketches['__profile__'].vertices.findAt((
675         TopPlate/2.0, -TopPlate/2.0),
676     ), entity2=mdb.models['Model-1'].sketches['__profile__'].vertices.
677         findAt((
678         -TopPlate/2.0, -TopPlate/2.0), ), midpoint=
679     mdb.models['Model-1'].sketches['__profile__'].vertices.findAt((0.0,
680         -TopPlate/2.0),
681     ))
682 mdb.models['Model-1'].sketches['__profile__'].Line(point1=(-TopPlate/2.0,
683     0.0), point2=(
684     TopPlate/2.0, 0.0))
685 mdb.models['Model-1'].sketches['__profile__'].HorizontalConstraint(
686     addUndoState=False, entity=
687     mdb.models['Model-1'].sketches['__profile__'].geometry.findAt((
688         -TopPlate/2.22, 0.0),
689     ))
690 mdb.models['Model-1'].sketches['__profile__'].PerpendicularConstraint(
691     addUndoState=False, entity1=
692     mdb.models['Model-1'].sketches['__profile__'].geometry.findAt((
693         -TopPlate/2.0,
694         -TopPlate/2.22), ), entity2=
695     mdb.models['Model-1'].sketches['__profile__'].geometry.findAt((
696         -TopPlate/2.22, 0.0),
697     ))
698 mdb.models['Model-1'].sketches['__profile__'].CoincidentConstraint(
699     addUndoState=False, entity1=
700     mdb.models['Model-1'].sketches['__profile__'].vertices.findAt((
701         -TopPlate/2.0, 0.0),
702     ), entity2=mdb.models['Model-1'].sketches['__profile__'].geometry.
703         findAt((
704         -TopPlate/2.0, -TopPlate/2.22), ))
705 mdb.models['Model-1'].sketches['__profile__'].EqualDistanceConstraint(
706     addUndoState=False, entity1=
707     mdb.models['Model-1'].sketches['__profile__'].vertices.findAt((
708         -TopPlate/2.0, -TopPlate/2.0),
709     ), entity2=mdb.models['Model-1'].sketches['__profile__'].vertices.
710         findAt((
711         -TopPlate/2.0, TopPlate/2.0), ), midpoint=
712     mdb.models['Model-1'].sketches['__profile__'].vertices.findAt((
713         -TopPlate/2.0, 0.0),
714     ))
715 mdb.models['Model-1'].sketches['__profile__'].CoincidentConstraint(
716     addUndoState=False, entity1=
717     mdb.models['Model-1'].sketches['__profile__'].vertices.findAt((

```



```
718         TopPlate/2.0, 0.0), )
719     , entity2=mdb.models['Model-1'].sketches['__profile__'].geometry.
720         findAt((
721         TopPlate/2.0, TopPlate/2.22), ))
722 mdb.models['Model-1'].sketches['__profile__'].EqualDistanceConstraint(
723     addUndoState=False, entity1=
724     mdb.models['Model-1'].sketches['__profile__'].vertices.findAt((
725     TopPlate/2.0, TopPlate/2.0), )
726     , entity2=mdb.models['Model-1'].sketches['__profile__'].vertices.
727     findAt((
728     TopPlate/2.0, -TopPlate/2.0), ), midpoint=
729     mdb.models['Model-1'].sketches['__profile__'].vertices.findAt((
730     TopPlate/2.0, 0.0),
731     ))
732 mdb.models['Model-1'].parts['SS_Top'].PartitionFaceBySketch(faces=
733     mdb.models['Model-1'].parts['SS_Top'].faces.findAt(((TopPlate/6.0,
734     TopPlate/6.0, PlatesDepth), )),
735     sketch=mdb.models['Model-1'].sketches['__profile__'], sketchUpEdge=
736     mdb.models['Model-1'].parts['SS_Top'].edges.findAt((-TopPlate/2.0,
737     -TopPlate/4.0, PlatesDepth),
738     ))
739 del mdb.models['Model-1'].sketches['__profile__']
740
741
742 #BottomPlate
743
744 # Sketch and Part
745 mdb.models['Model-1'].ConstrainedSketch(name='__profile__',
746     sheetSize=sheet_Size)
747 mdb.models['Model-1'].sketches['__profile__'].rectangle(point1=
748     (BottomPlate_, BottomPlate_),
749     point2=(-BottomPlate_, -BottomPlate_))
750 mdb.models['Model-1'].Part(dimensionality=THREE_D, name='SS_Bottom',
751     type=
752     DEFORMABLE_BODY)
753 mdb.models['Model-1'].parts['SS_Bottom'].BaseSolidExtrude(depth=
754     PlatesDepth, sketch=
755     mdb.models['Model-1'].sketches['__profile__'])
756 del mdb.models['Model-1'].sketches['__profile__']
757
758 # Partition Bottom Plate
759 mdb.models['Model-1'].ConstrainedSketch(gridSpacing=Grid,
760     name='__profile__',
761     sheetSize=sheet_Size, transform=
762     mdb.models['Model-1'].parts['SS_Bottom'].MakeSketchTransform(
763     sketchPlane=mdb.models['Model-1'].parts['SS_Bottom'].faces.findAt((
764     BottomPlate/6.0, BottomPlate/6.0, PlatesDepth), ),
```

```

765         sketchPlaneSide=SIDE1,
766         sketchUpEdge=mdb.models['Model-1'].parts['SS_Bottom'].edges.findAt((
767             -BottomPlate/2.0,
768             -BottomPlate/4.0, PlatesDepth), ), sketchOrientation=RIGHT,
769             origin=(0.0, 0.0, PlatesDepth)))
770 mdb.models['Model-1'].parts['SS_Bottom'].projectReferencesOntoSketch(
771     filter=
772         COPLANAR_EDGES, sketch=mdb.models['Model-1'].sketches['__profile__'])
773 mdb.models['Model-1'].sketches['__profile__'].Line(point1=(0.0,
774     BottomPlate/2.0), point2=(
775         0.0, -BottomPlate/2.0))
776 mdb.models['Model-1'].sketches['__profile__'].VerticalConstraint(
777     addUndoState=
778         False, entity=
779         mdb.models['Model-1'].sketches['__profile__'].geometry.findAt((0.0,
780             0.0),
781         ))
782 mdb.models['Model-1'].sketches['__profile__'].PerpendicularConstraint(
783     addUndoState=False, entity1=
784         mdb.models['Model-1'].sketches['__profile__'].geometry.findAt((
785             -BottomPlate/2.22, BottomPlate/2.0),
786         ), entity2=mdb.models['Model-1'].sketches['__profile__'].geometry.
787             findAt((
788                 0.0, 0.0), ))
789 mdb.models['Model-1'].sketches['__profile__'].CoincidentConstraint(
790     addUndoState=False, entity1=
791         mdb.models['Model-1'].sketches['__profile__'].vertices.findAt((0.0,
792             BottomPlate/2.0), )
793         , entity2=mdb.models['Model-1'].sketches['__profile__'].geometry.
794             findAt((
795                 -BottomPlate/2.22, BottomPlate/2.0), ))
796 mdb.models['Model-1'].sketches['__profile__'].EqualDistanceConstraint(
797     addUndoState=False, entity1=
798         mdb.models['Model-1'].sketches['__profile__'].vertices.findAt((
799             -BottomPlate/2.0, BottomPlate/2.0),
800         ), entity2=mdb.models['Model-1'].sketches['__profile__'].vertices.
801             findAt((
802                 BottomPlate/2.0, BottomPlate/2.0), ), midpoint=
803         mdb.models['Model-1'].sketches['__profile__'].vertices.findAt((0.0,
804             BottomPlate/2.0),
805         ))
806 mdb.models['Model-1'].sketches['__profile__'].CoincidentConstraint(
807     addUndoState=False, entity1=
808         mdb.models['Model-1'].sketches['__profile__'].vertices.findAt((0.0,
809             -BottomPlate/2.0),
810         ), entity2=mdb.models['Model-1'].sketches['__profile__'].geometry.
811             findAt((

```

```
812     BottomPlate/2.22, -BottomPlate/2.0), ))
813 mdb.models['Model-1'].sketches['__profile__'].EqualDistanceConstraint(
814     addUndoState=False, entity1=
815     mdb.models['Model-1'].sketches['__profile__'].vertices.findAt((
816         BottomPlate/2.0, -BottomPlate/2.0),
817     ), entity2=mdb.models['Model-1'].sketches['__profile__'].vertices.
818     findAt((
819         -BottomPlate/2.0, -BottomPlate/2.0), ), midpoint=
820     mdb.models['Model-1'].sketches['__profile__'].vertices.findAt((0.0,
821         -BottomPlate/2.0),
822     ))
823 mdb.models['Model-1'].sketches['__profile__'].Line(point1=(
824     -BottomPlate/2.0, 0.0), point2=(
825     BottomPlate/2.0, 0.0))
826 mdb.models['Model-1'].sketches['__profile__'].HorizontalConstraint(
827     addUndoState=False, entity=
828     mdb.models['Model-1'].sketches['__profile__'].geometry.findAt((
829         -BottomPlate/2.22, 0.0),
830     ))
831 mdb.models['Model-1'].sketches['__profile__'].PerpendicularConstraint(
832     addUndoState=False, entity1=
833     mdb.models['Model-1'].sketches['__profile__'].geometry.findAt((
834         -BottomPlate/2.0,
835         -BottomPlate/2.22), ), entity2=
836     mdb.models['Model-1'].sketches['__profile__'].geometry.findAt((
837         -BottomPlate/2.22, 0.0),
838     ))
839 mdb.models['Model-1'].sketches['__profile__'].CoincidentConstraint(
840     addUndoState=False, entity1=
841     mdb.models['Model-1'].sketches['__profile__'].vertices.findAt((
842         -BottomPlate/2.0, 0.0),
843     ), entity2=mdb.models['Model-1'].sketches['__profile__'].geometry.
844     findAt((
845         -BottomPlate/2.0, -BottomPlate/2.22), ))
846 mdb.models['Model-1'].sketches['__profile__'].EqualDistanceConstraint(
847     addUndoState=False, entity1=
848     mdb.models['Model-1'].sketches['__profile__'].vertices.findAt((
849         -BottomPlate/2.0, -BottomPlate/2.0),
850     ), entity2=mdb.models['Model-1'].sketches['__profile__'].vertices.
851     findAt((
852         -BottomPlate/2.0, BottomPlate/2.0), ), midpoint=
853     mdb.models['Model-1'].sketches['__profile__'].vertices.findAt((
854         -BottomPlate/2.0, 0.0),
855     ))
856 mdb.models['Model-1'].sketches['__profile__'].CoincidentConstraint(
857     addUndoState=False, entity1=
858     mdb.models['Model-1'].sketches['__profile__'].vertices.findAt((
```

```

859         BottomPlate/2.0, 0.0), )
860     , entity2=mdb.models['Model-1'].sketches['__profile__'].geometry.
861         findAt((
862         BottomPlate/2.0, BottomPlate/2.22), ))
863 mdb.models['Model-1'].sketches['__profile__'].EqualDistanceConstraint(
864     addUndoState=False, entity1=
865     mdb.models['Model-1'].sketches['__profile__'].vertices.findAt((
866         BottomPlate/2.0, BottomPlate/2.0), )
867     , entity2=mdb.models['Model-1'].sketches['__profile__'].vertices.
868         findAt((
869         BottomPlate/2.0, -BottomPlate/2.0), ), midpoint=
870     mdb.models['Model-1'].sketches['__profile__'].vertices.findAt((
871         BottomPlate/2.0, 0.0),
872     ))
873 mdb.models['Model-1'].parts['SS_Bottom'].PartitionFaceBySketch(faces=
874     mdb.models['Model-1'].parts['SS_Bottom'].faces.findAt(((
875         BottomPlate/6.0, BottomPlate/6.0,
876         PlatesDepth), )), sketch=mdb.models['Model-1'].sketches
877     ['__profile__'],
878     sketchUpEdge=mdb.models['Model-1'].parts['SS_Bottom'].edges.findAt((
879         -BottomPlate/2.0,
880         -BottomPlate/4.0, PlatesDepth), ))
881 del mdb.models['Model-1'].sketches['__profile__']
882
883 # Stainless Steel Properties
884 mdb.models['Model-1'].Material(name='Stainless_Steel')
885 mdb.models['Model-1'].materials['Stainless_Steel'].Density(table=
886     ((8000.0, ),
887     ))
888 mdb.models['Model-1'].materials['Stainless_Steel'].Elastic(table=((
889     200000000000.0, 0.28), ))
890 mdb.models['Model-1'].materials['Stainless_Steel'].Conductivity(table=
891     ((16.2,
892     20.0), (16.3, 70.0), (16.4, 120.0), (16.6, 170.0), (17.0, 210.0)),
893     temperatureDependency=ON)
894 mdb.models['Model-1'].materials['Stainless_Steel'].SpecificHeat(table=
895     ((500.0,
896     ), ))
897 mdb.models['Model-1'].materials['Stainless_Steel'].Expansion(table=
898     ((1.76e-05,
899     ), ))
900
901 # Section for Stainless Steels
902 mdb.models['Model-1'].HomogeneousSolidSection(material='Stainless_Steel',
903     name=
904     'SS-Section', thickness=None)
905 mdb.models['Model-1'].parts['SS_Top'].Set(cells=

```

```
906     mdb.models[ 'Model-1' ].parts[ 'SS_Top' ].cells.findAt(((TopPlate/2.0,
907         TopPlate/6.0, PlatesDepth/1.5),
908     )), name='TopPlate_Whole_Set')
909 mdb.models[ 'Model-1' ].parts[ 'SS_Top' ].SectionAssignment(offset=0.0,
910     offsetField='', offsetType=MIDDLE_SURFACE, region=
911     mdb.models[ 'Model-1' ].parts[ 'SS_Top' ].sets[ 'TopPlate_Whole_Set' ],
912     sectionName='SS-Section', thicknessAssignment=FROM_SECTION)
913 mdb.models[ 'Model-1' ].parts[ 'SS_Bottom' ].Set(cells=
914     mdb.models[ 'Model-1' ].parts[ 'SS_Bottom' ].cells.findAt(((
915         BottomPlate/2.0, BottomPlate/6.0,
916         PlatesDepth/1.5), )), name='BottomPlate_Whole_Set')
917 mdb.models[ 'Model-1' ].parts[ 'SS_Bottom' ].SectionAssignment(offset=0.0,
918     offsetField='', offsetType=MIDDLE_SURFACE, region=
919     mdb.models[ 'Model-1' ].parts[ 'SS_Bottom' ].sets
920     [ 'BottomPlate_Whole_Set' ],
921     sectionName='SS-Section', thicknessAssignment=FROM_SECTION)
922
923 # Steps for Heat Transfer
924 mdb.models[ 'Model-1' ].HeatTransferStep(deltmx=60.0, initialInc=0.1,
925     maxInc=time_Heat
926     , minInc=0.0004, name='Heat1', previous='Initial',
927     timePeriod=time_Heat)
928 mdb.models[ 'Model-1' ].HeatTransferStep(deltmx=60.0, initialInc=0.1,
929     maxInc=time_Couling
930     , minInc=0.0002, name='Cooling1', previous='Heat1',
931     timePeriod=time_Couling)
932 mdb.models[ 'Model-1' ].HeatTransferStep(deltmx=60.0, initialInc=0.1,
933     maxInc=time_Heat
934     , minInc=0.0004, name='Heat2', previous='Cooling1',
935     timePeriod=time_Heat)
936 mdb.models[ 'Model-1' ].HeatTransferStep(deltmx=60.0, initialInc=0.1,
937     maxInc=time_Couling
938     , minInc=0.0002, name='Cooling2', previous='Heat2',
939     timePeriod=time_Couling)
940 mdb.models[ 'Model-1' ].HeatTransferStep(deltmx=60.0, initialInc=0.1,
941     maxInc=time_Heat
942     , minInc=0.0004, name='Heat3', previous='Cooling2',
943     timePeriod=time_Heat)
944 mdb.models[ 'Model-1' ].HeatTransferStep(deltmx=60.0, initialInc=0.1,
945     maxInc=time_Couling
946     , minInc=0.0002, name='Cooling3', previous='Heat3',
947     timePeriod=time_Couling)
948
949 ## Assembly
950 mdb.models[ 'Model-1' ].rootAssembly.Instance(dependent=ON, name=
951     'Airborne-Composite-1', part=
952     mdb.models[ 'Model-1' ].parts[ 'Airborne-Composite' ])
```

```

953 mdb.models[ 'Model-1' ].rootAssembly.Instance(dependent=ON,
954     name='Teflon-1',
955     part=mdb.models[ 'Model-1' ].parts[ 'Teflon' ])
956 mdb.models[ 'Model-1' ].rootAssembly.translate(instanceList=(
957     'Airborne-Composite-1', ), vector=(0.0, 0.0, thickness))
958
959 # Assign Teflon Surf and Set
960 mdb.models[ 'Model-1' ].rootAssembly.Set(faces=
961     mdb.models[ 'Model-1' ].rootAssembly.instances[ 'Teflon-1' ].faces.findAt(((
962     Sides/6.0, -Sides/6.0, 0.0), ), ((Sides/3.0, Sides/6.0, 0.0), ),
963     ((-Sides/3.0, -Sides/6.0, 0.0), ), (
964     (-Sides/6.0, Sides/6.0, 0.0), ), ), name='Teflon-Set-Bottom')
965
966 mdb.models[ 'Model-1' ].rootAssembly.Surface(name='Teflon-Surf-Bottom',
967     side1Faces=
968     mdb.models[ 'Model-1' ].rootAssembly.instances[ 'Teflon-1' ].faces.
969     findAt(((
970     Sides/6.0, -Sides/6.0, 0.0), ), ((Sides/3.0, Sides/6.0, 0.0), ),
971     ((-Sides/3.0, -Sides/6.0, 0.0), ), (
972     (-Sides/6.0, Sides/6.0, 0.0), ), ))
973
974 mdb.models[ 'Model-1' ].rootAssembly.Surface(name='Teflon-Surf-Top',
975     side1Faces=
976     mdb.models[ 'Model-1' ].rootAssembly.instances[ 'Teflon-1' ].faces.
977     findAt(((
978     Sides/6.0, -Sides/3.0, thickness), ), ((-Sides/6.0, -Sides/6.0,
979     thickness), ), ((Sides/6.0, Sides/6.0,
980     thickness), ), ((-Sides/6.0, Sides/3.0, thickness), ), ))
981
982 # Create a set for the Laminate
983 p = mdb.models[ 'Model-1' ].parts[ 'Airborne-Composite' ]
984 p.Set(cells=lamina_Composite + lamina_Cohesive, name='C-Set-InitialTemp')
985
986 mdb.models[ 'Model-1' ].rootAssembly.Set(faces=
987     mdb.models[ 'Model-1' ].rootAssembly.instances[ 'Airborne-Composite-1' ].
988     faces.findAt(
989     ((Width/3.0, Length/6.0, Thickness_+thickness), ),
990     ((-Width/3.0, Length/6.0, Thickness_+thickness), ), ((Width/3.0,
991     -Length/6.0, Thickness_+thickness), ), ((-Width/6.0, -Length/6.0,
992     Thickness_+thickness), ), ), name='Comp-Set-Top')
993
994 # Surf for convection
995 p = mdb.models[ 'Model-1' ].parts[ 'Airborne-Composite' ]
996 s = p.faces
997 surf_contact_1_A=[]
998
999 surf_contact_1_A.append(s.findAt(

```

```

1000         ((Width_)/2.0,(Length_)/2.0, Thickness_ ),),
1001         ((-(Width_)/2.0,(Length_)/2.0, Thickness_ ),),
1002         ((Width_)/2.0,-(Length_)/2.0, Thickness_ ),),
1003         ((-(Width_)/2.0,-(Length_)/2.0, Thickness_ ),),))
1004
1005 surf_contact_1_A.append(s.findAt(
1006         ((Width_)/2.0,(Length_)/2.0, 0.0 ),),
1007         ((-(Width_)/2.0,(Length_)/2.0, 0.0 ),),
1008         ((Width_)/2.0,-(Length_)/2.0, 0.0 ),),
1009         ((-(Width_)/2.0,-(Length_)/2.0, 0.0 ),),))
1010 p.Surface(sidelFaces=surf_contact_1_A, name='C-Surf-Conv-Radiation')
1011
1012 # Top and bottom surfaces for composite
1013 p = mdb.models['Model-1'].parts['Airborne-Composite']
1014 s = p.faces
1015 p.Surface(sidelFaces=surf_contact_1_A[0], name='C-Surf-Top')
1016
1017 p = mdb.models['Model-1'].parts['Airborne-Composite']
1018 s = p.faces
1019 p.Surface(sidelFaces=surf_contact_1_A[1], name='C-Surf-Bottom')
1020
1021 # Assembly Plates
1022
1023 mdb.models['Model-1'].rootAssembly.Instance(dependent=ON,
1024     name='SS_Top-1',
1025     part=mdb.models['Model-1'].parts['SS_Top'])
1026 mdb.models['Model-1'].rootAssembly.translate(instanceList=('SS_Top-1', ),
1027     vector=(TopPlate, 0.0, 0.0))
1028 mdb.models['Model-1'].rootAssembly.rotate(angle=180.0,
1029     axisDirection=(TopPlate/2.0, 0.0,
1030     0.0), axisPoint=(TopPlate, 0.0, PlatesDepth), instanceList=
1031     ('SS_Top-1', ))
1032 mdb.models['Model-1'].rootAssembly.CoincidentPoint(fixedPoint=
1033     mdb.models['Model-1'].rootAssembly.instances['Airborne-Composite-1'].
1034     vertices.findAt(
1035     (0.0, 0.0, Thickness_+thickness), ), movablePoint=
1036     mdb.models['Model-1'].rootAssembly.instances['SS_Top-1'].vertices.
1037     findAt((
1038     TopPlate, 0.0, PlatesDepth), ))
1039 mdb.models['Model-1'].rootAssembly.Instance(dependent=ON,
1040     name='SS_Bottom-1',
1041     part=mdb.models['Model-1'].parts['SS_Bottom'])
1042 mdb.models['Model-1'].rootAssembly.translate(
1043     instanceList=('SS_Bottom-1', ),
1044     vector=(1.0, 0.0, 0.0))
1045 mdb.models['Model-1'].rootAssembly.CoincidentPoint(fixedPoint=
1046     mdb.models['Model-1'].rootAssembly.instances['Teflon-1'].vertices.

```

```

1047         findAt((
1048             0.0, 0.0, 0.0), ), movablePoint=
1049             mdb.models[ 'Model-1' ].rootAssembly.instances[ 'SS_Bottom-1' ].
1050                 vertices.findAt(
1051                     (1.0, 0.0, PlatesDepth), )
1052
1053 # Assign Sets and Surfaces for the Plates
1054
1055 mdb.models[ 'Model-1' ].rootAssembly.Set(faces=
1056     mdb.models[ 'Model-1' ].rootAssembly.instances[ 'SS_Top-1' ].faces.
1057         findAt(((
1058             -TopPlate/6.0, -TopPlate/6.0, Thickness_+thickness+PlatesDepth),
1059             )), name='SS_Top_Set')
1060 mdb.models[ 'Model-1' ].rootAssembly.Set(faces=
1061     mdb.models[ 'Model-1' ].rootAssembly.instances[ 'SS_Bottom-1' ].faces.
1062         findAt(((
1063             -BottomPlate/6.0, BottomPlate/6.0, -PlatesDepth), )),
1064         name='SS_Bottom_Set')
1065
1066 mdb.models[ 'Model-1' ].rootAssembly.Surface(name='SS_Top_Surf',
1067     side1Faces=
1068         mdb.models[ 'Model-1' ].rootAssembly.instances[ 'SS_Top-1' ].faces.
1069             findAt(((
1070                 TopPlate/6.0, TopPlate/3.0, thickness+Thickness_), ),
1071                 ((-TopPlate/6.0, TopPlate/6.0, thickness+Thickness_), ),
1072                 ((TopPlate/6.0, -TopPlate/6.0, thickness+Thickness_), ),
1073                 ((-TopPlate/6.0, -TopPlate/3.0, thickness+Thickness_), ), ))
1074 mdb.models[ 'Model-1' ].rootAssembly.Surface(name='SS_Bottom_Surf',
1075     side1Faces=
1076         mdb.models[ 'Model-1' ].rootAssembly.instances[ 'SS_Bottom-1' ].faces.
1077             findAt(((
1078                 BottomPlate/6.0, -BottomPlate/3.0, 0.0), ), ((-BottomPlate/6.0,
1079                 -BottomPlate/6.0, 0.0), ), ((BottomPlate/6.0,
1080                 BottomPlate/6.0, 0.0), ), ((-BottomPlate/6.0, BottomPlate/3.0, 0.0),
1081                 ), ))
1082
1083
1084 ## Surface Contact
1085
1086 # Assign Contact Property
1087 mdb.models[ 'Model-1' ].ContactProperty('Comp-Teflon')
1088 mdb.models[ 'Model-1' ].interactionProperties[ 'Comp-Teflon' ].
1089 TangentialBehavior(
1090     dependencies=0, directionality=ISOTROPIC, formulation=LAGRANGE,
1091     pressureDependency=OFF, shearStressLimit=None,
1092     slipRateDependency=OFF,
1093     table=((ContactValue, ), ), temperatureDependency=OFF)

```



```
1094 mdb.models[ 'Model-1' ].interactionProperties[ 'Comp-Teflon' ].
1095 NormalBehavior(
1096     allowSeparation=ON, clearanceAtZeroContactPressure=0.0,
1097     constraintEnforcementMethod=AUGMENTED_IAGRANGE,
1098     contactStiffness=DEFAULT,
1099     contactStiffnessScaleFactor=1.0, pressureOverclosure=HARD)
1100 mdb.models[ 'Model-1' ].interactionProperties[ 'Comp-Teflon' ].
1101 ThermalConductance(
1102     clearanceDepTable=((Thermal_Conductance_Comp_Teflon, 0.0),
1103         (0.0, 0.001)), clearanceDependency=ON,
1104     definition=TABULAR, dependenciesC=0, massFlowRateDependencyC=OFF,
1105     pressureDependency=OFF, temperatureDependencyC=OFF)
1106
1107 mdb.models[ 'Model-1' ].ContactProperty( 'Plates-Polymers' )
1108 mdb.models[ 'Model-1' ].interactionProperties[ 'Plates-Polymers' ].
1109 TangentialBehavior(
1110     dependencies=0, directionality=ISOTROPIC, formulation=LAGRANGE,
1111     pressureDependency=OFF, shearStressLimit=None,
1112     slipRateDependency=OFF,
1113     table=((ContactValue, ), ), temperatureDependency=OFF)
1114 mdb.models[ 'Model-1' ].interactionProperties[ 'Plates-Polymers' ].
1115 NormalBehavior(
1116     allowSeparation=ON, clearanceAtZeroContactPressure=0.0,
1117     constraintEnforcementMethod=AUGMENTED_IAGRANGE,
1118     contactStiffness=DEFAULT,
1119     contactStiffnessScaleFactor=1.0, pressureOverclosure=HARD)
1120 mdb.models[ 'Model-1' ].interactionProperties[ 'Plates-Polymers' ].
1121 ThermalConductance(
1122     clearanceDepTable=((Thermal_Conductance_Plates_Polymers, 0.0),
1123         (0.0, 0.001)), clearanceDependency=ON,
1124     definition=TABULAR, dependenciesC=0, massFlowRateDependencyC=OFF,
1125     pressureDependency=OFF, temperatureDependencyC=OFF)
1126
1127 # Assign interaction
1128 mdb.models[ 'Model-1' ].SurfaceToSurfaceContactStd(adjustMethod=
1129 OVERCLOSED,
1130     clearanceRegion=None, createStepName='Initial', datumAxis=None,
1131     initialClearance=OMIT, interactionProperty='Comp-Teflon', master=
1132     mdb.models[ 'Model-1' ].rootAssembly.surfaces[ 'Teflon-Surf-Top' ],
1133     name=
1134     'C-T-inter', slave=
1135     mdb.models[ 'Model-1' ].rootAssembly.instances[ 'Airborne-Composite-1' ].
1136     surfaces[ 'C-Surf-Bottom' ]
1137     , sliding=FINITE, surfaceSmoothing=AUTOMATIC, thickness=ON,
1138     tied=OFF)
1139 mdb.models[ 'Model-1' ].SurfaceToSurfaceContactStd(adjustMethod=
1140 OVERCLOSED,
```

```

1141     clearanceRegion=None, createStepName='Initial', datumAxis=None,
1142     initialClearance=OMIT, interactionProperty='Plates-Polymers',
1143     master=
1144     mdb.models['Model-1'].rootAssembly-surfaces['SS_Top_Surf'],
1145     name=
1146     'Comp-TopPlate', slave=
1147     mdb.models['Model-1'].rootAssembly-instances['Airborne-Composite-1'].
1148     surfaces['C-Surf-Top']
1149     , sliding=FINITE, surfaceSmoothing=AUTOMATIC, thickness=ON, tied=OFF)
1150 mdb.models['Model-1'].SurfaceToSurfaceContactStd(adjustMethod=OVERCLOSED,
1151     clearanceRegion=None, createStepName='Initial', datumAxis=None,
1152     initialClearance=OMIT, interactionProperty='Plates-Polymers',
1153     master=
1154     mdb.models['Model-1'].rootAssembly-surfaces['SS_Bottom_Surf'],
1155     name=
1156     'Teflon_BottomPlate', slave=
1157     mdb.models['Model-1'].rootAssembly-surfaces['Teflon-Surf-Bottom'],
1158     sliding=
1159     FINITE, surfaceSmoothing=AUTOMATIC, thickness=ON, tied=OFF)
1160
1161 # Convection
1162 mdb.models['Model-1'].rootAssembly.Surface(name='SS_Convection',
1163     side1Faces=
1164     mdb.models['Model-1'].rootAssembly-instances['SS_Top-1'].faces.
1165     findAt(((
1166     -TopPlate/6.0, -TopPlate/6.0, Thickness_+thickness+PlatesDepth), ),
1167     )+\
1168     mdb.models['Model-1'].rootAssembly-instances['SS_Bottom-1'].faces.
1169     findAt(((
1170     BottomPlate/6.0, -BottomPlate/6.0, -PlatesDepth), ), ))
1171 mdb.models['Model-1'].FilmCondition(createStepName='Cooling1',
1172     definition=
1173     EMBEDDED_COEFF, filmCoeff=Convection, filmCoeffAmplitude='',
1174     name='Convection_1',
1175     sinkAmplitude='', sinkDistributionType=UNIFORM, sinkFieldName='',
1176     sinkTemperature=sink_temperature, surface=
1177     mdb.models['Model-1'].rootAssembly-surfaces['SS_Convection'])
1178 mdb.models['Model-1'].FilmCondition(createStepName='Cooling2',
1179     definition=
1180     EMBEDDED_COEFF, filmCoeff=Convection, filmCoeffAmplitude='',
1181     name='Convection_2',
1182     sinkAmplitude='', sinkDistributionType=UNIFORM, sinkFieldName='',
1183     sinkTemperature=sink_temperature, surface=
1184     mdb.models['Model-1'].rootAssembly-surfaces['SS_Convection'])
1185 mdb.models['Model-1'].FilmCondition(createStepName='Cooling2',
1186     definition=
1187     EMBEDDED_COEFF, filmCoeff=Convection, filmCoeffAmplitude='',

```

```
1188         name='Convection_3',
1189         sinkAmplitude='', sinkDistributionType=UNIFORM, sinkFieldName='',
1190         sinkTemperature=sink_temperature, surface=
1191         mdb.models['Model-1'].rootAssembly-surfaces['SS_Convection'])
1192 mdb.models['Model-1'].interactions['Convection_1'].deactivate('Heat2')
1193 mdb.models['Model-1'].interactions['Convection_2'].deactivate('Heat3')
1194 mdb.models['Model-1'].interactions['Convection_3'].move('Cooling2',
1195 'Heat3')
1196 mdb.models['Model-1'].interactions['Convection_3'].move('Heat3',
1197 'Cooling3')
1198
1199 # Assign Temperature Loads
1200 # Loads
1201 mdb.models['Model-1'].TemperatureBC(amplitude=UNSET,
1202 createStepName='Heat1',
1203 distributionType=UNIFORM, fieldName='', fixed=OFF,
1204 magnitude=210.0, name=
1205 'Heat1_Top', region=mdb.models['Model-1'].rootAssembly.sets
1206 ['SS_Top_Set'])
1207 mdb.models['Model-1'].boundaryConditions['Heat1_Top'].deactivate
1208 ('Cooling1')
1209 mdb.models['Model-1'].TemperatureBC(amplitude=UNSET,
1210 createStepName='Heat2',
1211 distributionType=UNIFORM, fieldName='', fixed=OFF,
1212 magnitude=130.0, name=
1213 'Heat2_Top', region=mdb.models['Model-1'].rootAssembly.
1214 sets['SS_Top_Set'])
1215 mdb.models['Model-1'].boundaryConditions['Heat2_Top'].deactivate
1216 ('Cooling2')
1217 mdb.models['Model-1'].TemperatureBC(amplitude=UNSET,
1218 createStepName='Heat3',
1219 distributionType=UNIFORM, fieldName='', fixed=OFF, magnitude=80.0,
1220 name=
1221 'Heat3_Top', region=mdb.models['Model-1'].rootAssembly.
1222 sets['SS_Top_Set'])
1223 mdb.models['Model-1'].boundaryConditions['Heat3_Top'].deactivate
1224 ('Cooling3')
1225 mdb.models['Model-1'].TemperatureBC(amplitude=UNSET,
1226 createStepName='Heat1',
1227 distributionType=UNIFORM, fieldName='', fixed=OFF,
1228 magnitude=210.0, name=
1229 'Heat1_Bottom', region=
1230 mdb.models['Model-1'].rootAssembly.sets['SS_Bottom_Set'])
1231 mdb.models['Model-1'].TemperatureBC(amplitude=UNSET,
1232 createStepName='Heat2',
1233 distributionType=UNIFORM, fieldName='', fixed=OFF,
1234 magnitude=130.0, name=
```

```

1235     'Heat2_Bottom', region=
1236     mdb.models['Model-1'].rootAssembly.sets['SS_Bottom_Set'])
1237 mdb.models['Model-1'].boundaryConditions['Heat1_Bottom'].deactivate
1238 ('Cooling1')
1239 mdb.models['Model-1'].boundaryConditions['Heat2_Bottom'].deactivate
1240 ('Cooling2')
1241 mdb.models['Model-1'].TemperatureBC(amplitude=UNSET, createStepName
1242 ='Heat3',
1243     distributionType=UNIFORM, fieldName='', fixed=OFF, magnitude=80.0,
1244     name=
1245     'Heat3_Bottom', region=
1246     mdb.models['Model-1'].rootAssembly.sets['SS_Bottom_Set'])
1247 mdb.models['Model-1'].boundaryConditions['Heat3_Bottom'].deactivate
1248 ('Cooling3')
1249
1250 # Field Output (Thermal Analysis)
1251 mdb.models['Model-1'].FieldOutputRequest(createStepName='Heat1', name=
1252     'F-Output-1', variables=('NT', 'TEMP', 'FTEMP', 'HFL', 'HFLA', 'HTL',
1253     'HTLA', 'RFL', 'RFLA', 'RFL', 'CFL', 'NFLUX', 'RADFL', 'RADFLA', 'RADTL',
1254     'RADTLA', 'VFTOT', 'SJD', 'SJDA', 'SJDT', 'SJDTA', 'WEIGHT', 'FLUXS',
1255     'HBF', 'FILMCOEF', 'SINKTEMP'))
1256
1257 # History Output
1258 mdb.models['Model-1'].HistoryOutputRequest(createStepName='Heat1',
1259     name=
1260     'H-Output-1', variables=('FTEMP', 'HFLA', 'HTL', 'HTLA', 'RADFL',
1261     'RADFLA',
1262     'RADTL', 'RADTLA', 'VFTOT', 'SJD', 'SJDA', 'SJDT', 'SJDTA',
1263     'WEIGHT'))
1264
1265 # Mesh Generation for Laminate and Teflon
1266 p = mdb.models['Model-1'].parts['Airborne-Composite']
1267 p.seedPart(size=0.01, deviationFactor=0.1, minSizeFactor=0.1)
1268 p = mdb.models['Model-1'].parts['Airborne-Composite']
1269 p.generateMesh()
1270
1271 t = mdb.models['Model-1'].parts['Teflon']
1272 t.seedPart(deviationFactor=0.1, minSizeFactor=0.1, size=0.011)
1273 mdb.models['Model-1'].parts['Teflon'].generateMesh()
1274
1275 # Mesh Generation for Plates
1276
1277 mdb.models['Model-1'].parts['SS_Top'].seedPart(deviationFactor=0.1,
1278     minSizeFactor=0.1, size=0.03)
1279 mdb.models['Model-1'].parts['SS_Top'].generateMesh()
1280
1281 mdb.models['Model-1'].parts['SS_Bottom'].seedPart(deviationFactor=0.1,

```

```
1282     minSizeFactor=0.1, size=0.05)
1283 mdb.models[ 'Model-1' ].parts[ 'SS_Bottom' ].generateMesh()
1284
1285
1286 #Elements for Laminate and Teflon
1287 elemType1 = mesh.ElemType(elemCode=DC3D6, elemLibrary=STANDARD,
1288     secondOrderAccuracy=OFF, distortionControl=DEFAULT)
1289 elemType2 = mesh.ElemType(elemCode=DC3D4, elemLibrary=STANDARD)
1290 p = mdb.models[ 'Model-1' ].parts[ 'Airborne-Composite' ]
1291 c = p.cells
1292 cells = lamina_Composite + lamina_Cohesive
1293 pickedRegions =( cells , )
1294 p.setElementType( regions=pickedRegions, elemTypes=(elemType1,
1295     elemType2, ))
1296
1297 mdb.models[ 'Model-1' ].parts[ 'Teflon' ].setElementType(elemTypes=
1298     (ElemType(
1299         elemCode=DC3D8, elemLibrary=STANDARD), ElemType(elemCode=DC3D6,
1300         elemLibrary=STANDARD), ElemType(elemCode=DC3D4, elemLibrary=
1301         STANDARD)),
1302     regions=(mdb.models[ 'Model-1' ].parts[ 'Teflon' ].cells.findAt(((
1303         -Sides/6.0,
1304         Sides/6.0, 0.0), )), ))
1305 mdb.models[ 'Model-1' ].rootAssembly.regenerate()
1306
1307 # Elements for Plates
1308
1309 mdb.models[ 'Model-1' ].parts[ 'SS_Top' ].setElementType(elemTypes=
1310     (ElemType(
1311         elemCode=DC3D8, elemLibrary=STANDARD), ElemType(elemCode=DC3D6,
1312         elemLibrary=STANDARD), ElemType(elemCode=DC3D4, elemLibrary=
1313         STANDARD)),
1314     regions=(mdb.models[ 'Model-1' ].parts[ 'SS_Top' ].cells.findAt(((
1315         TopPlate/2.0, TopPlate/6.0,
1316         PlatesDepth/1.5), )), ))
1317
1318 mdb.models[ 'Model-1' ].parts[ 'SS_Bottom' ].setElementType(elemTypes=(
1319     ElemType(
1320         elemCode=DC3D8, elemLibrary=STANDARD), ElemType(elemCode=DC3D6,
1321         elemLibrary=STANDARD), ElemType(elemCode=DC3D4, elemLibrary=
1322         STANDARD)),
1323     regions=(mdb.models[ 'Model-1' ].parts[ 'SS_Bottom' ].cells.findAt(((
1324         BottomPlate/2.0,
1325         BottomPlate/6.0, PlatesDepth/1.5), )), ))
```



# B

## APPENDIX B

In the Appendix B, the Python code for the simulations from Chapter 4 will be provided. The structure was given in Appendix A, so in this appendix, the rest of the code that is needed to simulate the Cycles will be provided. Four smaller codes are typed, first is the simulation of the Cycles, second is the warpage simulation, third is the discrete plates scripting and fourth is the viscoelastic merging. Furthermore, the structure of the parts will only be shown in the simulation of the Cycles, where in the warpage model, only the most important changes will be given (such as the step).

### B.1. CYCLE'S SIMULATION

```
1 # Teflon Properties for Composite Material (change if not isotropic)
2
3 mdb.models['Model-1'].Material(name='Teflon-Composite')
4 mdb.models['Model-1'].materials['Teflon-Composite'].Density(
5 table=((2275.0, ),
6      ))
7 mdb.models['Model-1'].materials['Teflon-Composite'].Elastic(table=((
8     20375000000.0, 66500000000.0, 66500000000.0, 0.35, 0.35, 0.4,
9     44000000000.0,
10    44000000000.0, 3000000000.0, 20.0), (20000000000.0, 6500000000.0,
11    6500000000.0, 0.35, 0.35, 0.4, 4300000000.0, 4300000000.0,
12    2800000000.0,
13    70.0), (20000000000.0, 6200000000.0, 6200000000.0, 0.35, 0.35, 0.4,
14    4000000000.0, 4000000000.0, 2600000000.0, 120.0), (20000000000.0,
15    6000000000.0, 6000000000.0, 0.35, 0.35, 0.4, 3500000000.0,
16    3500000000.0,
17    2500000000.0, 170.0), (19000000000.0, 5900000000.0, 5900000000.0,
18    0.35,
19    0.35, 0.4, 3400000000.0, 3400000000.0, 2400000000.0, 210.0)),
20 temperatureDependency=ON, type=ENGINEERING_CONSTANTS)
```

```

21 mdb.models[ 'Model-1' ].materials[ 'Teflon-Composite' ].Expansion(
22   table=((2.7e-06,
23     0.000126, 0.000126, 20.0), (2.8e-06, 0.000127, 0.000127, 70.0),
24     (3e-06,
25     0.0002, 0.0002, 120.0), (3.1e-06, 0.0002, 0.0002, 160.0),
26     (3e-06, 0.00025,
27     0.00025, 210.0)), temperatureDependency=ON, type=ORTHOTROPIC)
28 mdb.models[ 'Model-1' ].materials[ 'Teflon-Composite' ].Conductivity(
29   table=((
30     0.4875, 0.3115, 0.3115, 20.0), (0.5, 0.32, 0.32, 70.0),
31     (0.52, 0.33, 0.33,
32     120.0), (0.55, 0.35, 0.35, 170.0), (0.6, 0.4, 0.4, 210.0)),
33   temperatureDependency=ON, type=ORTHOTROPIC)
34 mdb.models[ 'Model-1' ].materials[ 'Teflon-Composite' ].SpecificHeat(
35   table=((
36     1000.0, 20.0), (1050.0, 70.0), (1100.0, 120.0), (1150.0, 170.0),
37     (1200.0,
38     210.0)), temperatureDependency=ON)
39
40 # Section assigned for Teflon Composite and material orientation
41
42 mdb.models[ 'Model-1' ].HomogeneousSolidSection(material='Teflon-Composite',
43   name='Teflon-Composite-Section', thickness=None)
44 mdb.models[ 'Model-1' ].parts[ 'Teflon' ].Set(cells=
45   mdb.models[ 'Model-1' ].parts[ 'Teflon' ].cells.findAt(((Sides/2.0,
46     Sides/3.0, thickness/6.02),
47   ), ((Sides/6.0, Sides/6.0, thickness), ), ), name='Teflon_Set')
48 mdb.models[ 'Model-1' ].parts[ 'Teflon' ].SectionAssignment(offset=0.0,
49   offsetField='', offsetType=MIDDLE_SURFACE, region=
50   mdb.models[ 'Model-1' ].parts[ 'Teflon' ].sets[ 'Teflon_Set' ],
51   sectionName=
52   'Teflon-Composite-Section', thicknessAssignment=FROM_SECTION)
53 mdb.models[ 'Model-1' ].parts[ 'Teflon' ].MaterialOrientation(
54   additionalRotationField='', additionalRotationType=ROTATION_ANGLE,
55   angle=
56   0.0, axis=AXIS_3, fieldName='', localCsys=None,
57   orientationType=SYSTEM,
58   region=Region(cells=mdb.models[ 'Model-1' ].parts[ 'Teflon' ].cells.
59   findAt(((
60   Sides/6.0, Sides/6.0, thickness), ), ), ), stackDirection=STACK_3)
61 mdb.models[ 'Model-1' ].parts[ 'Teflon' ].MaterialOrientation(
62   additionalRotationField='', additionalRotationType=ROTATION_ANGLE,
63   angle=
64   90.0, axis=AXIS_3, fieldName='', localCsys=None,
65   orientationType=SYSTEM,
66   region=Region(cells=mdb.models[ 'Model-1' ].parts[ 'Teflon' ].cells.
67   findAt(((

```



```

68     Sides/2.0, Sides/3.0, thickness/6.02), ), ),
69     stackDirection=STACK_3)
70 mdb.models['Model-1'].rootAssembly.regenerate()
71
72 # Top Plate
73
74 # Sketch and Part
75 mdb.models['Model-1'].ConstrainedSketch(name='__profile__',
76     sheetSize=sheet_Size)
77 mdb.models['Model-1'].sketches['__profile__'].Line(
78     point1=(-TopPlate, 0.0), point2=
79     (0.0, 0.0))
80 mdb.models['Model-1'].sketches['__profile__'].HorizontalConstraint(
81     addUndoState=False, entity=
82     mdb.models['Model-1'].sketches['__profile__'].geometry.findAt(
83     (-TopPlate, 0.0),
84     ))
85 mdb.models['Model-1'].sketches['__profile__'].
86 ObliqueDimension(textPoint=(
87     -TopPlate, -TopPlate), value=TopPlate, vertex1=
88     mdb.models['Model-1'].sketches['__profile__'].vertices.findAt(
89     (-TopPlate, 0.0),
90     ), vertex2=mdb.models['Model-1'].sketches['__profile__'].
91     vertices.findAt((
92     0.0, 0.0), ))
93 mdb.models['Model-1'].Part(dimensionality=THREE_D,
94     name='Top_Plate', type=
95     ANALYTIC_RIGID_SURFACE)
96 mdb.models['Model-1'].parts['Top_Plate'].AnalyticRigidSurfExtrude(
97     depth=TopPlate,
98     sketch=mdb.models['Model-1'].sketches['__profile__'])
99 del mdb.models['Model-1'].sketches['__profile__']
100
101 # Partition Cross Section
102 mdb.models['Model-1'].ConstrainedSketch(gridSpacing=Grid,
103     name='__profile__',
104     sheetSize=sheet_Size, transform=
105     mdb.models['Model-1'].parts['Top_Plate'].MakeSketchTransform(
106     sketchPlane=mdb.models['Model-1'].parts['Top_Plate'].faces.findAt(
107     (-TopPlate/3.0,
108     0.0, -TopPlate/6.0), (0.0, 1.0, 0.0)), sketchPlaneSide=SIDE1,
109     sketchUpEdge=mdb.models['Model-1'].parts['Top_Plate'].edges.findAt(
110     (-TopPlate,
111     0.0, TopPlate/4.0), ), sketchOrientation=RIGHT,
112     origin=(-TopPlate/2.0, 0.0, 0.0)))
113 mdb.models['Model-1'].parts['Top_Plate'].projectReferencesOntoSketch(
114     filter=

```

```

115     COPLANAR_EDGES, sketch=mdb.models['Model-1'].sketches['__profile__'])
116 mdb.models['Model-1'].sketches['__profile__'].Line(
117     point1=(0.0, TopPlate/2.0), point2=(
118         0.0, -TopPlate/2.0))
119 mdb.models['Model-1'].sketches['__profile__'].VerticalConstraint(
120     addUndoState=
121         False, entity=
122         mdb.models['Model-1'].sketches['__profile__'].geometry.findAt(
123             (0.0, 0.0),
124         ))
125 mdb.models['Model-1'].sketches['__profile__'].PerpendicularConstraint(
126     addUndoState=False, entity1=
127         mdb.models['Model-1'].sketches['__profile__'].geometry.findAt(
128             (TopPlate/2.0, TopPlate/2.0),
129     ), entity2=mdb.models['Model-1'].sketches['__profile__'].geometry.
130         findAt((
131             0.0, 0.0), ))
132 mdb.models['Model-1'].sketches['__profile__'].CoincidentConstraint(
133     addUndoState=False, entity1=
134         mdb.models['Model-1'].sketches['__profile__'].vertices.findAt(
135             (0.0, TopPlate/2.0), )
136     , entity2=mdb.models['Model-1'].sketches['__profile__'].geometry.
137         findAt((
138             TopPlate/2.0, TopPlate/2.0), ))
139 mdb.models['Model-1'].sketches['__profile__'].EqualDistanceConstraint(
140     addUndoState=False, entity1=
141         mdb.models['Model-1'].sketches['__profile__'].vertices.findAt(
142             (TopPlate/2.0, TopPlate/2.0), )
143     , entity2=mdb.models['Model-1'].sketches['__profile__'].vertices.
144         findAt((
145             -TopPlate/2.0, TopPlate/2.0), ), midpoint=
146         mdb.models['Model-1'].sketches['__profile__'].vertices.findAt(
147             (0.0, TopPlate/2.0),
148     ))
149 mdb.models['Model-1'].sketches['__profile__'].CoincidentConstraint(
150     addUndoState=False, entity1=
151         mdb.models['Model-1'].sketches['__profile__'].vertices.findAt(
152             (0.0, -TopPlate/2.0),
153     ), entity2=mdb.models['Model-1'].sketches['__profile__'].geometry.
154         findAt((
155             -TopPlate/2.0, -TopPlate/2.0), ))
156 mdb.models['Model-1'].sketches['__profile__'].EqualDistanceConstraint(
157     addUndoState=False, entity1=
158         mdb.models['Model-1'].sketches['__profile__'].vertices.findAt(
159             (-TopPlate/2.0, -TopPlate/2.0),
160     ), entity2=mdb.models['Model-1'].sketches['__profile__'].vertices.
161         findAt((

```

```
162     TopPlate/2.0, -TopPlate/2.0), ), midpoint=
163     mdb.models['Model-1'].sketches['__profile__'].vertices.findAt(
164         (0.0, -TopPlate/2.0),
165     ))
166 mdb.models['Model-1'].sketches['__profile__'].Line(point1=
167 (-TopPlate/2.0, 0.0), point2=(
168     TopPlate/2.0, 0.0))
169 mdb.models['Model-1'].sketches['__profile__'].HorizontalConstraint(
170     addUndoState=False, entity=
171     mdb.models['Model-1'].sketches['__profile__'].geometry.findAt(
172         (-TopPlate/2.0, 0.0),
173     ))
174 mdb.models['Model-1'].sketches['__profile__'].PerpendicularConstraint(
175     addUndoState=False, entity1=
176     mdb.models['Model-1'].sketches['__profile__'].geometry.findAt(
177         (-TopPlate/2.0, TopPlate/2.0),
178     ), entity2=mdb.models['Model-1'].sketches['__profile__'].geometry.
179     findAt((
180     -TopPlate/2.0, 0.0), ))
181 mdb.models['Model-1'].sketches['__profile__'].CoincidentConstraint(
182     addUndoState=False, entity1=
183     mdb.models['Model-1'].sketches['__profile__'].vertices.findAt(
184         (-TopPlate/2.0, 0.0),
185     ), entity2=mdb.models['Model-1'].sketches['__profile__'].geometry.
186     findAt((
187     -TopPlate/2.0, TopPlate/2.0), ))
188 mdb.models['Model-1'].sketches['__profile__'].EqualDistanceConstraint(
189     addUndoState=False, entity1=
190     mdb.models['Model-1'].sketches['__profile__'].vertices.findAt(
191         (-TopPlate/2.0, TopPlate/2.0),
192     ), entity2=mdb.models['Model-1'].sketches['__profile__'].vertices.
193     findAt((
194     -TopPlate/2.0, -TopPlate/2.0), ), midpoint=
195     mdb.models['Model-1'].sketches['__profile__'].vertices.findAt(
196         (-TopPlate/2.0, 0.0),
197     ))
198 mdb.models['Model-1'].sketches['__profile__'].CoincidentConstraint(
199     addUndoState=False, entity1=
200     mdb.models['Model-1'].sketches['__profile__'].vertices.findAt(
201         (TopPlate/2.0, 0.0), )
202     , entity2=mdb.models['Model-1'].sketches['__profile__'].geometry.
203     findAt((
204     TopPlate/2.0, -TopPlate/2.0), ))
205 mdb.models['Model-1'].sketches['__profile__'].EqualDistanceConstraint(
206     addUndoState=False, entity1=
207     mdb.models['Model-1'].sketches['__profile__'].vertices.findAt(
208         (TopPlate/2.0, -TopPlate/2.0),
```

```

209     ), entity2=mdb.models['Model-1'].sketches['__profile__'].vertices.
210     findAt((
211     TopPlate/2.0, TopPlate/2.0), ), midpoint=
212     mdb.models['Model-1'].sketches['__profile__'].vertices.findAt(
213     (TopPlate/2.0, 0.0),
214     ))
215 mdb.models['Model-1'].parts['Top_Plate'].PartitionFaceBySketch(faces=
216     mdb.models['Model-1'].parts['Top_Plate'].faces.findAt((
217     (-TopPlate/3.0, 0.0, -TopPlate/6.0),
218     )), sketch=mdb.models['Model-1'].sketches['__profile__'],
219     sketchUpEdge=
220     mdb.models['Model-1'].parts['Top_Plate'].edges.findAt(
221     (-TopPlate, 0.0, TopPlate/4.0), ))
222 del mdb.models['Model-1'].sketches['__profile__']
223
224 # Reference Point
225 mdb.models['Model-1'].parts['Top_Plate'].ReferencePoint(point=
226     mdb.models['Model-1'].parts['Top_Plate'].vertices.findAt(
227     (-TopPlate/2.0, 0.0, 0.0),
228     ))
229
230 # Bottom Plate
231
232 # Sketch and Part
233 mdb.models['Model-1'].ConstrainedSketch(name='__profile__',
234     sheetSize=sheet_Size)
235 mdb.models['Model-1'].sketches['__profile__'].Line(point1=(-BottomPlate, 0.0),
236     point2=
237     (0.0, 0.0))
238 mdb.models['Model-1'].sketches['__profile__'].HorizontalConstraint(
239     addUndoState=False, entity=
240     mdb.models['Model-1'].sketches['__profile__'].geometry.findAt(
241     (-BottomPlate, 0.0),
242     ))
243 mdb.models['Model-1'].sketches['__profile__'].
244 ObliqueDimension(textPoint=(
245     -BottomPlate, -BottomPlate), value=BottomPlate, vertex1=
246     mdb.models['Model-1'].sketches['__profile__'].vertices.findAt(
247     (-BottomPlate, 0.0),
248     ), vertex2=mdb.models['Model-1'].sketches['__profile__'].vertices.
249     findAt((
250     0.0, 0.0), ))
251 mdb.models['Model-1'].Part(dimensionality=THREE_D, name='Bottom_Plate',
252     type=
253     ANALYTIC_RIGID_SURFACE)
254 mdb.models['Model-1'].parts['Bottom_Plate'].
255 AnalyticRigidSurfExtrude(depth=BottomPlate,

```

```

256     sketch=mdb.models['Model-1'].sketches['__profile__']
257 del mdb.models['Model-1'].sketches['__profile__']
258
259 # Partition Cross Section
260 mdb.models['Model-1'].ConstrainedSketch(gridSpacing=Grid,
261     name='__profile__',
262     sheetSize=sheet_Size, transform=
263     mdb.models['Model-1'].parts['Bottom_Plate'].MakeSketchTransform(
264     sketchPlane=mdb.models['Model-1'].parts['Bottom_Plate'].faces.
265     findAt((-BottomPlate/3.0,
266     0.0, -BottomPlate/6.0), (0.0, 1.0, 0.0)), sketchPlaneSide=SIDE1,
267     sketchUpEdge=mdb.models['Model-1'].parts['Bottom_Plate'].edges.
268     findAt((-BottomPlate,
269     0.0, BottomPlate/4.0), ), sketchOrientation=RIGHT,
270     origin=(-BottomPlate/2.0, 0.0, 0.0))
271 mdb.models['Model-1'].parts['Bottom_Plate'].
272 projectReferencesOntoSketch(filter=
273     COPLANAR_EDGES, sketch=mdb.models['Model-1'].sketches['__profile__'])
274 mdb.models['Model-1'].sketches['__profile__'].
275 Line(point1=(0.0, BottomPlate/2.0), point2=(
276     0.0, -BottomPlate/2.0))
277 mdb.models['Model-1'].sketches['__profile__'].
278 VerticalConstraint(addUndoState=
279     False, entity=
280     mdb.models['Model-1'].sketches['__profile__'].geometry.
281     findAt((0.0, 0.0),
282     ))
283 mdb.models['Model-1'].sketches['__profile__'].PerpendicularConstraint(
284     addUndoState=False, entity1=
285     mdb.models['Model-1'].sketches['__profile__'].geometry.findAt(
286     (BottomPlate/2.0, BottomPlate/2.0),
287     ), entity2=mdb.models['Model-1'].sketches['__profile__'].geometry.
288     findAt((
289     0.0, 0.0), ))
290 mdb.models['Model-1'].sketches['__profile__'].CoincidentConstraint(
291     addUndoState=False, entity1=
292     mdb.models['Model-1'].sketches['__profile__'].vertices.findAt(
293     (0.0, BottomPlate/2.0), )
294     , entity2=mdb.models['Model-1'].sketches['__profile__'].geometry.
295     findAt((
296     BottomPlate/2.0, BottomPlate/2.0), ))
297 mdb.models['Model-1'].sketches['__profile__'].EqualDistanceConstraint(
298     addUndoState=False, entity1=
299     mdb.models['Model-1'].sketches['__profile__'].vertices.findAt(
300     (BottomPlate/2.0, BottomPlate/2.0), )
301     , entity2=mdb.models['Model-1'].sketches['__profile__'].vertices.
302     findAt((

```

```

303     -BottomPlate/2.0, BottomPlate/2.0), ), midpoint=
304     mdb.models['Model-1'].sketches['__profile__'].vertices.findAt(
305         (0.0, BottomPlate/2.0),
306     )
307 mdb.models['Model-1'].sketches['__profile__'].CoincidentConstraint(
308     addUndoState=False, entity1=
309     mdb.models['Model-1'].sketches['__profile__'].vertices.findAt(
310         (0.0, -BottomPlate/2.0),
311     ), entity2=mdb.models['Model-1'].sketches['__profile__'].geometry.
312     findAt((
313     -BottomPlate/2.0, -BottomPlate/2.0), ))
314 mdb.models['Model-1'].sketches['__profile__'].EqualDistanceConstraint(
315     addUndoState=False, entity1=
316     mdb.models['Model-1'].sketches['__profile__'].vertices.findAt(
317         (-BottomPlate/2.0, -BottomPlate/2.0),
318     ), entity2=mdb.models['Model-1'].sketches['__profile__'].vertices.
319     findAt((
320     BottomPlate/2.0, -BottomPlate/2.0), ), midpoint=
321     mdb.models['Model-1'].sketches['__profile__'].vertices.findAt(
322         (0.0, -BottomPlate/2.0),
323     ))
324 mdb.models['Model-1'].sketches['__profile__'].
325 Line(point1=(-BottomPlate/2.0, 0.0), point2=(
326     BottomPlate/2.0, 0.0))
327 mdb.models['Model-1'].sketches['__profile__'].HorizontalConstraint(
328     addUndoState=False, entity=
329     mdb.models['Model-1'].sketches['__profile__'].geometry.
330     findAt((-BottomPlate/2.0, 0.0),
331     ))
332 mdb.models['Model-1'].sketches['__profile__'].PerpendicularConstraint(
333     addUndoState=False, entity1=
334     mdb.models['Model-1'].sketches['__profile__'].geometry.findAt(
335         (-BottomPlate/2.0, BottomPlate/2.0),
336     ), entity2=mdb.models['Model-1'].sketches['__profile__'].geometry.
337     findAt((
338     -BottomPlate/2.0, 0.0), ))
339 mdb.models['Model-1'].sketches['__profile__'].CoincidentConstraint(
340     addUndoState=False, entity1=
341     mdb.models['Model-1'].sketches['__profile__'].vertices.findAt(
342         (-BottomPlate/2.0, 0.0),
343     ), entity2=mdb.models['Model-1'].sketches['__profile__'].geometry.
344     findAt((
345     -BottomPlate/2.0, BottomPlate/2.0), ))
346 mdb.models['Model-1'].sketches['__profile__'].EqualDistanceConstraint(
347     addUndoState=False, entity1=
348     mdb.models['Model-1'].sketches['__profile__'].vertices.findAt(
349         (-BottomPlate/2.0, BottomPlate/2.0),

```

```

350     ), entity2=mdb.models['Model-1'].sketches['__profile__'].vertices.
351     findAt((
352     -BottomPlate/2.0, -BottomPlate/2.0), ), midpoint=
353     mdb.models['Model-1'].sketches['__profile__'].vertices.findAt(
354     (-BottomPlate/2.0, 0.0),
355     ))
356 mdb.models['Model-1'].sketches['__profile__'].CoincidentConstraint(
357     addUndoState=False, entity1=
358     mdb.models['Model-1'].sketches['__profile__'].vertices.findAt(
359     (BottomPlate/2.0, 0.0), )
360     , entity2=mdb.models['Model-1'].sketches['__profile__'].geometry.
361     findAt((
362     BottomPlate/2.0, -BottomPlate/2.0), ))
363 mdb.models['Model-1'].sketches['__profile__'].EqualDistanceConstraint(
364     addUndoState=False, entity1=
365     mdb.models['Model-1'].sketches['__profile__'].vertices.findAt(
366     (BottomPlate/2.0, -BottomPlate/2.0),
367     ), entity2=mdb.models['Model-1'].sketches['__profile__'].vertices.
368     findAt((
369     BottomPlate/2.0, BottomPlate/2.0), ), midpoint=
370     mdb.models['Model-1'].sketches['__profile__'].vertices.findAt(
371     (BottomPlate/2.0, 0.0),
372     ))
373 mdb.models['Model-1'].parts['Bottom_Plate'].PartitionFaceBySketch(faces=
374     mdb.models['Model-1'].parts['Bottom_Plate'].faces.findAt((
375     (-BottomPlate/3.0, 0.0, -BottomPlate/6.0),
376     )), sketch=mdb.models['Model-1'].sketches['__profile__'],
377     sketchUpEdge=
378     mdb.models['Model-1'].parts['Bottom_Plate'].edges.findAt(
379     (-BottomPlate, 0.0, BottomPlate/4.0), ))
380 del mdb.models['Model-1'].sketches['__profile__']
381
382 # Reference Point
383 mdb.models['Model-1'].parts['Bottom_Plate'].ReferencePoint(point=
384     mdb.models['Model-1'].parts['Bottom_Plate'].vertices.findAt(
385     (-BottomPlate/2.0, 0.0, 0.0),
386     ))
387
388
389 ## Assembly
390 # Connect Comp with Teflon
391 mdb.models['Model-1'].rootAssembly.Instance(dependent=ON, name=
392     'Airborne-Composite-1', part=
393     mdb.models['Model-1'].parts['Airborne-Composite'])
394 mdb.models['Model-1'].rootAssembly.Instance(dependent=ON,
395     name='Teflon-1',
396     part=mdb.models['Model-1'].parts['Teflon'])

```

```

397 mdb.models[ 'Model-1' ].rootAssembly.translate(instanceList=(
398     'Airborne-Composite-1', ), vector=(0.0, 0.0, thickness))
399
400
401 # Connect Bottom Plate and assign Set(RP) and Surf
402 mdb.models[ 'Model-1' ].rootAssembly.DatumCsysByDefault(CARTESIAN)
403 mdb.models[ 'Model-1' ].rootAssembly.Instance(dependent=ON,
404     name='Bottom_Plate-1'
405     , part=mdb.models[ 'Model-1' ].parts[ 'Bottom_Plate' ])
406 mdb.models[ 'Model-1' ].rootAssembly.rotate(angle=90.0,
407     axisDirection=(-BottomPlate/2.0, 0.0,
408     0.0), axisPoint=(-BottomPlate/2.0, 0.0, 0.0),
409     instanceList=('Bottom_Plate-1', ))
410
411 mdb.models[ 'Model-1' ].rootAssembly.CoincidentPoint(fixedPoint=
412     mdb.models[ 'Model-1' ].rootAssembly.instances[ 'Teflon-1' ].vertices.
413     findAt((
414     0.0, 0.0, 0.0), ), movablePoint=
415     mdb.models[ 'Model-1' ].rootAssembly.instances[ 'Bottom_Plate-1' ].
416     referencePoints[3])
417
418
419 # Assign RP and surf for contact
420 mdb.models[ 'Model-1' ].rootAssembly.Set(name='BottomPlate_RP',
421     referencePoints=(
422     mdb.models[ 'Model-1' ].rootAssembly.instances[ 'Bottom_Plate-1' ].
423     referencePoints[3],
424     ))
425 mdb.models[ 'Model-1' ].rootAssembly.Surface(name='BottomPlate_Surf',
426     side2Faces=
427     mdb.models[ 'Model-1' ].rootAssembly.instances[ 'Bottom_Plate-1' ].
428     faces.findAt(
429     ((0.,0.,0),)) )
430
431 # Connect Top Plate and assign Set(RP) and Surf
432 mdb.models[ 'Model-1' ].rootAssembly.Instance(dependent=ON,
433     name='Top_Plate-1',
434     part=mdb.models[ 'Model-1' ].parts[ 'Top_Plate' ])
435 mdb.models[ 'Model-1' ].rootAssembly.rotate(angle=90.0,
436     axisDirection=(-TopPlate/2.0, 0.0,
437     0.0), axisPoint=(-TopPlate/1.5, 0.0, 0.0),
438     instanceList=('Top_Plate-1', ))
439 mdb.models[ 'Model-1' ].rootAssembly.CoincidentPoint(fixedPoint=
440     mdb.models[ 'Model-1' ].rootAssembly.instances[ 'Airborne-Composite-1' ].
441     vertices.findAt(
442     (0.0, 0.0, thickness+Thickness_), ), movablePoint=
443     mdb.models[ 'Model-1' ].rootAssembly.instances[ 'Top_Plate-1' ].

```



```

444         referencePoints[3])
445
446 # Assign RP and surf for contact
447 mdb.models['Model-1'].rootAssembly.Set(name='TopPlate_RP',
448     referencePoints=(
449         mdb.models['Model-1'].rootAssembly.instances['Top_Plate-1'].
450             referencePoints[3],
451     ))
452 mdb.models['Model-1'].rootAssembly.Surface(name='TopPlate_Surf',
453     side1Faces=
454         mdb.models['Model-1'].rootAssembly.instances['Top_Plate-1'].faces.
455             findAt(
456                 ((0.,0.,thickness+Thickness_)),) )
457
458
459 # Assign Teflon Surf and Set
460 mdb.models['Model-1'].rootAssembly.Set(cells=
461     mdb.models['Model-1'].rootAssembly.instances['Teflon-1'].cells.
462         findAt(((
463             -Sides/6.0, Sides/6.0, 0.0), )), name='Teflon_Set')
464
465 mdb.models['Model-1'].rootAssembly.Set(faces=
466     mdb.models['Model-1'].rootAssembly.instances['Teflon-1'].faces.
467         findAt(((
468             Sides/6.0, -Sides/6.0, 0.0), ), ((Sides/3.0, Sides/6.0, 0.0), ),
469             ((-Sides/3.0, -Sides/6.0, 0.0), ), (
470             (-Sides/6.0, Sides/6.0, 0.0), ), ), name='Teflon-Set-Bottom')
471
472 mdb.models['Model-1'].rootAssembly.Surface(name='Teflon-Surf-Bottom',
473     side1Faces=
474         mdb.models['Model-1'].rootAssembly.instances['Teflon-1'].faces.
475             findAt(((
476             Sides/6.0, -Sides/6.0, 0.0), ), ((Sides/3.0, Sides/6.0, 0.0), ),
477             ((-Sides/3.0, -Sides/6.0, 0.0), ), (
478             (-Sides/6.0, Sides/6.0, 0.0), ), ))
479
480 mdb.models['Model-1'].rootAssembly.Surface(name='Teflon-Surf-Top',
481     side1Faces=
482         mdb.models['Model-1'].rootAssembly.instances['Teflon-1'].faces.
483             findAt(((
484             Sides/6.0, -Sides/3.0, thickness), ), ((-Sides/6.0, -Sides/6.0,
485             thickness), ), ((Sides/6.0, Sides/6.0,
486             thickness), ), ((-Sides/6.0, Sides/3.0, thickness), ), ))
487
488 # Set for the whole laminate
489 p = mdb.models['Model-1'].parts['Airborne-Composite']
490 p.Set(cells=lamina_Composite + lamina_Cohesive,

```

```

491 name='C-Set-InitialTemp')
492
493 mdb.models['Model-1'].rootAssembly.Set(faces=
494     mdb.models['Model-1'].rootAssembly.
495     instances['Airborne-Composite-1'].faces.findAt(
496     ((Width/3.0, Length/6.0, Thickness_+thickness), ),
497     ((-Width/3.0, Length/6.0, Thickness_+thickness), ), ((Width/3.0,
498     -Length/6.0, Thickness_+thickness), ),
499     ((-Width/6.0, -Length/6.0, Thickness_+thickness), ), ), ),
500     name='Comp-Set-Top')
501
502 # Surf for convection
503 p = mdb.models['Model-1'].parts['Airborne-Composite']
504 s = p.faces
505 surf_contact_1_A=[]
506
507 surf_contact_1_A.append(s.findAt(
508     ((Width_)/2.0, (Length_)/2.0, Thickness_ ),),
509     ((-Width_)/2.0, (Length_)/2.0, Thickness_ ),),
510     ((Width_)/2.0, -(Length_)/2.0, Thickness_ ),),
511     ((-Width_)/2.0, -(Length_)/2.0, Thickness_ ),),)
512
513 surf_contact_1_A.append(s.findAt(
514     ((Width_)/2.0, (Length_)/2.0, 0.0 ),),
515     ((-Width_)/2.0, (Length_)/2.0, 0.0 ),),
516     ((Width_)/2.0, -(Length_)/2.0, 0.0 ),),
517     ((-Width_)/2.0, -(Length_)/2.0, 0.0 ),),)
518 p.Surface(sidelFaces=surf_contact_1_A, name='C-Surf-Conv-Radiation')
519
520 # Top and bottom surfaces for composite
521 p = mdb.models['Model-1'].parts['Airborne-Composite']
522 s = p.faces
523 p.Surface(sidelFaces=surf_contact_1_A[0], name='C-Surf-Top')
524
525 p = mdb.models['Model-1'].parts['Airborne-Composite']
526 s = p.faces
527 p.Surface(sidelFaces=surf_contact_1_A[1], name='C-Surf-Bottom')
528
529 # Creation of Step with Damping
530
531 mdb.models['Model-1'].CoupledTempDisplacementStep
532 (adaptiveDampingRatio=DampingFactor,
533     continueDampingFactors=True, deltmx=100.0,
534     initialInc=1e-08, maxInc=time,
535     minInc=1e-015, name='Heat_1', nlgeom=ON, previous='Initial',
536     stabilizationMethod=DAMPING_FACTOR, timePeriod=time)
537

```

```
538 ## Surface Contact
539
540 # Contact Control
541 mdb.models[ 'Model-1' ].StdContactControl( dampFactor=ContactControl_Damp,
542     name='ContCtrl-1',
543     stabilizeChoice=AUTOMATIC)
544
545 # Assign Contact Properties
546 # Between Composite and Teflon
547 mdb.models[ 'Model-1' ].ContactProperty( 'Comp-Teflon' )
548 mdb.models[ 'Model-1' ].interactionProperties[ 'Comp-Teflon' ].
549 TangentialBehavior(
550     dependencies=0, directionality=ISOTROPIC,
551     elasticSlipStiffness=None,
552     formulation=PENALTY, fraction=0.005, maximumElasticSlip=FRACTION,
553     pressureDependency=OFF, shearStressLimit=None,
554     slipRateDependency=OFF,
555     table=((0.4, ), ), temperatureDependency=OFF)
556 mdb.models[ 'Model-1' ].interactionProperties[ 'Comp-Teflon' ].
557 NormalBehavior(
558     allowSeparation=ON, constraintEnforcementMethod=DEFAULT,
559     pressureOverclosure=HARD)
560 mdb.models[ 'Model-1' ].interactionProperties[ 'Comp-Teflon' ].
561 ThermalConductance(
562     clearanceDepTable=((Thermal_Conductance_Comp_Teflon, 0.0),
563         (0.0, 0.001)),
564     clearanceDependency=ON,
565     definition=TABULAR, dependenciesC=0, massFlowRateDependencyC=OFF,
566     pressureDependency=OFF, temperatureDependencyC=OFF)
567
568 # Between Composite and Top Plate
569 mdb.models[ 'Model-1' ].ContactProperty( 'Comp-TP' )
570 mdb.models[ 'Model-1' ].interactionProperties[ 'Comp-TP' ].
571 TangentialBehavior(
572     formulation=FRICITIONLESS)
573 mdb.models[ 'Model-1' ].interactionProperties[ 'Comp-TP' ].
574 NormalBehavior(
575     allowSeparation=ON, constraintEnforcementMethod=DEFAULT,
576     pressureOverclosure=HARD)
577 mdb.models[ 'Model-1' ].interactionProperties[ 'Comp-TP' ].
578 ThermalConductance(
579     clearanceDepTable=((Thermal_Conductance_Plates, 0.0),
580         (0.0, 0.001)),
581     clearanceDependency=ON,
582     definition=TABULAR, dependenciesC=0, massFlowRateDependencyC=OFF,
583     pressureDependency=OFF, temperatureDependencyC=OFF)
584
```

```

585 # Between Teflon and Bottom Plate
586 mdb.models[ 'Model-1' ].ContactProperty( 'Teflon-BP' )
587 mdb.models[ 'Model-1' ].interactionProperties[ 'Teflon-BP' ].
588 TangentialBehavior(
589     dependencies=0, directionality=ISOTROPIC,
590     elasticSlipStiffness=None,
591     formulation=PENALTY, fraction=0.005, maximumElasticSlip=FRACTION,
592     pressureDependency=OFF, shearStressLimit=None,
593     slipRateDependency=OFF,
594     table=((0.04, ), ), temperatureDependency=OFF)
595 mdb.models[ 'Model-1' ].interactionProperties[ 'Teflon-BP' ].
596 NormalBehavior(
597     allowSeparation=ON, constraintEnforcementMethod=DEFAULT,
598     pressureOverclosure=HARD)
599 mdb.models[ 'Model-1' ].interactionProperties[ 'Teflon-BP' ].
600 ThermalConductance(
601     clearanceDepTable=((Thermal_Conductance_Plates, 0.0),
602     (0.0, 0.001)),
603     clearanceDependency=ON,
604     definition=TABULAR, dependenciesC=0, massFlowRateDependencyC=OFF,
605     pressureDependency=OFF, temperatureDependencyC=OFF)
606
607 # Assign interaction between surfaces, Teflon-BP and Comp-TP
608 mdb.models[ 'Model-1' ].SurfaceToSurfaceContactStd(
609     adjustMethod=OVERCLOSED,
610     clearanceRegion=None, createStepName='Initial', datumAxis=None,
611     initialClearance=OMIT, interactionProperty='Comp-TP', master=
612     mdb.models[ 'Model-1' ].rootAssembly.surfaces[ 'TopPlate_Surf' ],
613     name=
614     'Comp-TP', slave=
615     mdb.models[ 'Model-1' ].rootAssembly.instances[ 'Airborne-Composite-1' ].
616     surfaces[ 'C-Surf-Top' ]
617     , sliding=FINITE, surfaceSmoothing=AUTOMATIC, thickness=ON,
618     tied=OFF)
619 mdb.models[ 'Model-1' ].interactions[ 'Comp-TP' ].setValuesInStep(
620     contactControls=
621     'ContCtrl-1', stepName='Heat_1')
622
623
624 mdb.models[ 'Model-1' ].SurfaceToSurfaceContactStd(
625     adjustMethod=OVERCLOSED,
626     clearanceRegion=None, createStepName='Initial', datumAxis=None,
627     initialClearance=OMIT, interactionProperty='Teflon-BP', master=
628     mdb.models[ 'Model-1' ].rootAssembly.surfaces[ 'BottomPlate_Surf' ],
629     name=
630     'Teflon-BP', slave=
631     mdb.models[ 'Model-1' ].rootAssembly.surfaces[ 'Teflon-Surf-Bottom' ],

```

```
632         sliding=
633         FINITE, surfaceSmoothing=AUTOMATIC, thickness=ON, tied=OFF)
634 mdb.models[ 'Model-1' ].interactions[ 'Teflon-BP' ].setValuesInStep (
635     contactControls='ContCtrl-1', stepName='Heat_1')
636
637 # Tie Composite with Teflon
638 mdb.models[ 'Model-1' ].Tie(adjust=ON, master=
639     mdb.models[ 'Model-1' ].rootAssembly.surfaces[ 'Teflon-Surf-Top' ],
640     name='Tie',
641     positionToleranceMethod=COMPUTED, slave=
642     mdb.models[ 'Model-1' ].rootAssembly.instances[ 'Airborne-Composite-1' ].
643     surfaces[ 'C-Surf-Bottom' ]
644     , thickness=ON, tieRotations=ON)
645
646 # Loads and Boundaries, Predifinied and Amplitude for Temperature Loads
647
648 mdb.models[ 'Model-1' ].SmoothStepAmplitude(data=((0.0, 0.0), (1.0, 0.2),
649     (2.0,
650     0.4), (5.0, 0.6), (10.0, 0.9), (12.0, 1.0)), name='Amp-1',
651     timeSpan=STEP)
652
653 mdb.models[ 'Model-1' ].EncastreBC(createStepName='Initial',
654     localCsys=None,
655     name='Bottom_Encastre', region=
656     mdb.models[ 'Model-1' ].rootAssembly.sets[ 'BottomPlate_RP' ])
657
658 mdb.models[ 'Model-1' ].TemperatureBC(amplitude='Amp-1',
659     createStepName='Heat_1',
660     distributionType=UNIFORM, fieldName='', fixed=OFF,
661     magnitude=Cycle1_Heat, name=
662     'Bottom_Temp', region=
663     mdb.models[ 'Model-1' ].rootAssembly.sets[ 'Teflon-Set-Bottom' ])
664
665 mdb.models[ 'Model-1' ].TemperatureBC(amplitude='Amp-1',
666     createStepName='Heat_1',
667     distributionType=UNIFORM, fieldName='', fixed=OFF,
668     magnitude=Cycle1_Heat, name=
669     'Top_Temp', region=
670     mdb.models[ 'Model-1' ].rootAssembly.sets[ 'Comp-Set-Top' ])
671
672 mdb.models[ 'Model-1' ].Temperature(createStepName='Initial',
673     crossSectionDistribution=CONSTANT_THROUGH_THICKNESS,
674     distributionType=
675     UNIFORM, magnitudes=(Predifinied_Heat, ),
676     name='Temp_Uniform_Composite',
677     region=
678     mdb.models[ 'Model-1' ].rootAssembly.
```

```

679         instances [ 'Airborne-Composite-1' ]. sets [ 'C-Set-InitialTemp' ])
680
681 mdb.models [ 'Model-1' ]. Temperature (createStepName= 'Initial' ,
682     crossSectionDistribution=CONSTANT_THROUGH_THICKNESS,
683     distributionType=
684     UNIFORM, magnitudes=( Predifinied_Heat , ) , name= 'Temp_Uniform_Teflon' ,
685     region=
686     mdb.models [ 'Model-1' ]. rootAssembly . sets [ 'Teflon_Set' ])
687
688 mdb.models [ 'Model-1' ]. ConcentratedForce ( cf3=Top_Force ,
689     createStepName= 'Heat_1'
690     , distributionType=UNIFORM, field=' ' , localCsys=None,
691     name= 'Top_Force' ,
692     region=mdb.models [ 'Model-1' ]. rootAssembly . sets [ 'TopPlate_RP' ])
693
694 # Mesh Generation
695 p = mdb.models [ 'Model-1' ]. parts [ 'Airborne-Composite' ]
696 p.seedPart (size=0.01, deviationFactor=0.1, minSizeFactor=0.1)
697 p = mdb.models [ 'Model-1' ]. parts [ 'Airborne-Composite' ]
698 p.generateMesh ()
699
700 t = mdb.models [ 'Model-1' ]. parts [ 'Teflon' ]
701 t.seedPart (deviationFactor=0.1, minSizeFactor=0.1, size=0.011)
702 mdb.models [ 'Model-1' ]. parts [ 'Teflon' ]. generateMesh ()
703
704 # Elements Assign
705 # Composite
706 elemType1 = mesh.ElemType (elemCode=C3D8T, elemLibrary=STANDARD,
707     secondOrderAccuracy=OFF, distortionControl=DEFAULT)
708 elemType2 = mesh.ElemType (elemCode=C3D6T, elemLibrary=STANDARD)
709 elemType3 = mesh.ElemType (elemCode=C3D4T, elemLibrary=STANDARD)
710 p = mdb.models [ 'Model-1' ]. parts [ 'Airborne-Composite' ]
711 c = p.cells
712 cells = lamina_Composite + lamina_Cohesive
713 pickedRegions =( cells , )
714 p.setElementType (regions=pickedRegions, elemTypes=(elemType1,
715     elemType2,
716     elemType3))
717
718
719 # Teflon
720 mdb.models [ 'Model-1' ]. parts [ 'Teflon' ]. setElementType (elemTypes=
721 (ElemType (
722     elemCode=C3D8T, elemLibrary=STANDARD, secondOrderAccuracy=OFF,
723     distortionControl=DEFAULT) , ElemType (elemCode=C3D6T, elemLibrary=
724     STANDARD) ,
725     ElemType (elemCode=C3D4T, elemLibrary=STANDARD) ) , regions=(

```

```

726     mdb.models[ 'Model-1' ].parts[ 'Teflon' ].cells.findAt((( -Sides/6.0,
727         Sides/6.0, 0.0),
728     )), ))

```

## B.2. WARPAGE SIMULATION

```

1  ## Python script for the warpage. Here, only the step, Predifined
2  #Stress Field and Boundary conditions are provided. The structure
3  #can be simulated from the code of the Cycles removing the Plates.
4
5  # Assign Static Step
6  mdb.models[ 'Model-1' ].StaticStep(adaptiveDampingRatio=0.05,
7      continueDampingFactors=False, initialInc=1e-10, maxInc=40.0,
8      minInc=1e-15,
9      name='Springback', nlgeom=ON, previous='Initial',
10     stabilizationMagnitude=
11     0.0002, stabilizationMethod=DISSIPATED_ENERGY_FRACTION,
12     timePeriod=40.0)
13
14 # Predifined Stress Field -- In the "filename, the name of the
15 # file that produces the desirable profile must be used (here is one
16 # my own files)
17 #
18 mdb.models[ 'Model-1' ].Stress(distributionType=FROM_FILE, fileName=
19     '/home/harris/temp/14June/Heat1_Test2_NP.odb', increment=45,
20     name='Stress_Field', step=1)
21
22 # Boundary Conditions, Fix Composite and Teflon Nodes
23 mdb.models[ 'Model-1' ].EncastreBC(createStepName='Initial',
24     localCsys=None,
25     name='Comp_Encastre', region=
26     mdb.models[ 'Model-1' ].rootAssembly.sets[ 'Comp_Set_Enc' ])
27
28 mdb.models[ 'Model-1' ].EncastreBC(createStepName='Initial',
29     localCsys=None,
30     name='Teflon_Encastre', region=
31     mdb.models[ 'Model-1' ].rootAssembly.sets[ 'Teflon_Set_Encastre' ])

```

## B.3. DISCRETE RIGID PLATES

Another type of rigid plates is the Discrete rigid plates. The difference between those two is that discrete plates can be meshed as a real deformable part, but they have properties of a rigid plate. The user can try with both plates in order to compare the outcome, as discrete plates manipulate the contact regions better.

```

1  # Discrete Plate
2  mdb.models[ 'Model-1' ].ConstrainedSketch(name='__profile__',
3      sheetSize=1.0)
4  mdb.models[ 'Model-1' ].sketches[ '__profile__' ].rectangle(point1=

```

```

5 (Plate / 2.0, Plate / 2.0),
6     point2=(-Plate / 2.0, -Plate / 2.0))
7 mdb.models['Model-1'].sketches['__profile__'].ObliqueDimension(textPoint=
8 (
9     -Plate / 6.0, Plate / 75.0), value=Plate, vertex1=
10    mdb.models['Model-1'].sketches['__profile__'].vertices.findAt(
11        (-Plate / 2.0, Plate / 2.0),
12    ), vertex2=mdb.models['Model-1'].sketches['__profile__'].vertices.
13    findAt((
14        -Plate / 2.0, -Plate / 2.0), ))
15 mdb.models['Model-1'].sketches['__profile__'].ObliqueDimension(textPoint=
16 (
17     -Plate / 15.0, -Plate / 6.0), value=0.6, vertex1=
18    mdb.models['Model-1'].sketches['__profile__'].vertices.findAt(
19        (-Plate / 2.0,
20        -Plate / 2.0), ), vertex2=
21    mdb.models['Model-1'].sketches['__profile__'].vertices.findAt(
22        (Plate / 2.0,
23        -Plate / 2.0), ))
24 mdb.models['Model-1'].Part(dimensionality=THREE_D, name='Top_Plate',
25     type=
26     DISCRETE_RIGID_SURFACE)
27 mdb.models['Model-1'].parts['Top_Plate'].BaseSolidExtrude(depth=
28     PlatesDepth, sketch=
29     mdb.models['Model-1'].sketches['__profile__'])
30 del mdb.models['Model-1'].sketches['__profile__']
31
32 # Partition
33 mdb.models['Model-1'].ConstrainedSketch(gridSpacing=Grid,
34     name='__profile__',
35     sheetSize=sheet_Size, transform=
36     mdb.models['Model-1'].parts['Top_Plate'].MakeSketchTransform(
37     sketchPlane=mdb.models['Model-1'].parts['Top_Plate'].faces.findAt(
38         (Plate / 6.0,
39         Plate / 6.0, PlatesDepth), ), sketchPlaneSide=SIDE1,
40     sketchUpEdge=mdb.models['Model-1'].parts['Top_Plate'].edges.findAt(
41         (-Plate / 2.0,
42         -Plate / 4.0, PlatesDepth), ), sketchOrientation=RIGHT, origin=(0.0,
43         0.0, PlatesDepth)))
44 mdb.models['Model-1'].parts['Top_Plate'].projectReferencesOntoSketch(
45     filter=
46     COPLANAR_EDGES, sketch=mdb.models['Model-1'].sketches['__profile__'])
47 mdb.models['Model-1'].sketches['__profile__'].Line(point1=(0.0,
48     Plate / 2.0), point2=(
49     0.0, -Plate / 2.0))
50 mdb.models['Model-1'].sketches['__profile__'].VerticalConstraint(
51     addUndoState=

```



```
52     False, entity=
53     mdb.models['Model-1'].sketches['__profile__'].geometry.findAt((0.0,
54         0.0),
55     ))
56 mdb.models['Model-1'].sketches['__profile__'].PerpendicularConstraint(
57     addUndoState=False, entity1=
58     mdb.models['Model-1'].sketches['__profile__'].geometry.findAt(
59         (-Plate/2.22, Plate/2.0),
60     ), entity2=mdb.models['Model-1'].sketches['__profile__'].geometry.
61         findAt((
62         0.0, 0.0), ))
63 mdb.models['Model-1'].sketches['__profile__'].CoincidentConstraint(
64     addUndoState=False, entity1=
65     mdb.models['Model-1'].sketches['__profile__'].vertices.findAt((0.0,
66         Plate/2.0), )
67     , entity2=mdb.models['Model-1'].sketches['__profile__'].geometry.
68         findAt((
69         -Plate/2.22, Plate/2.0), ))
70 mdb.models['Model-1'].sketches['__profile__'].EqualDistanceConstraint(
71     addUndoState=False, entity1=
72     mdb.models['Model-1'].sketches['__profile__'].vertices.findAt(
73         (-Plate/2.0, Plate/2.0),
74     ), entity2=mdb.models['Model-1'].sketches['__profile__'].vertices.
75         findAt((
76         Plate/2.0, Plate/2.0), ), midpoint=
77     mdb.models['Model-1'].sketches['__profile__'].vertices.findAt(
78         (0.0, Plate/2.0),
79     ))
80 mdb.models['Model-1'].sketches['__profile__'].CoincidentConstraint(
81     addUndoState=False, entity1=
82     mdb.models['Model-1'].sketches['__profile__'].vertices.findAt(
83         (0.0, -Plate/2.0),
84     ), entity2=mdb.models['Model-1'].sketches['__profile__'].geometry.
85         findAt((
86         Plate/2.22, -Plate/2.0), ))
87 mdb.models['Model-1'].sketches['__profile__'].EqualDistanceConstraint(
88     addUndoState=False, entity1=
89     mdb.models['Model-1'].sketches['__profile__'].vertices.findAt(
90         (Plate/2.0, -Plate/2.0),
91     ), entity2=mdb.models['Model-1'].sketches['__profile__'].vertices.
92         findAt((
93         -Plate/2.0, -Plate/2.0), ), midpoint=
94     mdb.models['Model-1'].sketches['__profile__'].vertices.findAt(
95         (0.0, -Plate/2.0),
96     ))
97 mdb.models['Model-1'].sketches['__profile__'].Line(point1=(-Plate/2.0,
98     0.0), point2=(
```

```

99     Plate / 2.0, 0.0))
100 mdb.models['Model-1'].sketches['__profile__'].HorizontalConstraint(
101     addUndoState=False, entity=
102     mdb.models['Model-1'].sketches['__profile__'].geometry.findAt(
103         (-Plate / 2.22, 0.0),
104     ))
105 mdb.models['Model-1'].sketches['__profile__'].PerpendicularConstraint(
106     addUndoState=False, entity1=
107     mdb.models['Model-1'].sketches['__profile__'].geometry.findAt((
108         -Plate / 2.0,
109         -Plate / 2.22), ), entity2=
110     mdb.models['Model-1'].sketches['__profile__'].geometry.findAt(
111         (-Plate / 2.22, 0.0),
112     ))
113 mdb.models['Model-1'].sketches['__profile__'].CoincidentConstraint(
114     addUndoState=False, entity1=
115     mdb.models['Model-1'].sketches['__profile__'].vertices.findAt(
116         (-Plate / 2.0, 0.0),
117     ), entity2=mdb.models['Model-1'].sketches['__profile__'].geometry.
118     findAt((
119         -Plate / 2.0, -Plate / 2.22), ))
120 mdb.models['Model-1'].sketches['__profile__'].EqualDistanceConstraint(
121     addUndoState=False, entity1=
122     mdb.models['Model-1'].sketches['__profile__'].vertices.findAt(
123         (-Plate / 2.0, -Plate / 2.0),
124     ), entity2=mdb.models['Model-1'].sketches['__profile__'].vertices.
125     findAt((
126         -Plate / 2.0, Plate / 2.0), ), midpoint=
127     mdb.models['Model-1'].sketches['__profile__'].vertices.findAt(
128         (-Plate / 2.0, 0.0),
129     ))
130 mdb.models['Model-1'].sketches['__profile__'].CoincidentConstraint(
131     addUndoState=False, entity1=
132     mdb.models['Model-1'].sketches['__profile__'].vertices.findAt(
133         (Plate / 2.0, 0.0), )
134     , entity2=mdb.models['Model-1'].sketches['__profile__'].geometry.
135     findAt((
136         Plate / 2.0, Plate / 2.22), ))
137 mdb.models['Model-1'].sketches['__profile__'].EqualDistanceConstraint(
138     addUndoState=False, entity1=
139     mdb.models['Model-1'].sketches['__profile__'].vertices.findAt(
140         (Plate / 2.0, Plate / 2.0), )
141     , entity2=mdb.models['Model-1'].sketches['__profile__'].vertices.
142     findAt((
143         Plate / 2.0, -Plate / 2.0), ), midpoint=
144     mdb.models['Model-1'].sketches['__profile__'].vertices.findAt(
145         (Plate / 2.0, 0.0),

```

```

146     ))
147     mdb.models['Model-1'].parts['Top_Plate'].PartitionFaceBySketch(faces=
148         mdb.models['Model-1'].parts['Top_Plate'].faces.findAt(((Plate/6.0,
149             Plate/6.0, PlatesDepth),
150         )), sketch=mdb.models['Model-1'].sketches['__profile__'],
151         sketchUpEdge=
152         mdb.models['Model-1'].parts['Top_Plate'].edges.findAt(
153             (-Plate/2.0, -Plate/4.0,
154             PlatesDepth), ))
155 del mdb.models['Model-1'].sketches['__profile__']

```

## B.4. VISCOELASTIC SCRIPTS

In this section, the basic extra script for merging the isotropic viscoelastic and the orthotropic elastic parts will be provided. These scripts are for Chapter 5. The rest of the scripts are the same from Chapter 4.

```

1 # Viscoelastic Isotropic
2 # Sketch and Part
3 mdb.models['Model-1'].ConstrainedSketch(name='__profile__',
4     sheetSize= sheet_Size)
5 mdb.models['Model-1'].sketches['__profile__'].rectangle(point1=
6     ( Width_, Length_),
7     point2=( -Width_, -Length_))
8 mdb.models['Model-1'].Part(dimensionality=THREE_D,
9     name='Airborne-Composite-Viscoelastic', type=
10     DEFORMABLE_BODY)
11 mdb.models['Model-1'].parts['Airborne-Composite-Viscoelastic'].
12     BaseSolidExtrude(depth=Thickness_, sketch=
13         mdb.models['Model-1'].sketches['__profile__'])
14 del mdb.models['Model-1'].sketches['__profile__']
15
16 # Merging
17 mdb.models['Model-1'].rootAssembly._previewMergeMeshes(instances=(
18     mdb.models['Model-1'].rootAssembly.instances['Airborne-Composite-1'],
19     mdb.models['Model-1'].rootAssembly.instances
20         ['Airborne-Composite-Viscoelastic-1'])
21     , mergeBoundaryOnly=False, nodeMergingTolerance=1e-06)
22 mdb.models['Model-1'].rootAssembly.InstanceFromBooleanMerge(domain=MESH,
23     instances=(
24     mdb.models['Model-1'].rootAssembly.instances['Airborne-Composite-1'],
25     mdb.models['Model-1'].rootAssembly.
26         instances['Airborne-Composite-Viscoelastic-1'])
27     , mergeNodes=ALL, name='Part-1', nodeMergingTolerance=1e-06,
28     originalInstances=DELETE)
29
30
31 # Viscoelastic Properties

```

```
32 mdb.models['Model-1'].Material(name='Viscoelastic')
33 mdb.models['Model-1'].materials['Viscoelastic'].Density(table=((1200.0,
34   ), ))
35 mdb.models['Model-1'].materials['Viscoelastic'].Elastic(
36   type=ISOTROPIC, table=((
37     2250000000.0, 0.3, 20.0), (2200000000.0, 0.3, 70.0), (2000000000.0,
38     0.3,
39     120.0), (1700000000.0, 0.3, 170.0)), temperatureDependency=ON)
40 mdb.models['Model-1'].materials['Viscoelastic'].Viscoelastic(domain=TIME,
41   table=(), time=RELAXATION_TEST_DATA)
42 mdb.models['Model-1'].materials['Viscoelastic'].viscoelastic.
43 ShearTestData(
44   shrink=0.45, table=((1, 0.001), (0.9, 50.0), (0.72, 100.0), (0.55,
45     200.0), (0.45,
46     300.0)))
```

# C

## APPENDIX C

In this Appendix, the basic knowledge concerning the first steps of obtaining data and also how to do a sensitivity analysis will be illustrated. No solutions or results are given, but only the basic steps for future work, as due to limited time frame, the author couldn't retrieve any result. Also, due to the big amount of coding (many Matlab and Python scripts), here, only the main concept and some basic coding will be given.

For Data retrieveing, a Matlab code was created. The work is about changing important input parameters in the model in order to observe how it behaves in terms of output results. In our case, how the parameters of the system affect the warpage is the main topic. There are several parameters from material properties to system parameters. To mention a few:

1. Laminate's thermal and mechanical properties (such as thermal expansion and Young's Modulus).
2. Laminate's imperfections and fiber misalignment.
3. Teflon's thermal and mechanical properties.
4. Friction coefficients between the plates, Teflon and Laminate.
5. Pressure and Temperature configurations of the system.

Also, a combination of these properties may have different outcome. So, in order to have a full observation, a Design of Experiments must be implemented. What this does is to create a dimensional space of combination of parameters that the user chooses to analyze. The user must provide the Upper and the Lower bound which is the range of values for analysis. After the DOE (Design Of Experiments) is created, simulations using each pair of parameters must take place. Every pair will correspond to a specific output, which will be extracted using post-processing techniques concerning the software that the user uses.

After the data is extracted, many data-analysis methods can be implemented such as sensitivity analysis which show how sensitive the output is concerning a specific parameter

or a pair of those. Another method of analysis is the well-known machine learning, which will show how the warpage is affected by the change of the most important parameters, mapping the inputs with the output.

To give an example, let us assume that the desirable parameters to be analyzed are the applied force from the top plate and the fiber misalignment of the first layer of the composite. Two ways can be used.

Through the Matlab code:

```

1 UserSettings.DoE_file_name = 'DOE'; % Name of the file
2 UserSettings.DoE_size     = 1000; % Number of DoE points
3 % Input design variables names
4 UserSettings.DoE_vars     = {'Force' , 'FiberMisal_layer'};
5 UserSettings.DoE_LowerBounds = [100e3, 0];
6 UserSettings.DoE_UpperBounds = [500e3, 90];

```

The 2<sup>nd</sup> way is by using a Python library called Salib which can be used either through Python compiler or from a terminal/command line [72] (the example here is through Python):

```

1 # Input Parameters
2 parameter_dict = {'num_vars':2 # Number of Input variables
3 'names':['Force', 'FiberMisal_layer'] # The parameters
4 'bounds':[[100e3,500e3], # Upper and Lower bounds
5 [0,90]]}
6
7 # Design of Experiments using Morris Method
8 model_input = SALib.sample.morris.sample(parameter_dict,10)

```

The next step is to run the simulations. Using the Matlab code, 6 smaller codes (except of the main one which run all the smaller codes).

1. Structure design and mesh of the Cycles 1 and 2 models (Python into Matlab)
2. Two input file codes which are the loads and boundary conditions for the two Cycles (Input file into Matlab)
3. Structure design and mesh of the Warpage model (Python into Matlab)
4. Input file that runs the Warpage model (Input file into Matlab)
5. Post-processing for extracting the node displacement U3

The input files (.inp) mentioned is a different way that Abaqus uses to run its simulations. In this case, Matlab provides ways to script different languages such as Python and also Input files.

After the output displacements are obtained, sensitivity analysis can be done using the input and the outputs:

```

1 # This step is just for illustration that to get the output,
2 # important is to run the simulations

```

```
3 model_output = run_simulation(model_input)
4
5 # The Python code below analyze the model using the input parameters
6 # and the output warpage to calculate how sensitive each parameter is.
7 Si = morris . analyze (problem , model_input , model_output)
```

Concerning sensitivity analysis, documentation is provided through articles, through Python developers and also online video seminars for better understanding [73].